DIFFRACTION OF TRANSIENT ELASTIC WAVES BY A SPHERICAL CAVITY

Thesis by

Frederick Reyes Norwood

In Partial Fulfillment of the Requirements

For the Degree of

Doctor of Philosophy

California Institute of Technology

Pasadena, California

1967

(Submitted September 12, 1966)

ACKNOWLEDGMENTS

The author desires to gratefully acknowledge the guidance and encouragement given by his advisor, Professor J. Miklowitz.

The author is further indebted to the National Aeronautics and Space Administration for a three year NASA traineeship (1963-1966) and to the California Institute of Technology for a teaching assistantship (1962-1963) and for its fine facilities and stimulating atmosphere.

This thesis is dedicated to my mother who instilled in me the desire to learn, to my father who encouraged me, and to my wife who has continued the work of my parents.

ABSTRACT

The diffraction of transient elastic waves by a spherical cavity is treated. Two cases are considered: (a) a suddenly applied normal point load, and (b) the impingement of a plane transient pulse on the cavity. The method used determines the solution only in the shadow zones; that is, those points which cannot be connected to the source of disturbance by straight-line rays. Analytical results are obtained and evaluated for the displacements at the cavity wall.

The analysis is based on the Laplace transform (on time) and the Watson transformation. This well-known transformation makes it possible to convert an infinite series involving a discrete real wave number into one involving a generalized wave number. This leads to transient solutions the components of which have a one-to-one correspondence with the modes of the underlying frequency equation. These solutions have a form convenient for numerical analysis and for obtaining approximate solutions.

The results given here are for the displacements evaluated at the cavity wall. It is found that the behavior of the diffracted wave fronts is similar to that associated with the simpler equations governing scalar diffraction problems (see Friedlander, Sound Pulses, Cambridge, 1958). In both problems the Rayleigh disturbance predominates for long time, being singular at its arrival time in the point load case and non-singular in the plane wave case.

TABLE OF CONTENTS

LIST OF FIGURES

NOMENCLATURE

Latin Symbols

a	a constant
$\mathcal{A}$	see equation (2.2-10)
Ai(z)	Airy function
$A(\nu, \Omega)$	see equation (A.9)
b	a constant
$\mathcal{B}$	see equation (2.2-10)
Bi(z)	Airy function
c	a constant
C	integration contour for inversion of Laplace transform
C_d	dilatation wave speed
C_R	Rayleigh wave speed
C_s	shear wave speed
C_W	integration contour for Watson's transformation
$\mathcal{D}$	see equation (2.2-10)
$\mathcal{E}$	see equation (2.2-10)
f(p)	Laplace transform of F(t)
$f_2(\nu)$	see equation (2.4-9)
$f_3(\nu)$	see equation (3.4-12)
F(t)	a prescribed function of t
$F(\nu, \Omega)$	see equation (2,4-2)
$\mathfrak{F}(\nu, \Omega)$	see equation (3.4-1)
$\mathcal{G}$	see equation (3.2-7)
$\tilde{\mathcal{G}}^*$	see equation (3.4-7)

$h = \frac{p}{C_d}$

h_i a curve in the ν - plane

$H(t)$ Heaviside step-function

$H_\nu^{(1;2)}(\Omega)$ Hankel function of the first or second kind

$I_\nu(z)$ modified Bessel function of the first kind

j mode number

$J_\nu(z)$ Bessel function

J_1 see equation (B. 2)

J_2 see equation (B. 2)

$k = \frac{p}{C_s}$

$K_\nu(z)$ modified Bessel function of the second kind

$m = \frac{C_s}{C_d}$

$\mathcal{M}(\nu)$ see equation (2. 4-2)

n an integer

$\mathcal{N}(\nu)$ see equation (3. 4-1)

p Laplace transform parameter

P a constant

$P_n(\cos\theta)$ Legendre polynomial

q see equation (2. 2-14)

$Q(p)$ see equation (2. 2-14)

r radial coordinate

r_o radius of cavity

R	Rayleigh wave mode designation
s	an integer
$S_{\nu}^{(1,2)}(\Omega)$	see Table A1
$\mathcal{S}$	see equation (3.2-7)
$\tilde{\mathcal{S}}^{*}$	see equation (3.4-8)
t	time
T	dimensionless time
T_2	see equation (2.7-22)
T_3	see equation (2.7-40)
T_4	see equation (2.7-40)
T_5	see equation (3.6-15)
T_6	see equation (3.6-31)
T_7	see equation (3.6-32)
u	general displacement
u_r	Laplace transform of U_r
u_θ	Laplace transform of U_θ
$U_o = \frac{P}{r_o(\lambda+2\mu)}$	normalization constant for displacements
$U_1 = \frac{\tau_o r_o}{\lambda+2\mu}$	normalization constant for displacements
U_r	radial displacement
U_θ	tangential displacement
$v = \frac{\omega r}{C_s}$	dimensionless frequency
w	a complex variable

x	Cartesian coordinate
y	Cartesian coordinate
$y(\theta)$	see equation (2. 7-17)
z	Cartesian coordinate
z	general complex variable
z_j	the zeros of Ai(z)

Greek Symbols

α	see equation (A. 9)
β	coordinate angle
γ	see equation (A. 2)
$\Gamma(z)$	gamma function
$\delta(\theta)$	Dirac delta function
δ_{ij}	Kronecker delta
Δ	see equation (2. 2-12)
ϵ	a small positive constant
ε_{ij}	strain component
ζ_o	root of equation (C. 8)
η	see equation (A. 29)
θ	coordinate angle
κ	lineal wave number
λ	Lamé elastic constant
λ	see equation (A. 2)
μ	Lamé elastic constant
ν	Watson transformation parameter

ν_j	root of $\Delta = 0$
ν_R	Rayleigh root
ν_{1j}	the roots ν_j close to $\nu = \Omega$
ν_{2j}	the roots ν_j close to $\nu = m\Omega$
ξ	see equation (A. 29)
ρ	density
σ	Poisson's ratio
σ_o	imaginary part of ν_R
σ_A	an average value of σ_o
σ_{ij}	Laplace transform of τ_{ij}
τ_{ij}	stress component
φ	Laplace transform of Φ
$\varphi_{\nu-\frac{1}{2}}$	see equations (2.4-12) and (3.4-15)
Φ	scalar displacement potential
$\varphi_o(p)$	Laplace transform of $\Phi_o(p)$
$\Phi_o(t)$	see equations (3.1-2) and (3.1-3)
ψ	Laplace transform of Ψ
$\psi_{\nu-\frac{1}{2}}$	see equations (2.4-13) and (3.4-16)
Ψ	vector displacement potential
$\omega = \pm ip$	angular frequency
$\Omega = \frac{\omega r_o}{C_s}$	dimensionless frequency

Subscripts and Superscripts

$(\ )^{inc}$	incident part of solution
$(\ )^{sc}$	scattered part of solution
$(\tilde{\ }) = (\ )\Big\vert_{n=\nu-\frac{1}{2}}$	
$(\ )^{*}$	see equations (3.4-7) - (3.4-11)
$\overline{(\ )}$	complex conjugate
$(\ )_{o}$	evaluated at $r=r_o$
$(\ )_{R}$	corresponding to the Rayleigh root

CHAPTER 1

INTRODUCTION

The purpose of the present investigation is to analyze the diffraction of a stress pulse by a spherical cavity embedded in an infinite, linear, homogeneous, isotropic, elastic medium. Two cases are considered: (a) a suddenly applied normal point load on the surface of the cavity, and (b) the impingement of a plane transient pulse on the cavity.

The work presented here is based on the results given by several authors for harmonic waves. Nagase (1) treated the case of harmonic elastic waves. For the case of an exterior point source, he obtained the high frequency approximations of the displacements by employing Watson's transformation. A modified Watson transformation will be used here to extend Nagase's results to the case of transient disturbances.

The work of Nussenzveig (2) which treats the case of an acoustic harmonic plane wave has also been important to the present study. To evaluate the high frequency contributions, Nussenzveig used a modified Watson transformation and Poisson's summation formula; he showed that for his problem the two techniques were equivalent. He gave a rigorous proof of Watson's transformation and of the convergence of the residue series which arise from it. In the present work, his findings are used to obtain equivalent information for the case of transient elastic waves.

A further guide in the analytical work for the present spherical problem is the analogous work done by Miklowitz (3, 4) and Peck (5) for the cylindrical cavity. The work of these authors is based on a technique developed by Friedlander (6) for representing a diffracted wave as a sum of its cylindrically propagating components. Their work also developed inversion procedures of double integral transforms (Laplace on time and Fourier on the cylindrical angle) that yielded transient solutions the components of which have a one-to-one correspondence with the modes of the underlying frequency equation. These exact solutions were shown to have a form convenient for numerical analysis and for getting certain approximate solutions. The use of double integral transforms yielded expressions containing two complex variables. In the present work, a Laplace transform on time is used. A spatial transform on θ is not possible, but Watson's transformation supplies the needed tool.

It is of interest to point out that in recent years there has been considerable importance attached to these problems because the point source in the cavity is related to the detection of underground nuclear explosions; and the plane wave case is related to the design of underground structures which will withstand severe ground shock environments (see, for example, Mow's work (7)). However, beyond this, the problems have fundamental significance as two of the most elementary examples of the diffraction of stress waves by a smooth curvilinear boundary. A good discussion of the analogous case of acoustic wave diffraction is given by Levy and Keller (8) for the

cylindrical and spherical cavities.

Following the theme in (3, 4, 5), the formal solutions to the problems in the present investigation are obtained by the Laplace transform on time, residue theory, and contour integration. Evaluation of the solutions is effected through asymptotic approximations of the functions involved. The final expressions are valid in the respective shadow zones of the problems. Expressions valid in the lit region may be found by using the techniques in references (1), (2), and (9).

The procedure for deriving the solutions is as follows: the first step is to apply the Laplace transform and perform a contour integration along the imaginary axis of the transform parameter. This gives formal solutions to the problems which involve the wave frequency. The next step is to introduce Watson's transformation (or Poisson's summation formula (2)) and to determine the roots of the characteristic equation relating frequency and wave number, for the solutions are based on a residue series associated with the poles of these roots. The characteristic equation involves Bessel functions of complex order, the wave number and frequency being the order and argument of these functions, respectively. The roots were approximated by Nagase (10) for large order and large argument. Termwise contour integration over the modes completes the solution.

The geometrical optics of these problems is similar to that of the cylinder; in fact, Figs. 4 and 7 of reference (3) are now the meridional section of the fronts, and the actual fronts are obtained by

rotating them about their axes of symmetry. Hence there is an important new feature: the portions $\theta = 0$ and $\theta = \pi$ of the axis in Fig. 1 are now caustics of the diffracted fronts. Consequently, different representations of the field are required for $0 < \theta < \pi$ and $\theta = 0$ or π.

The results given here are for the displacements evaluated at the cavity wall. It is found that the behavior of the diffracted wave fronts is similar to that associated with the simpler equations governing scalar diffraction problems (6). In both problems the Rayleigh disturbance predominates for long time, being singular at its arrival time in the point load case and non-singular in the plane wave case, in agreement with reference (3). The analytical information on the frequency equation given here could be employed for a more complete evaluation of the response by numerical techniques. Peck (5) devised a scheme for such an evaluation of the diffracted waves. His numerical scheme could be used in the present problems.

It should also be pointed out that the results found here can be extended to the linear viscoelastic case using a correspondence principle as was done in reference (3).

CHAPTER 2

POINT SOURCE ON THE SURFACE OF THE CAVITY

2.1. Statement of the Problem

In a spherical coordinate system, consider a spherical cavity of radius r_o centered at the origin. A normal point load PF(t) is suddenly applied, at time $t=0$, to the cavity wall $r=r_o$ at $\theta=0$ (see Figs. 1 and 2). P is a magnitude constant and F(t) describes the time behavior of the input. The governing wave equations are

$$\nabla^2\Phi=\frac{1}{C_d^2}\cdot\frac{\partial^2\Phi}{\partial t^2}\ , \qquad \nabla^2\vec{\Psi}^*=\frac{1}{C_s}\cdot\frac{\partial^2\vec{\Psi}^*}{\partial t^2}\ , \tag{2.1-1}$$

where $\vec{\Psi}^*=\Psi\vec{e}_\beta$. The potentials Φ and Ψ are related to the displacements through

$$\vec{U}=\nabla\Phi+\nabla\times\vec{\Psi}^* \tag{2.1-2}$$

where ∇^2 is the Laplacian spherical operator,

$$\nabla^2\Phi=\frac{1}{r^2}\cdot\frac{\partial}{\partial r}\left(r^2\frac{\partial\Phi}{\partial r}\right)+\frac{1}{r^2\sin\theta}\cdot\frac{\partial}{\partial\theta}\left(\sin\theta\frac{\partial\Phi}{\partial\theta}\right)+\frac{1}{r^2\sin^2\theta}\cdot\frac{\partial^2\Phi}{\partial\beta^2}\ ,$$

C_d and C_s are the dilatational and equivoluminal body wave speeds respectively, and are defined by $C_d^2=\frac{\lambda+2\mu}{\rho}$ and $C_s^2=\mu/\rho$, where λ and μ are the Lame constants, and ρ is the material density.

In spherical coordinates the stress-strain relations needed in the sequel are as follows:

$$\tau_{ij} = \lambda \nabla^2 \Phi \delta_{ij} + 2\mu \varepsilon_{ij} \tag{2.1-3}$$

where

$$\varepsilon_{rr} = \frac{\partial U_r}{\partial r}, \qquad \varepsilon_{r\theta} = \left(\frac{\partial U_\theta}{\partial r} - \frac{U_\theta}{r} + \frac{1}{r} \cdot \frac{\partial U_r}{\partial \theta}\right)\frac{1}{2} \tag{2.1-4}$$

The boundary conditions (at $r=r_o$) for the problem are

$$\left.\begin{aligned} \tau_{rr}(r_o, \theta, t) &= -\frac{P F(t) \delta(\theta)}{2\pi r_o^2 \sin\theta}, \\ \tau_{r\theta}(r_o, \theta, t) &= 0 \end{aligned}\right\} \tag{2.1-5}$$

where $\delta(\theta)$ is the Dirac delta function. The potentials Φ and Ψ (and hence the displacements and stresses) are required to vanish as $r \to \infty$, that is,

$$\lim_{r \to \infty} (\Phi, \Psi, U_r, U_\theta, \text{etc.}) = 0 . \tag{2.1-6}$$

The initial conditions are taken as

$$\Phi(r,\theta,0) = \Psi(r,\theta,0) = \frac{\partial \Phi(r,\theta,0)}{\partial t} = \frac{\partial \Psi(r,\theta,0)}{\partial \theta} = 0 \tag{2.1-7}$$

representing quiescence at $t=0$.

2.2. Formal Solution

Here the Laplace transform of a quantity will be denoted by a small case letter*, for example,

$$\phi = \mathcal{L}\{\Phi\} = \int_0^\infty \Phi\, e^{-pt}\, dt, \quad \Phi = \frac{1}{2\pi i}\int_{Br_1} \phi\, e^{pt}\, dp \ , \qquad (2.2\text{-}1)$$

where p is the Laplace transform parameter and Br_1 is the well-known contour in the right half of the p-plane.

Application of the transform to equations (2.1-1) using (2.1-7) gives

$$\nabla^2\phi = \frac{p^2}{C_d^2}\phi, \quad \nabla^2\chi = \frac{p^2}{C_s^2}\chi \ , \qquad \psi = \frac{\partial \chi}{\partial \theta} \ . \qquad (2.2\text{-}2)$$

A solution of (2.2-2) satisfying the transform of (2.1-6) is given by

$$\phi = \sum_{n=0}^{\infty} A_n \frac{K_{n+1/2}(hr)}{\sqrt{hr}} P_n(\cos\theta), \quad \psi = \sum_{n=0}^{\infty} B_n \frac{K_{n+1/2}(kr)}{\sqrt{kr}} \cdot \frac{dP_n(\cos\theta)}{d\theta}, \qquad (2.2\text{-}3)$$

where $h = p/C_d$, $k = p/C_s$, $K_{n+1/2}(z)$ is the modified Bessel function of the second kind of order $n + 1/2$, and $P_n(\cos\theta)$ is the Legendre polynomial of order n.

---

* Except for $\sigma_{ij} = \mathcal{L}\{\tau_{ij}\}$.

Since

$$K_{1/2}(z)=\left(\frac{\pi}{2z}\right)^{1/2}e^{-z}, \quad K_{\nu+1}=\frac{\nu}{z}K_{\nu}-\frac{dK_{\nu}}{dz}, \tag{2.2-4}$$

$K_{n+\frac{1}{2}}(z)$ may be expressed as

$$K_{n+\frac{1}{2}}(z)=\left(\frac{\pi}{2z}\right)^{1/2}e^{-z}\sum_{s=0}^{n}\frac{\Gamma(1+n+s)}{s!\,\Gamma(1+n-s)}(2z)^{-s} \tag{2.2-5}$$

where $\Gamma(x)$ is the gamma function. Clearly

$$\frac{K_{n+1/2}(z)}{\sqrt{z}} \tag{2.2-6}$$

does not have a branch point at $z = 0$.

The transforms of equations (2.1-2)-(2.1-4) may be written as

$$\left.\begin{aligned} &u_r=\frac{\partial\phi}{\partial r}+\frac{1}{r\sin\theta}\frac{\partial}{\partial\theta}(\sin\theta\,\psi), \quad u_\theta=\frac{1}{r}\frac{\partial\phi}{\partial\theta}-\frac{1}{r}\frac{\partial}{\partial r}(r\psi),\\ &e_{rr}=\frac{\partial u_r}{\partial r}, \quad \nabla^2\phi=\frac{p^2}{c_d^2}\phi, \quad e_{r\theta}=\frac{1}{2}\left(\frac{\partial u_\theta}{\partial r}-\frac{u_\theta}{r}+\frac{1}{r}\frac{\partial u_r}{\partial\theta}\right),\\ &\sigma_{rr}=\lambda h^2\phi+2\mu e_{rr}, \quad \sigma_{r\theta}=2\mu e_{r\theta}. \end{aligned}\right\} \tag{2.2-7}$$

Using the relations

$$-\frac{P\,f(p)\,\delta(\theta)}{2\pi r_o^2\sin\theta}=\sum_{n=0}^{\infty}Q(p)\,(2n+1)P_n(\cos\theta), \quad Q(p)=-\frac{P\,f(p)}{4\pi r_o^2},$$

the boundary conditions are transformed into

$$\sigma_{rr}(r_o, \theta, p) = Q(p) \sum_{n=0}^{\infty} (2n+1) P_n(\cos\theta), \quad \sigma_{r\theta}(r_o, \theta, p) = 0 . \qquad (2.2\text{-}8)$$

By (2.2-3), (2.2-7),

$$\sigma_{rr} = \sum_{n=0}^{\infty} \left[A_n \mathcal{A} + B_n \mathcal{B} \right] P_n(\cos\theta), \quad \sigma_{r\theta} = \mu \sum_{n=0}^{\infty} \left[A_n \mathcal{D} + B_n \mathcal{E} \right] \frac{dP_n(\cos\theta)}{d\theta}, \qquad (2.2\text{-}9)$$

where

$$\left.\begin{aligned} \mathcal{A} &= \frac{K_{n+1/2}(hr)}{\sqrt{hr}} \left\{ k^2 + 2\frac{n(n+1)}{r^2} \right\} \mu - \frac{4\mu}{r} \frac{d}{dr} \left(\frac{K_{n+1/2}(hr)}{\sqrt{hr}} \right), \\ \mathcal{B} &= -2\mu n(n+1) \frac{d}{dr} \left(\frac{1}{r} \frac{K_{n+1/2}(kr)}{\sqrt{kr}} \right), \quad \mathcal{D} = 2 \frac{d}{dr} \left(\frac{1}{r} \cdot \frac{K_{n+1/2}(hr)}{\sqrt{hr}} \right), \\ \mathcal{E} &= \frac{2}{r} \cdot \frac{d}{dr} \left(\frac{K_{n+1/2}(kr)}{\sqrt{kr}} \right) + \frac{K_{n+1/2}(kr)}{\sqrt{kr}} \left\{ \frac{2 - 2n(n+1)}{r^2} - k^2 \right\} . \end{aligned}\right\} \qquad (2.2\text{-}10)$$

The application of (2.2-8) to (2.2-9) yields

$$\left.\begin{aligned} \sum_{n=0}^{\infty} \left[A_n \mathcal{A}_o + B_n \mathcal{B}_o \right] P_n(\cos\theta) &= \sum_{n=0}^{\infty} Q(p)(2n+1) P_n(\cos\theta), \\ \sum_{n=0}^{\infty} \left[A_n \mathcal{D}_o + B_n \mathcal{E}_o \right] \frac{dP_n(\cos\theta)}{d\theta} &= 0, \end{aligned}\right\} \qquad (2.2\text{-}11)$$

in which $\mathcal{A}_o = \mathcal{A} \,/_{r=r_o}$, etc. Solving for A_n and B_n, one obtains

$$\left.\begin{aligned} A_n &= Q(p) \frac{(2n+1)}{\Delta(r_o, p, n)} \mathcal{E}_o , \quad B_n = - A_n \frac{\mathcal{D}_o}{\mathcal{E}_o}, \\ \Delta(r_o, p, n) &= \mathcal{A}_o \mathcal{E}_o - \mathcal{B}_o \mathcal{D}_o . \end{aligned}\right\} \qquad (2.2\text{-}12)$$

Substitution of (2. 2-12) into (2. 2-3) gives

$$\left.\begin{aligned} \phi &= Q(p)\sum_{n=0}^{\infty}(2n+1)\frac{\mathcal{E}_o}{\Delta(r_o,p,n)}\cdot\frac{K_{n+1/2}(hr)}{\sqrt{hr}}P_n(\cos\theta) \\ \psi &= -Q(p)\sum_{n=0}^{\infty}(2n+1)\frac{\mathcal{D}_o}{\Delta(r_o,p,n)}\cdot\frac{K_{n+1/2}(kr)}{\sqrt{kr}}\cdot\frac{dP_n(\cos\theta)}{d\theta} \end{aligned}\right\} \quad (2.2\text{-}13)$$

Clearly, in view of (2. 2-5), except for possible branch points of Q(p), ϕ and ψ are meromorphic functions of p in the whole p-plane. For the special case of a delta function in time,

$$F(t) = \delta(t)\ , \qquad Q(p) = -\frac{P\,f(p)}{4\pi r_o^2} = \frac{-P}{4\pi r_o^2} = q\ ; \qquad (2.2\text{-}14)$$

for a step function in time,

$$F(t) = H(t)\ , \qquad Q(p) = \frac{q}{p} \qquad (2.2\text{-}15)$$

Convergence of the Series. It seems appropriate to consider now the convergence of (2. 2-13) for p on the Bromwich contour Re p = c>0, $-R \leq \text{Im } p \leq R$, $R \to \infty$. The potential functions ϕ and ψ are assumed to be analytic on the contour. Select the compact subset of the Bromwich contour given by Re p = c > 0, $-R < -Y \leq \text{Im } p \leq Y < R$, and recall the inequalities

$$\left|P_n(\cos\theta)\right| \leq 1, \qquad \left|\frac{dP_n(\cos\theta)}{d\theta}\right| \leq n^2\ .$$

Then, by writing

$$\phi = \sum_{n=0}^{\infty} \phi_n \quad , \qquad \psi = \sum_{n=0}^{\infty} \psi_n \, , \tag{2.2-16}$$

one sees that for large n

$$|\phi_n| \sim \frac{r_0^2}{4\mu} \left(\frac{r_0}{r}\right)^{n+1} e^{-c(r-r_0)} \left| P_n(\cos\theta) \right| ,$$

$$|\psi_n| \sim \frac{r_0^2}{4\mu} \left(\frac{r_0}{r}\right)^{n+1} \frac{e^{-c(r-r_0)}}{n} \left| \frac{dP_n(\cos\theta)}{d\theta} \right| ,$$

independently of Im p. Therefore, for $0 \leq \theta \leq \pi$, $r \geq r_0 + \epsilon$, $\epsilon > 0$, the series in (2.2-13) converge uniformly on the Bromwich contour.

2.3. Exact Inversion

Since the series are uniformly convergent on the Bromwich contour, the Laplace transforms in (2.2-13) may be inverted by term-wise integration. Alternatively, these transforms may be inverted by integrating along a contour equivalent to the Bromwich contour. One such contour will now be determined.

For the present case, selecting $F(t) = H(t)$, the Bromwich contour $\mathrm{Re}\, p = c > 0$, $-R \leq \mathrm{Im}\, p \leq R$, $R \to \infty$, is completed down the imaginary axis, as shown in Figure 3, by the contour $C + C_R + C_{-R}$, where $C = C_U + C_L + C_0$. This selection is inherent in the foregoing analysis since it takes p through its physical values. No branch cuts are required*.

---

* A cut at the origin was required in the cylindrical case.

The singularities of (2. 2-13) can come only from the vanishing of $\Delta(r_o, p, n)$ and from the character of $Q(p)$. Poles in the right half-plane are ruled out by the boundedness in time requirement of the solution.

On the basis of the previous discussion and the Cauchy-Goursat theorem, the solution to the problem is given by

$$\begin{Bmatrix} \Phi \\ \Psi \end{Bmatrix} = \frac{1}{2\pi i} \int_{Br_1} \begin{Bmatrix} \phi \\ \psi \end{Bmatrix} e^{pt} dp = \frac{1}{2\pi i} \int_{C+C_R+C_{-R}} \begin{Bmatrix} \phi \\ \psi \end{Bmatrix} e^{pt} dp, \qquad (2.3\text{-}1)$$

where the paths of integration are shown in Figure 3. For large p,

$$\phi_n \sim \frac{1}{p^3} \exp[-h(r-r_o)],$$

$$\psi_n \sim \frac{1}{p^5} \exp[-k(r-r_o)]$$

where ϕ_n and ψ_n were defined by the expressions (2. 2-16). Consequently the integrands of (2. 3-1) vanish uniformly on C_R and C_{-R} as $R \to \infty$ and, therefore, the above expression for the potentials reduces to

$$\begin{Bmatrix} \Phi \\ \Psi \end{Bmatrix} = \frac{1}{2\pi i} \int_{C} \begin{Bmatrix} \phi \\ \psi \end{Bmatrix} e^{pt} dp = \frac{1}{2\pi i} \int_{Br_1} \begin{Bmatrix} \phi \\ \psi \end{Bmatrix} e^{pt} dp \qquad (2.3\text{-}2)$$

and thus it has been shown that the path C is <u>equivalent</u> to the Bromwich contour.

Since for real

$$\frac{K_{n+1/2}(-i\Omega)}{(-i\Omega)^{1/2}} = \overline{\left[\frac{K_{n+1/2}(i\Omega)}{(i\Omega)^{1/2}}\right]}, \qquad (2.3\text{-}3)$$

where the vinculum indicates the complex conjugate, then, by (2.2-10), (2.2-12), and (2.2-13),

$$\left\{\begin{matrix}\Phi\\ \Psi\end{matrix}\right\}_{p=-i\omega} = \overline{\left\{\begin{matrix}\Phi\\ \Psi\end{matrix}\right\}_{p=i\omega}} \tag{2.3-4}$$

and

$$\left.\begin{aligned}\left\{\begin{matrix}\Phi_1\\ \Psi_1\end{matrix}\right\} &= \frac{1}{2\pi i}\int_{C_v+C_L}\left\{\begin{matrix}\Phi\\ \Psi\end{matrix}\right\}e^{pt}\,dp,\\ &= \frac{1}{2\pi i}\int_0^{\infty i}\left\{\begin{matrix}\Phi\\ \Psi\end{matrix}\right\}_{p=i\omega}e^{i\omega t}\,d(i\omega) + \frac{1}{2\pi i}\int_{-i\infty}^{0}\left\{\begin{matrix}\Phi\\ \Psi\end{matrix}\right\}_{p=-i\omega}e^{-i\omega t}\,d(-i\omega)\end{aligned}\right\} \tag{2.3-5}$$

or

$$\left\{\begin{matrix}\Phi_1\\ \Psi_1\end{matrix}\right\} = \frac{Re}{\pi}\int_0^{\infty}\left\{\begin{matrix}\Phi\\ \Psi\end{matrix}\right\}_{p=i\omega}e^{i\omega t}\,d\omega, \tag{2.3-6}$$

in which

$$\left.\begin{aligned}\Phi\Big|_{i\omega} &= Q(i\omega)\sum_{n=0}^{\infty}(2n+1)\frac{\mathcal{E}_0|_{p=i\omega}}{\Delta(r_0,i\omega,n)}\cdot\frac{K_{n+1/2}\left(\frac{i\omega}{C_d}r\right)}{\left(\frac{i\omega r}{C_d}\right)^{1/2}}P_n(\cos\theta),\\ \Psi\Big|_{i\omega} &= -Q(i\omega)\sum_{n=0}^{\infty}(2n+1)\frac{\mathcal{D}_0|_{p=i\omega}}{\Delta(r_0,i\omega,n)}\cdot\frac{K_{n+1/2}\left(\frac{i\omega r}{C_s}\right)}{\left(\frac{i\omega r}{C_s}\right)^{1/2}}\cdot\frac{dP_n(\cos\theta)}{d\theta}.\end{aligned}\right\} \tag{2.3-7}$$

In the rest of the chapter, reference will be made to these expressions as the partial-wave expansions for $\Phi\Big|_{i\omega}$ and $\Psi\Big|_{i\omega}$. The subscript $i\omega$ is henceforth deleted.

2.4. Watson's Transformation

It has long been known that for harmonic wave diffraction by spheres and circular cylinders the Fourier series type of solution converges increasingly slowly as the frequency is increased. The number of terms one must keep in the partial-wave expansions is of the order of $\frac{\omega r_0}{c_s} >> 1$, so that (2.3-7) becomes useless at high frequencies. However, since high frequency is associated with short time through integral transform theory, it is necessary to estimate the values of Φ and Ψ for large ω .

It was discovered that the convergence could be resolved by changing the form of the solution through the use of Watson's transformation (2, 8, 11, 12) or of Poisson's summation formula (2, 5, 13, 14). Here it is shown that these two techniques are equivalent for the present problem.

(a) Watson's Transformation. This transformation is based upon the following formula:

$$\sum_{n=0}^{\infty} f(n+1/2) = \frac{1}{2}\int_{C_W} f_0(\nu)\,\frac{\exp(-i\pi\nu)}{\cos\pi\nu}\,d\nu, \qquad (2.4\text{-}1)$$

where C_W is the contour shown in Figure 4. This formula may easily be checked by evaluating the residues at $\nu = n + 1/2$.

$f_0(\nu)$ must be such that it reproduces $f(n + 1/2)$ at $\nu = n + 1/2$ and be regular in a neighborhood of the real axis; thus the integral may be computed by residue theory. In practice the choice of $f_0(\nu)$ is dictated by the requirement of appropriate behavior at infinity in

the ν -plane, since the next step in Watson's transformation will be to deform the contour C_W away from the real axis.

Before writing the particular form of the Watson transformation to be used in the problem, it is convenient to introduce the notation

$$\left.\begin{aligned} m=\frac{c_s}{c_d}=\left(\frac{1-2\sigma}{2-2\sigma}\right)^{1/2}, \quad \Omega=\frac{\omega r_o}{c_s} \quad , \quad v=\frac{\omega r}{c_s}, \\ F(\nu,\Omega)=\frac{d}{d\Omega}\left(\ln H_\nu^{(2)}(\Omega)\right), \quad \mathcal{M}(\nu)=\frac{\pi}{2i}\, e^{-i\frac{\pi\nu}{2}}, \\ \tilde{\mathcal{S}}=\mathcal{S}\Big|_{n=\nu-1/2}, \end{aligned}\right\} \quad (2.4\text{-}2)$$

where $\mathcal{S}=\mathcal{A}, \mathcal{B}, \mathcal{D}, \mathcal{E}$ and $H_\nu^{(2)}(\Omega)$ is the Hankel function of the second kind.

With this notation and the relation

$$K_\nu(e^{i\pi/2}\Omega)=\mathcal{M}(\nu)\, H_\nu^{(2)}(\Omega), \quad (2.4\text{-}3)$$

one immediately finds that

$$\frac{r^2(mve^{i\pi/2})^{1/2}}{\mu\,\mathcal{M}(\nu)}\cdot\frac{\tilde{\mathcal{A}}}{H_\nu^{(2)}(mv)}=\left(\frac{3+4\nu^2}{2}-v^2\right)-4mvF(\nu,mv), \quad (2.4\text{-}4)$$

$$\frac{r^2(ve^{i\pi/2})^{1/2}}{\mu\,\mathcal{M}(\nu)}\cdot\frac{\tilde{\mathcal{B}}}{H_\nu^{(2)}(v)}=-\left(\nu^2-\tfrac{1}{4}\right)\left(2vF(\nu,v)-3\right), \quad (2.4\text{-}5)$$

$$\frac{r^2(mve^{i\pi/2})^{1/2}}{\mathcal{M}(\nu)}\cdot\frac{\tilde{\mathcal{D}}}{H_\nu^{(2)}(mv)}=2mvF(\nu,mv)-3, \quad (2.4\text{-}6)$$

$$\frac{r^2(\nu e^{i\pi/2})^{1/2}}{\mathcal{M}(\nu)}\cdot\frac{\tilde{\xi}}{H_\nu^{(2)}(\nu)} = 2\nu F(\nu,\nu)+\left(\frac{3-4\nu^2}{2}+\nu^2\right), \tag{2.4-7}$$

$$\frac{\Delta(r_0,i\omega,\nu-1/2)}{H_\nu^{(2)}(\Omega)H_\nu^{(2)}(m\Omega)} = \frac{4\sqrt{m}\,\mu\mathcal{M}^2(\nu)\Omega(\nu^2-9/4)}{r_0^4\,e^{i\pi/2}}\,f_2(\nu), \tag{2.4-8}$$

and

$$f_2(\nu) = -\frac{\nu^2-1/4}{m\Omega^2}\left(1-\frac{\Omega^2}{2(\nu^2-9/4)}\right)^2+\left\{F(\nu,m\Omega)-\frac{1}{2m\Omega}\left(1+\frac{\Omega^2}{\nu^2-9/4}\right)\right\}\times \tag{2.4-9}$$
$$\times\left\{F(\nu,\Omega)+\frac{1}{2\Omega}\left(1-\frac{2\Omega^2}{\nu^2-9/4}\right)\right\}.$$

On applying formula (2.4-1) to the expressions for ϕ and ψ, and using the relation $P_n(\cos\theta) = \exp(i\pi n)\,P_n(-\cos\theta)$, one obtains

$$\left.\begin{aligned}\phi &= Q(i\omega)\int_{C_W}\nu\,\frac{\phi_{\nu-1/2}(r_0,r,\nu-1/2)}{\Delta(r_0,i\omega,\nu-1/2)}P_{\nu-1/2}(\cos\theta)\,\frac{\exp(-i\pi\nu)}{\cos\nu\pi}\,d\nu,\\ \psi &= Q(i\omega)\int_{C_W}\nu\,\frac{\psi_{\nu-1/2}(r_0,r,\nu-1/2)}{\Delta(r_0,i\omega,\nu-1/2)}\cdot\frac{dP_{\nu-1/2}(\cos\theta)}{d\theta}\cdot\frac{\exp(-i\pi\nu)}{\cos\nu\pi}\,d\nu,\end{aligned}\right\} \tag{2.4-10}$$

or

$$\left.\begin{aligned}\phi &= \frac{Q(i\omega)}{i}\int_{C_W}\frac{\phi_{\nu-1/2}(r_0,r,\nu-1/2)}{\Delta(r_0,i\omega,\nu-1/2)}P_{\nu-1/2}(-\cos\theta)\,\frac{\nu\,d\nu}{\cos\nu\pi},\\ \psi &= \frac{Q(i\omega)}{i}\int_{C_W}\frac{\psi_{\nu-1/2}(r_0,r,\nu-1/2)}{\Delta(r_0,i\omega,\nu-1/2)}\cdot\frac{dP_{\nu-1/2}(-\cos\theta)}{d\theta}\cdot\frac{\nu\,d\nu}{\cos\nu\pi},\end{aligned}\right\} \tag{2.4-11}$$

where

$$\phi_{\nu-1/2}(r_0, r, \nu-1/2) = \tilde{\mathcal{E}}_0 \frac{\mathcal{M}(\nu) H_\nu^{(2)}(m\nu)}{(m\nu e^{i\pi/2})^{1/2}}, \tag{2.4-12}$$

$$\psi_{\nu-1/2}(r_0, r, \nu-1/2) = -\tilde{\mathcal{D}}_0 \frac{\mathcal{M}(\nu) H_\nu^{(2)}(\nu)}{(\nu e^{i\pi/2})^{1/2}}. \tag{2.4-13}$$

(b) Poisson's Sum. For the present problem Poisson's summation formula (2) may be written as

$$\sum_{n=0}^{\infty} f(n+1/2) = \sum_{s=-\infty}^{\infty} (-1)^s \int_0^\infty f(\nu) \exp(2\pi i s \nu)\, d\nu.$$

The application of this formula to the partial-wave expansions for ϕ and ψ yields

$$\phi = \frac{2Q(i\omega)}{i} \sum_{s=-\infty}^{\infty} (-1)^s \int_0^\infty \nu \frac{\phi_{\nu-1/2}(r_0, r, \nu-1/2)}{\Delta(r_0, i\omega, \nu-1/2)} P_{\nu-1/2}(\cos(\pi-\theta)) \exp[i\pi\nu(2s+1)]\, d\nu$$

$$\psi = \frac{2Q(i\omega)}{i} \sum_{s=-\infty}^{\infty} (-1)^s \int_0^\infty \nu \frac{\psi_{\nu-1/2}(r_0, r, \nu-1/2)}{\Delta(r_0, i\omega, \nu-1/2)} \cdot \frac{dP_{\nu-1/2}(\cos(\pi-\theta))}{d\theta} \exp[i\pi\nu(2s+1)]\, d\nu$$

By substituting $-\nu$ for $+\nu$ in the integrals corresponding to the sum from s = - 1 to $-\infty$ and using the identities

$$P_{-\lambda-1/2}(\cos(\pi-\theta)) = P_{\lambda-1/2}(\cos(\pi-\theta)), \tag{2.4-14}$$

$$H^{(2)}_{-\nu}(\Omega) = e^{-\nu\pi i} H^{(2)}(\Omega) \quad , \tag{2.4-15}$$

the above expressions become

$$\left.\begin{aligned} \phi &= \frac{2Q(i\omega)}{i} \sum_{s=0}^{\infty} (-1)^s \int_{-\infty}^{\infty} \nu \frac{\phi_{\nu-1/2}}{\Delta} P_{\nu-1/2}(\cos(\pi-\theta)) \exp\left[i\pi\nu(2s+1)\right] d\nu \\ \psi &= \frac{2Q(i\omega)}{i} \sum_{s=0}^{\infty} (-1)^s \int_{-\infty}^{\infty} \nu \frac{\psi_{\nu-1/2}}{\Delta} \cdot \frac{dP_{\nu-1/2}(\cos(\pi-\theta))}{d\theta} \exp\left[i\pi\nu(2s+1)\right] d\nu . \end{aligned}\right\} \tag{2.4-16}$$

Figure 5 shows the path of integration for these expressions.

This result may be shown to be equivalent to (2.4-10) and (2.4-11) as follows: by (2.4-14) and (2.4-15), the integrands of (2.4-10) and (2.4-11) are odd functions of ν, so that the lower half of the contour C_W may be replaced by its reflection about the origin (see dashed line in Fig. 4). This contour and the upper half of C_W is equivalent to the straight line D located above the real axis and on which the expansion

$$\frac{1}{\cos\nu\pi} = 2\sum_{s=0}^{\infty} (-1)^s \exp\left[i\pi\nu(2s+1)\right] \tag{2.4-17}$$

is valid. Substitution of this result in (2.4-11) gives (2.4-16).

2.5. The Zeros of $\Delta(r_o, i\omega, \nu - 1/2)$

To deform the path of integration in (2.4-10), (2.4-11) and (2.4-16), away from the real axis, it is necessary to know the singularities of the integrands as functions of ν. The integrands are meromorphic functions of ν and their poles are the zeros of $\cos \nu\pi$ and of $\Delta(r_o, i\omega, \nu - 1/2)$.

The behavior of the roots of Δ for large values of Ω is needed for the short-time solution. The required asymptotic expansions for the Hankel functions are given in Appendix A. These expansions are used in Appendix B to determine the properties of the function $F(\nu, \Omega)$ defined in (2.4-2).

Nagase (10) found that the zeros of Δ are equivalent to the zeros of $f_2(\nu)$, equation (2.4-9). He also found, analogous to the case of the cylindrical cavity (5), that there exist three groups of zeros of the first order in the fourth quadrant of the ν-plane and no zeros lie on the real or imaginary axes*; the zeros in the second quadrant are merely the negative of those in the fourth quadrant. Only the first approximations are given below because they are satisfactory for wave-front expansions.

As indicated above, and just as in the case of the cylindrical cavity (5, 4), for $\Omega >> 1$ the roots split into three types. First, an infinite set of shear type roots lying asymptotically along the curve

---

* The real value obtained for the Rayleigh root comes from the imperfection of the approximations used.

h_{2s} in Fig. 6. This curve starts from $\nu = \Omega$, makes an angle of $-\pi/3$ with the positive real axis and goes off to $-i\infty$. The first several zeros, which are of the greatest physical importance here, are given by

$$\nu_{1j} \sim \Omega + 2^{-1/3} e^{\frac{5\pi i}{3}} (e^{-i\pi} z_j) \Omega^{1/3} + O(\Omega^0), \quad j = 1, 2, 3, \ldots .$$

The second type is an infinite set of dilatational type lying asymptotically along the curve h_{2d} in Figure 6 (the zeros of $H_\nu^{(2)}(m\Omega)$ lie asymptotically along this curve). The first several zeros are given by

$$\nu_{2j} \sim m\Omega + 2^{-1/3} e^{\frac{5\pi i}{3}} (e^{-i\pi} z_j) (m\Omega)^{1/3} + O(\Omega^0), \quad j = 1, 2, 3, \ldots .$$

And third, a single root of the Rayleigh type

$$\nu_R \sim \frac{C_S}{C_R} \Omega + O(\Omega^0) ,$$

where the imaginary part of ν_R vanishes exponentially as $\Omega \to \infty$. The z_j are the roots of $Ai(z) = 0$, which are real and negative, where $Ai(z)$ is the Airy function, and C_R is the Rayleigh surface wave speed. The imaginary part of ν_R is of the form

$$\mathrm{Im}\, \nu_R \sim -a\Omega e^{-b\Omega} , \qquad a, b > 0,$$

just as in the cylindrical case. In Appendix C the expressions for a and b are given. These expressions differ from those appearing in (10).

Clearly, even though the frequency equations in the cylindrical and in the spherical case are different, the first approximations to the roots given here are the complex conjugate of the roots given by formulas (3.8), (3.9), and the first of page 34 in Peck's work for the cylindrical case (5). In fact, if $H_\nu^{(1)}(\Omega)$ were used here instead of $H_\nu^{(2)}(\Omega)$, then the first approximate values of the roots would be identical in the two cases.

Thus it is seen that for large $|\nu|$, vanishingly small imaginary part, and large ω, there is a limiting real root $\nu_R = \kappa_R r_o = \frac{\omega r_o}{C_R}$ (κ being the wave number) corresponding to the Rayleigh surface wave on the half-space. This result follows logically since $\nu_R = \kappa_R r_o \to \infty$ can be interpreted as $\kappa_R \to \infty$ for fixed r_o; hence this very short wave "does not see the curvature". One would expect, therefore, as Miklowitz (3, 4) has shown for the cylindrical case, that this root would yield the predominant disturbance in the long time solution for the present transient problem.

2.6. The Residue Series

In section 2.4, Watson's transformation and Poisson's summation formula were applied to the series for $\varphi|_{i\omega}$ and $\psi|_{i\omega}$ which converge very slowly for large ω. The next step in the solution is to determine the conditions under which the expressions (2.4-11) and the integrals in (2.4-16) may be reduced to a series of residues evaluated at the zeros of $\Delta(r_o, i\omega, \nu-\frac{1}{2})$. This is done

by considering a sequence of paths C_n, shown in Fig. 5, which passes between these zeros and is such that

$$\lim_{n\to\infty} \int_{C_n} f(r,\theta;\nu, s)\, d\nu = 0 \qquad (2.6\text{-}1)$$

where $f(r,\theta;\nu, s)$ is a generic expression for the integrands of (2.4-16). Here the analysis is much simpler than that given by Nussenzveig (2), and leads to the same conclusions when applied to the problem treated there. Instead of the asymptotic expansions employed in (2), the power series

$$H_\nu^{(2)}(z) = -\frac{1}{i\pi}\left[\sum_{s=0}^{\infty}\frac{\Gamma(\nu-s)}{s!}\left(\frac{z}{2}\right)^{2s-\nu} + e^{i\nu\pi}\sum_{s=0}^{\infty}\frac{\Gamma(-\nu-s)}{s!}\left(\frac{z}{2}\right)^{2s+\nu}\right]$$

is used here. This expansion is valid for all ν and z.

On C_n, the dominant terms of $H_\nu^{(2)}(z)$ are

$$\frac{i}{\sin\nu\pi}\left[\frac{\left(\frac{z}{2}\right)^{-\nu}}{\Gamma(1-\nu)} - \exp(\nu\pi i)\frac{\left(\frac{z}{2}\right)^{\nu}}{\Gamma(1+\nu)}\right], \qquad (2.6\text{-}2)$$

where the second term in the brackets is significant only in the neighborhood of the imaginary axis. Therefore

$$\nu\frac{\phi_{\nu-1/2}(r_o,r,\nu-1/2)}{\Delta(r_o,i\omega,\nu-1/2)} \sim \frac{r_o^2}{4\mu\nu}\left(\frac{r_o}{r}\right)^{1/2}\left[\left(\frac{r_o}{r}\right)^{\nu} \text{ or } \left(\frac{r}{r_o}\right)^{\nu}\right],$$

$$\nu\frac{\psi_{\nu-1/2}(r_o,r,\nu-1/2)}{\Delta(r_o,i\omega,\nu-1/2)} \sim \frac{r_o^2}{4\mu\nu^3}\left(\frac{r_o}{r}\right)^{1/2}\left[\left(\frac{r_o}{r}\right)^{\nu} \text{ or } \left(\frac{r}{r_o}\right)^{\nu}\right], \qquad (2.6\text{-}3)$$

where the second term in each bracket is valid close to the imaginary axis.

From Appendix D, for $0<\theta<\pi$,

$$P_{\nu-\frac{1}{2}}(\cos(\pi-\theta)) \sim (2\pi\nu\sin\theta)^{-\frac{1}{2}} \exp\left[-i\nu(\pi-\theta)+\frac{i\pi}{4}\right] \tag{2.6-4}$$

on C_n, and therefore

$$\left.\begin{aligned} &P_{\nu-\frac{1}{2}}(\cos(\pi-\theta))\exp i\pi\nu(2s+1) \sim (2\nu\pi\sin\theta)^{-\frac{1}{2}} \exp\left[i\nu(2\pi s+\theta)\right] \\ &\frac{dP_{\nu-\frac{1}{2}}(\cos(\pi-\theta))}{d\theta}\exp i\pi\nu(2s+1) \sim i\nu(2\pi\nu\sin\theta)^{-\frac{1}{2}}\exp\left[i\nu(2\pi s+\theta)\right]. \end{aligned}\right\} \tag{2.6-5}$$

Since the paths of integration avoid the singularities of the integrands, the application of Jordan's lemma gives

$$\lim_{n\to\infty}\int_{C_n} f(r,\theta;\nu,s)\,d\nu = 0 \tag{2.6-6}$$

for all θ, $0<\theta<\pi$. Also, since $P_{\nu-\frac{1}{2}}(1) = 1$, it is easily verified that all of the above results remain true if $\theta = \pi$. Near $\theta = 0$, however, the equations (2.4-16) can no longer be employed, for $P_{\nu-\frac{1}{2}}(\cos(\pi-\theta))$ has a logarithmic singularity at this point.

In view of the foregoing discussion, it follows that the integrals in (2.4-16) can be written as

$$I(r,\theta;s)=\int_{-\infty}^{\infty}\frac{\phi_{\nu-1/2}(r_0,r,\nu-1/2)}{\Delta(r_0,i\omega,\nu-1/2)}P_{\nu-1/2}(\cos(\pi-\theta))\exp\left[i\pi\nu(2s+1)\right]\nu\,d\nu$$

$$=2\pi i\sum_{\nu_j}\left\{\frac{\phi_{\nu-1/2}}{\partial\Delta/\partial\nu}P_{\nu-1/2}(\cos(\pi-\theta))\exp\left[i\pi\nu(2s+1)\right]\nu\right\}_{\nu=\nu_j},\qquad(2.6\text{-}7)$$

$$II(r,\theta,s)=\int_{-\infty}^{\infty}\frac{\psi_{\nu-1/2}(r_0,r,\nu-1/2)}{\Delta(r_0,i\omega,\nu-1/2)}\cdot\frac{dP_{\nu-1/2}(\cos(\pi-\theta))}{d\theta}\exp\left[i\pi\nu(2s+1)\right]d\nu$$

$$=2\pi i\sum_{\nu_j}\left\{\frac{\psi_{\nu-1/2}}{\partial\Delta/\partial\nu}\cdot\frac{dP_{\nu-1/2}(\cos(\pi-\theta))}{d\theta}\exp\left[i\pi\nu(2s+1)\right]\nu\right\}_{\nu=\nu_j},\qquad(2.6\text{-}8)$$

for $0<\theta\leq\pi$, where the ν_j are the zeros of $\Delta(r_o, i\omega, \nu-1/2)$ in the second quadrant.

The functions $\phi/_{i\omega}$ and $\psi/_{i\omega}$ are then given by

$$\phi=4\pi Q(i\omega)\sum_{s=0}^{\infty}(-1)^s\sum_{\nu_j}\left\{\frac{\phi_{\nu-1/2}}{\partial\Delta/\partial\nu}P_{\nu-1/2}(\cos(\pi-\theta))\exp\left[i\pi\nu(2s+1)\right]\nu\right\}_{\nu=\nu_j},$$

$$\psi=4\pi Q(i\omega)\sum_{s=0}^{\infty}(-1)^s\sum_{\nu_j}\left\{\frac{\psi_{\nu-1/2}}{\partial\Delta/\partial\nu}\cdot\frac{dP_{\nu-1/2}(\cos(\pi-\theta))}{d\theta}\exp\left[i\pi\nu(2s+1)\right]\nu\right\}_{\nu=\nu_j},\qquad(2.6\text{-}9)$$

or, equivalently, by

$$\left.\begin{aligned}\phi &= 2\pi Q(i\omega)\sum_{\nu_j}\left\{\frac{\phi_{\nu-1/2}}{\partial\Delta/\partial\nu}P_{\nu-1/2}(\cos(\pi-\theta))\frac{\nu}{\cos\nu\pi}\right\}_{\nu=\nu_j},\\ \psi &= 2\pi Q(i\omega)\sum_{\nu_j}\left\{\frac{\psi_{\nu-1/2}}{\partial\Delta/\partial\nu}\cdot\frac{dP_{\nu-1/2}(\cos(\pi-\theta))}{d\theta}\cdot\frac{\nu}{\cos\nu\pi}\right\}_{\nu=\nu_j},\end{aligned}\right\} \qquad (2.6\text{-}10)$$

where relation (2.4-17) has been employed. These last forms of the result are also obtained directly from (2.4-11).

2.7. Evaluation of the Transient Response

2.7.1. Introduction. The ultimate goal of the present investigation is the analytical evaluation of the solution. The solution is the inverse Laplace transform of equations (2.2-13). The task of evaluating the exact inversion of (2.2-13) (see section 2.3) is a formidable one for the complete ranges in time and space. However, important approximate solutions valid only for certain ranges in the time and space domains can be obtained with less difficulty. It is well known that the behavior of a diffracted wave near its front is correlated with the behavior of its Laplace transform for large p. This fact was used by Friedlander (6), and by Gilbert and Knopoff (15) to obtain wave front expansions in diffraction problems. This is the type of information that was found here also.

The analysis which has been performed here is different from that employed in (6) and (15), and leads to the same conclusions when applied to the problems treated there. In section 2.3 it was indicated that the series in (2.2-13) are meromorphic function of p with poles

at the origin and to the left of the imaginary axis; the path C in Fig. 3 was shown to be equivalent to the Bromwich contour. In sections 2.4, 2.5, and 2.6, several properties of the functions $\varphi(r,\theta, p=i\omega)$ and $\psi(r,\theta, p=i\omega)$ were deduced. The final forms obtained in section 2.6 give the behavior of the functions for $\omega\to\infty$. Hence, using for φ and ψ the expressions given in (2.6-9) or (2.6-10), one finds that

$$\begin{Bmatrix}\Phi\\ \Psi\end{Bmatrix} = \frac{1}{2\pi i}\int_C \begin{Bmatrix}\varphi\\ \psi\end{Bmatrix} d(i\omega)\ e^{i\omega t} \qquad (2.7\text{-}1)$$

is valid for short times. But the path C is equivalent to the Bromwich contour and, therefore, one can set $i\omega = p$ in (2.6-9) and (2.6-10) and obtain

$$\begin{Bmatrix}\Phi\\ \Psi\end{Bmatrix} = \frac{1}{2\pi i}\int_C \begin{Bmatrix}\varphi\\ \psi\end{Bmatrix} e^{i\omega t}\, d(i\omega) = \frac{1}{2\pi i}\int_{Br_1} \begin{Bmatrix}\varphi\\ \psi\end{Bmatrix}_{i\omega=p} e^{pt}\ dp\ , \qquad (2.7\text{-}2)$$

which is valid for short times.

A similar analysis shows that the transforms of the displacements possess the same properties found for φ and ψ. Hence, one may write, for $0 < \theta \le \pi$, $\omega\to\infty$,

$$u_r = \sum_{S=0}^{\infty}(-1)^S \sum_{\nu_j}^{S} \nu P_{\nu-\frac{1}{2}}(\cos(\pi-\theta))\exp\left[i\pi\nu(2S+1)\right] u_r^*\ , \qquad (2.7\text{-}3)$$

$$u_\theta = \sum_{s=0}^{\infty} (-1)^s \sum_j \nu \frac{dP_{\nu-1/2}(\cos(\pi-\theta))}{d\theta} \exp\left[i\pi\nu(2s+1)\right] u_\theta^* , \qquad (2.7\text{-}4)$$

where

$$u_r^* = \frac{4\pi Q(i\omega)}{r}\left\{\phi_{\nu-1/2}\left(m\nu\, F(\nu, m\nu) - \frac{1}{2}\right) - \left(\nu^2 - \frac{1}{4}\right)\psi_{\nu-1/2}\right\}\left(\frac{\partial\Delta}{\partial\nu}\right)^{-1},$$

$$u_\theta^* = \frac{4\pi Q(i\omega)}{r}\left\{\phi_{\nu-1/2} - \psi_{\nu-1/2}\left(\nu F(\nu, \nu) + \frac{1}{2}\right)\right\}\left(\frac{\partial\Delta}{\partial\nu}\right)^{-1},$$

and the ν_j are the roots of $\Delta(r_o, i\omega, \nu - 1/2)$ in the second quadrant. Thus, to find the displacements at the wave fronts, it remains to apply one of the inversion formulas (2.7-2) to (2.7-3) and (2.7-4). This will now be done for the displacements at $r = r_o$. A step function input will be assumed. The normalization constant

$$U_o = \frac{P}{r_o(\lambda + 2\mu)} \qquad (2.7\text{-}5)$$

is introduced in the final expressions.

2.7.2. Contributions from the Roots ν_{2j} Corresponding to Dilatational Waves. In this vicinity, the dominant term of $\Delta(r_o, i\omega, \nu - 1/2)$ is given by*

---

* The corresponding equation for the cylindrical cavity (5) is given by

$$D(\nu, -i\omega) \sim \left(\frac{\pi}{2}\right)^2 e^{\nu\pi i}\left(2\nu^2 - \Omega^2\right) H_\nu^{(1)}(\Omega)\, H_\nu^{(1)}(m\Omega) .$$

$$\Delta(r_o, i\omega, \nu-1/2) \sim \mu \frac{M^2(\nu) e^{i\pi/2}}{\sqrt{m}\,\Omega r_o^4} (2\nu^2-\Omega^2)^2 H_\nu^{(2)}(\Omega) H_\nu^{(2)}(m\Omega). \quad (2.7\text{-}6)$$

From Appendix A it follows that the transitional asymptotic expansion applies for $H_\nu^{(2)}(m\Omega)$ and that the non-transitional asymptotic expansion applies for $H_\nu^{(2)}(\Omega)$. Thus in this region the zeros of $\Delta(r_o, i\omega, \nu - \frac{1}{2})$ are the same as the zeros of $H_\nu^{(2)}(m\Omega)$ to this degree of approximation (this, of course agrees with references (5) and (10)). In the vicinity of the zeros,

$$H_\nu^{(2)}(m\Omega) \sim (\nu-\nu_{2j}) \left.\frac{\partial H_\nu^{(2)}(m\Omega)}{\partial \nu}\right|_{\nu=\nu_{2j}} \quad (2.7\text{-}7)$$

where

$$\nu_{2j} \sim -m\Omega + 2^{-1/3} e^{2/3\pi i} (e^{-i\pi} z_j) (m\Omega)^{1/3}, \quad (2.7\text{-}8)$$

and the z_j are the zeros of Ai(z). The first ten z_j appear in Table E1. From equations (2.7-3) and (2.7-4), it follows that

$$u_r = b_o \left(\frac{i\omega r_o}{C_d}\right)^{-1/2} \sum_{s=0}^{\infty} (-1)^s \sum_{\nu_{2j}} \left\{ e^{i\nu[2\pi(s+1)-\theta]} + e^{i\nu[2\pi s+\theta]} \right\}, \quad (2.7\text{-}9)$$

$$u_\theta = -2b_o(1-m^2)^{1/2} m^2 \left(\frac{i\omega r_o}{C_d}\right)^{-5/2} \sum_{s=0}^{\infty} (-1)^s \sum_{\nu_{2j}} \left\{ e^{i\nu[2\pi(s+1)-\theta]} - e^{i\nu[2\pi s+\theta]} \right\} \quad (2.7\text{-}10)$$

in which

$$b_o = \frac{m P}{C_d \mu (2m^2-1)^2 \sqrt{2\pi \sin\theta}} ,$$

where equations (2.7-8) and (D.8) have been used.

In practice, even though (2.6-9), (2.6-10), and (2.7-9), (2.7-10), converge for all θ in $0 < \theta \leq \pi$, their usefulness is restricted to the domain where their terms on ν_j are rapidly decreasing from the beginning so that only the first few terms need to be considered. Thus

$$\left| \exp\left[i \nu_{2j} (2\pi - \theta) \right] \right| = \exp\left\{ -\frac{\sqrt{3}}{2} \left(e^{-i\pi} z_j \right) \left(\frac{m\Omega}{2} \right)^{1/3} (2\pi - \theta) \right\} , \quad (2.7\text{-}11)$$

$$\left| \exp\left(i \nu_{2j} \theta \right) \right| = \exp\left\{ -\frac{\sqrt{3}}{2} \left(e^{-i\pi} z_j \right) \left(\frac{m\Omega}{2} \right)^{1/3} \theta \right\} , \quad (2.7\text{-}12)$$

must both be rapidly decreasing functions of z_j. This will be true provided that

$$\theta >> \Omega^{-1/3} , \qquad 2\pi - \theta >> \Omega^{-1/3} \quad (2.7\text{-}13)$$

These inequalities are satisfied in the shadow region. Setting $m\Omega = 100$, (2.7-12) is evaluated below for various values of θ and z_j.

	$\theta = 0.1$	$\theta = 0.2$	$\theta = 0.5$	$\theta = 1.0$
z_1	0.4747	0.2249	0.02399	0.00058
z_2	0.2714	0.0736	0.00134	0.000002
z_3	0.1718	0.0295	0.00015	
z_4	0.1152	0.0132		
z_5	0.079	0.006		
z_6	0.056	0.003		
z_7	0.041			

Thus it is obvious that (2.7-9) and (2.7-10) are useful for the deep shadow region.

The infinite sums appearing here have a physical interpretation which agrees with geometrical optics (2, 3, 5, 6, 8). For simplicity consider only points on the surface of the cavity (see Figure 7). At short wave lengths one may employ the concept of propagation along rays. The source excites a series of surface waves. As these waves travel along the surface, they shed radiation along tangential directions, leading to the decay factor (2.7-12). Upon reaching $\theta = \pi$, these waves are reflected toward their original direction. Thus, a point (r_o, θ) is reached by the waves coming from the source and also by those being reflected at $\theta = \pi$. The corresponding angles travelled along the surface by the first waves and their reflection are, according to Figure 7,

$$\theta_1 = \theta$$

$$\theta_2 = 2\pi - \theta \quad ,$$

in agreement with (2. 7-9) and (2. 7-10) for $s = 0$. The paths along the cavity surface are called "diffracted rays" in Keller's geometrical theory of diffraction (8).

In (2. 7-9) and (2. 7-14), the terms with $s \geq 1$ correspond to waves which have encircled the sphere $2s$ times, so that the corresponding angular paths are increased by $2\pi s$. This interpretation is corroborated by the solution to the problem of diffraction by a pulse (6), where one can follow the diffracted wave front around the sphere.

Substituting $p = i\omega$ into (2. 7-8), (2. 7-9), and (2. 7-10), one obtains

$$i\nu_{zj} = -p\frac{m r_0}{C_s} - \left(e^{-i\pi}\overline{z}_j\right)\left(p\frac{m r_0}{2C_s}\right)^{1/3}, \tag{2.7-14}$$

and, by applying (2. 7-2),

$$\frac{U_r}{U_0} = \frac{(2m^2-1)^{-2}}{m\sqrt{2\pi\sin\theta}}\sum_{s=0}^{\infty}(-1)^s\sum\left\{\frac{1}{2\pi i}\int_{Br_1}\frac{r_0}{C_d}\left(p\frac{r_0}{C_d}\right)^{-1/2}y\left(2\pi s+\theta\right)dp\right\}$$

$$+\frac{(2m^2-1)^{-2}}{m\sqrt{2\pi\sin\theta}}\sum_{s=0}^{\infty}(-1)^s\sum_{\nu_{zj}}\left\{\frac{1}{2\pi i}\int_{Br_1}\frac{r_0}{C_d}\left(p\frac{r_0}{C_d}\right)^{-1/2}y\left(2\pi(s+1)-\theta\right)dp\right\}, \tag{2.7-15}$$

$$\frac{U_\theta}{U_0} = \frac{2(1-m^2)^{1/2} m}{(2m^2-1)^2\sqrt{2\pi\sin\theta}} \sum_{s=0}^{\infty}(-1)^s \sum_{\nu_{2j}} \left\{ \frac{1}{2\pi i} \int_{Br_1} \frac{r_0}{C_d} \left(\rho \frac{r_0}{C_d}\right)^{-5/2} y\,(2\pi s + \theta)\, d\rho \right\}$$

$$- \frac{2(1-m^2)^{1/2} m}{(2m^2-1)^2\sqrt{2\pi\sin\theta}} \sum_{s=0}^{\infty}(-1)^s \sum_{\nu_{2j}} \left\{ \frac{1}{2\pi i} \int_{Br_1} \frac{r_0}{C_d} \left(\rho \frac{r_0}{C_d}\right)^{-5/2} y\,(2\pi(s+1) - \theta)\, d\rho \right\}, \qquad (2.7\text{-}16)$$

where

$$y(\theta) = \exp\left\{\rho \frac{r_0}{C_d}\left(\frac{tC_d}{r_0} - \theta\right)\right\} \exp\left\{z_j \left(\rho \frac{r_0}{2C_d}\right)^{1/3}\right\}. \qquad (2.7\text{-}17)$$

The form of $y(\theta)$ indicates that the inverse Laplace transform of each mode ν_{2j} is zero for $tC_d < r_0\theta$. This agrees with the geometrical optics of the problem.

The integrals in the above expressions have the form*

$$\tilde{I} = \frac{1}{2\pi i} \int_{Br_1} \rho^{-\chi} \exp\left(T\rho - b_j \rho^{1/3}\right) d\rho, \qquad (2.7\text{-}18)$$

---

* An extensive treatment of integrals of this type appears in reference (16).

where

$$\left.\begin{aligned} \rho &= p\frac{r_o}{c_d}, \qquad b_j = \begin{cases} -z_j\,(2\pi S+\theta)\,2^{-1/3} > 0 \\ \text{or} \\ -z_j\,[2\pi(S+1)-\theta]\,2^{-1/3} > 0 \end{cases}, \\ \chi &= \begin{cases} 1/2 \\ \text{or} \\ 5/2 \end{cases}, \qquad T = \begin{cases} \dfrac{tc_d}{r_o} - (2\pi S+\theta) \\ \text{or} \\ \dfrac{tc_d}{r_o} - [2\pi(S+1)-\theta] \end{cases}. \end{aligned}\right\} \tag{2.7-19}$$

If 3x were an integer, then this integral could be expressed in terms of the Airy function discussed in Appendix E. For this problem the approximation of the integral for small values of T is needed. For such values of T (6),

$$\tilde{I} \sim \frac{3^{1/4(6\chi-1)}\, b^{1/4(3-6\chi)}\, T^{1/4(6\chi-5)}}{2\sqrt{\pi}} \exp\left\{-\frac{2b_j^{3/2}}{3^{3/2}T^{1/2}}\right\} H(T)\,\chi \times \left\{1+O\left(\frac{T^{1/2}}{b_j^{3/2}}\right)\right\}, \qquad b_j^{3/2} > 0 \text{ and real.} \tag{2.7-20}$$

The magnitude of the error term limits the applicability of the technique. Since $0 > z_1 > z_2 > z_3 \ldots$, the leading term of any mode of order $j > 1$ tends to zero more rapidly than the error term of the first mode. Since the error term is to be neglected, it follows that the results must be confined to a range of T in which the error

term for $s = 0$ is smaller than the contributions from the higher modes. Then only the terms $s = 0$, $j = 1$ need be taken into account for $\theta \gg 1$, and thus the final expressions are

$$\frac{U_r}{U_o} = \frac{(2m^2-1)^{-2}\sqrt{3}}{m(2\pi\sin\theta)^{1/2}} \cdot \frac{T_2^{-1/2}}{2\sqrt{\pi}} \exp\left(-0.9742\theta^{3/2}T_2^{-1/2}\right) H(T_2), \qquad (2.7\text{-}21)$$

$$\frac{U_\theta}{U_o} = \frac{2(1-m^2)^{1/2} m\, 3^{7/2}}{(2m^2-1)^2\sqrt{2\pi\sin\theta}} \cdot \frac{T_2^{5/2}}{2(2.34\theta)^3} \exp\left(-0.9742\theta^{3/2}T_2^{-1/2}\right) H(T_2), \qquad (2.7\text{-}22)$$

in which

$$T_2 = \frac{t\, C_d}{r_o} - \theta \quad , \qquad (2.7\text{-}23)$$

and the inequalities

$$1 < \theta < \pi \, , \qquad \frac{t\, C_d}{r_o} < \min\left(\frac{\theta}{m},\ 2\pi - \theta\right), \qquad (2.7\text{-}24)$$

must hold. When $m = 0.5$ (Poisson's ratio of one-third), these expressions reduce to

$$\frac{U_r}{U_o} = \frac{0.195\, T_2^{-1/2}}{\sqrt{\sin\theta}} \exp\left(-0.9742\theta^{3/2}T_2^{-1/2}\right) H(T_2), \qquad (2.7\text{-}25)$$

$$\frac{U_\theta}{U_o} = \frac{2.85\, T_2^{5/2}}{\theta^3\sqrt{\sin\theta}} \exp\left(-0.9742\theta^{3/2}T_2^{-1/2}\right) H(T_2). \qquad (2.7\text{-}26)$$

Reflecting upon the results for the half-space (see de Hoop (17)), one sees that the dilatational wave generates a head wave at its point of contact with the free surface. Furthermore, at the surface this head wave travels with the speed of the dilatational wave. Since here the evaluations have been made at the surface, the head wave is contained in the expressions given above for the displacements.

2.7.3. Contributions from the Rayleigh Root. In this vicinity the non-transitional asymptotic expansions apply for $H_\nu^{(2)}(\Omega)$, $H_\nu^{(2)}(m\Omega)$, $F(\nu,\Omega)$, and $F(\nu, m\Omega)$. The dominant term of $\Delta(r_o, i\omega, \nu-\frac{1}{2})$ is given by

$$\Delta(r_o, i\omega, \nu-\tfrac{1}{2}) \sim \frac{4\sqrt{m}\,\mu M^2(\nu)\Omega(\nu^2-9/4)}{r_o^4\, e^{i\pi/2}} H_\nu^{(2)}(\Omega) H_\nu^{(2)}(m\Omega) f_2(\nu), \quad (2.7\text{-}27)$$

where

$$f_2(\nu) \sim \frac{\Omega^2}{m\nu^2}\left[\frac{\nu^2}{\Omega^2}\left(\frac{\nu^2}{\Omega^2}-1\right)^{1/2}\left(\frac{\nu^2}{\Omega^2}-m^2\right)^{1/2} - \left(\frac{\nu^2}{\Omega^2}-\frac{1}{2}\right)^2\right],$$

and the required cuts are given in Fig. 6. In accordance with Appendix C, there is only one root which approaches the real ν-axis as $|\nu|\to\infty$ and whose limiting phase velocity is the Rayleigh velocity. The real part of this root is given asymptotically by

$$\nu_R \sim \nu_o = -\zeta_o^{1/2}\Omega \quad , \quad (2.7\text{-}28)$$

where ζ_o is the unique real root of the cubic equation

$$16(1-m^2)\zeta^3 - 8(3-2m^2)\zeta^2 + 8\zeta - 1 = 0 \ ;$$

ζ_o is greater than one; $\zeta_o = 1.15$ when $m = 0.5$. The imaginary part of this root, σ_o, has the form

$$\text{Im } \nu_R = \sigma_o \sim \text{const } \Omega\, e^{-\text{const } \Omega} \quad , \tag{2.7-29}$$

where const > 0.

When $m = 0.5$, (2.7-3) and (2.7-4) give

$$u_{\theta R} = -\frac{0.672\,P}{4\mu c_s \sqrt{2\pi \sin\theta}} \left(\frac{i\omega r_o}{c_s}\right)^{-1/2} \sum_{s=0}^{\infty} \left\{ e^{i\nu_R[2\pi(s+1)-\theta]} - e^{i\nu_R[2\pi s+\theta]} \right\}, \tag{2.7-30}$$

$$u_{rR} = \frac{0.475\,P}{2\mu c_s \sqrt{2\pi \sin\theta}} \left(\frac{i\omega r_o}{c_s}\right)^{-1/2} \sum_{s=0}^{\infty} \left\{ e^{i\nu_R[2\pi(s+1)-\theta]} + e^{i\nu_R[2\pi s+\theta]} \right\}. \tag{2.7-31}$$

The physical interpretation of the infinite sums is the same as that for (2.7-9) and (2.7-10). As was indicated in 2.7.2 for the roots ν_{2j}, the source excites a series of surface waves and, as these waves travel along the surface, they shed radiation along tangential directions, leading to the decay factors (2.7-11) and (2.7-12). Since $0 > z_1 > z_2 > z_3 \cdots$, the higher ν_{2j} modes decay faster than the lower modes. The corresponding decay factors for the Rayleigh root are

$$\left| \exp\left[i \nu_R (2\pi - \theta) \right] \right| = \exp\left\{ -\sigma_o (2\pi - \theta) \right\}, \tag{2.7-32}$$

$$\left| \exp\left(i \nu_R \theta \right) \right| = \exp\left\{ -\sigma_o \theta \right\}. \tag{2.7-33}$$

Since $\sigma_o << -z_j \Omega$, it follows that the predominant disturbance for long time is given by the Rayleigh root, in agreement with Miklowitz (3, 4) who showed this to be the case for the cylindrical cavity diffraction problems. It is of interest to note that Miklowitz (3) first deduced the analogous result for the cylindrical case by comparing his final expressions with the results of Lamb's problem (see, for example, equation (2-114) ref. (19)) of the elastic half-space subjected to a surface impulsive line load.

The analysis now follows closely the technique given in (3) and (4). Hence the following need only be brief. The application of (2.7-2) gives

$$\begin{Bmatrix} U_{rR} \\ U_{\theta R} \end{Bmatrix} = \frac{1}{2\pi i} \int_{\substack{C \\ i\omega = p}} \begin{Bmatrix} u_{rR} \\ u_{\theta R} \end{Bmatrix} e^{pt} dp$$

and, since the semi-circle C_o in Fig. 3 gives no contribution to the integrals, these integrals reduce to

$$\begin{Bmatrix} U_{rR} \\ U_{\theta R} \end{Bmatrix} = \frac{Re}{\pi} \int_0^\infty \begin{Bmatrix} u_{rR} \\ u_{\theta R} \end{Bmatrix} e^{i\omega t} d\omega, \qquad (2.7\text{-}34)$$

where property (2.3-4) has been used. More explicitly,

$$\frac{U_{rR}}{U_o} = \frac{Re\ 4}{6\pi\sqrt{\pi \sin\theta}} \sum_{s=0}^{\infty} \int_0^\infty \frac{1}{\Omega^{1/2}} \left\{ e^{i\nu_R[2\pi(s+1)-\theta]} + e^{i\nu_R[2\pi s+\theta]} \right\} e^{i\omega t} d\Omega, \qquad (2.7\text{-}35)$$

$$\frac{U_{\theta R}}{U_o} = -\frac{Re\ 0.672}{\pi\sqrt{2\pi \sin\theta}} \sum_{s=0}^{\infty} \int_0^\infty \frac{1}{\Omega^{1/2}} \left\{ e^{i\nu_R[2\pi(s+1)-\theta]} - e^{i\nu_R[2\pi s+\theta]} \right\} e^{i\omega t} d\Omega, \qquad (2.7\text{-}36)$$

where

$$i\,\nu_R = -\,i\,1.072\,\Omega - \sigma_o = -\,i\,\frac{C_S}{C_R}\,\Omega - \sigma_o \quad . \qquad (2.7\text{-}37)$$

For the approximations being determined here, it is sufficient to assume a certain value of σ_o, denoted by σ_A (see ref. (4)). The above expressions then become (20)

$$\frac{U_{rR}}{U_o} = \frac{0.145}{\sqrt{\sin\theta}} \sum_{s=N_o}^{N} \left\{ \frac{H(T_3)\, e^{-\sigma_A[2\pi s+\theta]}}{|T_3|^{1/2}} + \frac{H(T_4)\, e^{-\sigma_A[2\pi(s+1)-\theta]}}{|T_4|^{1/2}} \right\}, \qquad (2.7\text{-}38)$$

$$\frac{U_{\theta R}}{U_o} = \frac{0.963}{\sqrt{\sin\theta}} \sum_{s=N_o}^{N} \left\{ \frac{H(T_3)\, e^{-\sigma_A[2\pi s+\theta]}}{|T_3|^{1/2}} - \frac{H(T_4)\, e^{-\sigma_A[2\pi(s+1)-\theta]}}{|T_4|^{1/2}} \right\}, \qquad (2.7\text{-}39)$$

where

$$T_3 = \frac{t\,C_R}{r_o} - (2\pi s + \theta), \quad T_4 = \frac{t\,C_R}{r_o} - [2\pi(s+1) - \theta], \qquad (2.7\text{-}40)$$

$H(T_{3,4})$ is the two-sided step function

$$H(T) = \begin{cases} -\frac{1}{2}, & T < 0 \\ 0, & T = 0 \\ \frac{1}{2}, & T > 0 \end{cases} , \qquad (2.7\text{-}41)$$

N and N_o are large numbers determined by the number of periodic waves occurring in a certain domain of large time.

The discontinuities represented in this expression are two-sided phenomena having tails and heads which extend in front and behind their arrival time. However, since the heads and tails are negligible relative to the infinite discontinuities. N needs to be only slightly greater than N_o. It can be seen from these expressions that their singular nature renders them as periodic non-decaying disturbances, as was found in reference (3) for the cylindrical case.

The form of the individual expressions (2.7-38) and (2.7-39) agree with those of Chao (21) for a half-space subjected to a concentrated surface force. There it was deduced that the Rayleigh disturbance is of the form

$$U_r \sim \left| C_R t - r \right|^{-\frac{1}{2}} , \qquad (2.7\text{-}42)$$

where C_R is the Rayleigh surface wave speed.

2.7.4. Discussion of the Results. The diffraction of scalar pulses by continuously curved obstacles has been considered by several authors (6, 8). It is found that the diffracted pulses near the front are always of the form

$$u \sim C T^{b} \exp(-\delta T^{-\frac{1}{2}}) \ , \qquad (2.7\text{-}43)$$

where T is the time counted from the arrival of the diffracted front, C and δ are functions of position, and b is a constant. This diffraction formula implies that u and all its derivatives with respect to time vanish at the diffracted front. Hence u increases at first more slowly than any power of T. By referring to equations (2.7-25), (2.7-26), and the Figures 8 and 9, it is found that these qualitative results hold in the present problem. For the cylindrical cavity, Gilbert (22) and Peck (5) also found these qualitative properties. Therefore, it may be conjectured that (2.7-43) is a general diffraction formula valid near the diffracted front.

The technique employed here for the ν_{2j} roots is useful for regular wave fronts. However, the shear wave front is two-sided at the surface of the cavity, as may be seen in Figure 11. Consequently, the contributions from the ν_{1j} roots cannot be assessed by this technique. Nevertheless, the ν_{1j} roots have been included here because they are needed for a numerical evaluation of the response (5) and for further work on the regular wave fronts. For a detailed

discussion of regular and two-sided wave fronts see Rosenfeld and Miklowitz (23).

The qualitative results for the Rayleigh root contributions, which are similar in behavior to those in (3), are shown in Figure 10. The infinite discontinuities are, of course, directly dependent on the nature of the input function F(t) which, it should be recalled, was taken to be a step function H(t). These discontinuities were also found for the problem of a half-space subjected to a concentrated surface force (21). This proves the validity of the technique employed here.

CHAPTER 3

INCIDENT PLANE WAVE

3.1 Statement of the Problem

Using the cavity described in Chapters 1 and 2 the problem of an incoming plane wave will now be considered. The geometry of this problem is depicted in Figure 12 where the coordinate system of Figure 1 is used.

For the problem of an incoming plane wave, the boundary conditions are

$$\tau_r^{sc}(r_o, \theta, t) = -\tau_r^{inc}(r_o, \theta, t)$$
$$\tau_{rr}^{sc}(r_o, \theta, t) = -\tau_{rr}^{inc}(r_o, \theta, t) \quad , \tag{3.1-1}$$

such that the total stress at the surface of the cavity is zero. The superscripts $(\ )^{sc}$ and $(\ )^{inc}$ denote the scattered and incident parts respectively. The incident plane dilatational wave is specified by the function $\Phi_o(t)$ in

$$\Phi^{inc}(r, \theta, t) = \Phi_o\left(\frac{t\, C_d}{r} - \cos\theta\right) \; H\left(\frac{t\, C_d}{r} - \cos\theta\right) \quad . \tag{3.1-2}$$

For an associated step-function stress (τ_{zz} in Fig. 12) of amplitude τ_o,

$$\Phi_o(t) = \frac{\tau_o C_d^2}{\lambda + 2\mu} \cdot \frac{t^2}{2} \quad . \tag{3.1-3}$$

Equations (2.1-1) - (2.1-6), with (2.1-5) replaced by (3.1-1), apply in this case when the superscripts $(\ )^{sc}$ and $(\ )^{inc}$ are attached to them. Hence, equations (2.2-3) also apply, where A_n and B_n need to be determined for this case.

The total field is given by adding the scattered field to the incident field, that is,

$$\Phi = \Phi_T = \Phi^{sc}(r, \theta, t) + \Phi^{inc}(r, \theta, t) ,$$
$$\Psi = \Psi_T = \Psi^{sc}(r, \theta, t) . \qquad (3.1-4)$$

3.2 Formal Solution

Here use of the bilateral Laplace transform will be made. Such a transform of a quantity will be denoted by a small case letter*, for example,

$$\varphi = \mathcal{L}\{\Phi\} = \int_{-\infty}^{\infty} \Phi\, e^{-pt}\, dt , \quad \Phi = \frac{1}{2\pi i} \int_{Br_1} \varphi\, e^{pt}\, dp .$$

The application of this transform to (3.1-2) and (3.1-3) yields

$$\varphi^{inc}(r, \theta, p) = \varphi_o(p)\, e^{-hr\cos\theta} ,$$

where, for a step input in stress,

---

* Except for $\sigma_{ij} = \mathcal{L}\{\tau_{ij}\}$

$$\varphi_o(p) = \frac{\tau_o C_d^2}{\lambda + 2\mu} p^{-3} \quad . \tag{3.2-1}$$

From reference (24), it follows that

$$\varphi^{inc}(r, \theta, p) = \sum_{n=0}^{\infty} C_n \frac{I_{n+\frac{1}{2}}(hr)}{\sqrt{hr}} P_n(\cos\theta) \quad , \tag{3.2-2}$$

where

$$C_n = \varphi_o(p) \sqrt{\frac{\pi}{2}} (2n+1) (-1)^n \quad , \tag{3.2-3}$$

and $I_{n+\frac{1}{2}}(z)$ is the modified Bessel function of the first kind of order $n+\frac{1}{2}$. Since

$$I_{n+1/2}(z) = \frac{1}{(2\pi z)^{1/2}} \left\{ e^{z} \sum_{s=0}^{n} \frac{(-1)^s (n+s)!}{s!(n-s)!(2z)^s} + \right.$$

$$\left. + (-1)^{n+1} e^{-z} \sum_{s=0}^{n} \frac{(n+s)!}{s!(n-s)!(2z)^s} \right\}, \tag{3.2-4}$$

then, for the input of (3.2-1), $\varphi^{inc}(r, \theta, p)$ is a meromorphic function of p.

The boundary conditions are transformed into

$$\sigma_r^{sc}(r_o, \theta, p) = - \sigma_r^{inc}(r_o, \theta, p), \quad \sigma_{rr}^{sc}(r_o, \theta, p) = - \sigma_{rr}^{inc}(r_o, \theta, p) \tag{3.2-5}$$

By (3.2-2) and (2.2-7), one finds that

$$\sigma_{rr}^{inc} = \sum_{n=0}^{\infty} C_n \mathcal{Y} P_n(\cos\theta), \quad \sigma_{r\theta}^{inc} = \mu \sum_{n=0}^{\infty} C_n \mathcal{S} \frac{dP_n(\cos\theta)}{d\theta} \tag{3.2-6}$$

where

$$\left.\begin{aligned} \mathcal{Y} &= \frac{I_{n+1/2}(hr)}{\sqrt{hr}}\left(k^2 + 2\frac{n(n+1)}{r^2}\right)\mu - \frac{4\mu}{r}\cdot\frac{d}{dr}\cdot\frac{I_{n+1/2}(hr)}{\sqrt{hr}} \\ \mathcal{S} &= 2\frac{d}{dr}\left(\frac{1}{r}\cdot\frac{I_{n+1/2}(hr)}{\sqrt{hr}}\right). \end{aligned}\right\} \tag{3.2-7}$$

The application of (3.2-5) to (3.2-6) amd (2.2-9) yields in this case

$$\left.\begin{aligned} \sum_{n=0}^{\infty}\left[A_n \mathcal{A}_0 + B_n \mathcal{B}_0\right] P_n(\cos\theta) &= -\sum_{n=0}^{\infty} C_n \mathcal{Y} P_n(\cos\theta), \\ \sum_{n=0}^{\infty}\left[A_n \mathcal{D}_0 + B_n \mathcal{E}_0\right] \frac{dP_n(\cos\theta)}{d\theta} &= -\sum_{n=0}^{\infty} C_n \mathcal{S}_0 \frac{dP_n(\cos\theta)}{d\theta}, \end{aligned}\right\} \tag{3.2-8}$$

where $\mathcal{A}, \mathcal{B}, \mathcal{D}, \mathcal{E}$ are given by (2.2-10).

Solving (3.2-8) for A_n and B_n, one obtains

$$\left.\begin{aligned} A_n &= C_n \frac{\mathcal{B}_0 \mathcal{S}_0 - \mathcal{Y}_0 \mathcal{E}_0}{\Delta(r_0, p, n)}, \\ B_n &= C_n \frac{\mathcal{D}_0 \mathcal{Y}_0 - \mathcal{A}_0 \mathcal{S}_0}{\Delta(r_0, p, n)}, \end{aligned}\right\} \tag{3.2-9}$$

where $\Delta(r_o, p, n)$ is given by (2. 2-12). The substitution of (3. 2-9) into (2. 2-3) gives

$$\left.\begin{aligned} \phi^{sc} &= \sqrt{\frac{\pi}{2}}\,\phi_o(p)\sum_{n=0}^{\infty}(2n+1)(-1)^n \frac{\mathcal{B}_o \mathcal{L}_o - \mathcal{Y}_o \mathcal{E}_o}{\Delta(r_o, p, n)} \cdot \frac{K_{n+1/2}(hr)}{\sqrt{hr}} P_n(\cos\theta) \\ \psi^{sc} &= \sqrt{\frac{\pi}{2}}\,\phi_o(p)\sum_{n=0}^{\infty}(2n+1)(-1)^n \frac{\mathcal{D}_o \mathcal{Y}_o - \mathcal{A}_o \mathcal{L}_o}{\Delta(r_o, p, n)} \cdot \frac{K_{n+1/2}(kr)}{\sqrt{kr}} \cdot \frac{dP_n(\cos\theta)}{d\theta} \end{aligned}\right\} \quad (3.\ 2\text{-}10)$$

The Laplace transform of the total field is then given by

$$\begin{aligned} \varphi = \varphi_T &= \varphi^{inc}(r, \theta, p) + \varphi^{sc}(r, \theta, p) \\ \psi = \psi_T &= \psi^{sc}(r, \theta, p) \ . \end{aligned} \quad (3.\ 2\text{-}11)$$

Clearly, in view of equations (2. 2-5) and (3. 2-4), φ and ψ are meromorphic functions of p in the whole p-plane.

Convergence of the Series. As in Chapter 2, the convergence of (3. 2-10) is considered now for p on the Bromwich contour $\mathrm{Re}\ p = c > 0$, $-R \le \mathrm{Im}\ p \le R$, $R \to \infty$. The potential functions φ^{sc} and ψ^{sc} are assumed to be analytic on the contour. Select the compact subset of the Bromwich contour given by $\mathrm{Re}\ p = c > 0$, $-R < -Y \le \mathrm{Im}\ p \le Y < R$, and recall the inequalities

$$\left|P_n(\cos\theta)\right| \le 1, \quad \left|\frac{dP_n(\cos\theta)}{d}\right| \le n^2 \ .$$

Then, by denoting

$$\varphi^{sc} = \sum_{n=o}^{\infty} \varphi_n \quad , \qquad \psi^{sc} = \sum_{n=o}^{\infty} \psi_n \quad ,$$

one sees that for large n,

$$\left| \varphi_n^{sc} \right| \sim \frac{\Gamma(2n+1)}{\Gamma(n+1)2^n} \left| P_n(\cos\theta) \right| \frac{1}{(hr)^{n+1}}$$

$$\left| \psi_n^{sc} \right| \sim \frac{\Gamma(2n+1)}{\Gamma(n+1)2^n} \left| \frac{dP_n(\cos\theta)}{d\theta} \right| \frac{1}{(hr)^{n+1}} \quad .$$

Therefore, by the ratio test, one concludes that the series in (3.2-10) converge uniformly on the Bromwich contour. Hence, one also concludes that (3.2-11) are uniformly convergent.

3.3. Exact Inversion

Since the series in (3.2-10) are uniformly convergent on the Bromwich contour, the Laplace transforms in (3.2-11) may be inverted by term-wise integration. By the arguments given in section 2.3, and assuming that the paths C_R and C_{-R} in Figure 3 do not contribute to the integral, one finds that the paths Br_1 and C are equivalent; that is

$$\begin{Bmatrix} \Phi \\ \Psi \end{Bmatrix} = \frac{1}{2\pi i} \int_{Br_1} \begin{Bmatrix} \varphi \\ \psi \end{Bmatrix} e^{pt}\, dp = \frac{1}{2\pi i} \int_{C} \begin{Bmatrix} \varphi \\ \psi \end{Bmatrix} e^{pt}\, dp. \quad (3.3\text{-}1)$$

As in Chapter 2, the singular points of φ and ψ are also those where $\Delta(r_o, p, n)$ vanishes.

Since for real Ω

$$\frac{I_{n+1/2}(-i\Omega)}{(-i\Omega)^{1/2}} = \overline{\left[\frac{I_{n+1/2}(i\Omega)}{(i\Omega)^{1/2}}\right]}, \quad (3.3\text{-}2)$$

then, by (2.3-3), (2.2-10), (3.2-7), and (3.2-10), one may write

$$\begin{Bmatrix} \varphi \\ \psi \end{Bmatrix}_{p=-i\omega} = \overline{\begin{Bmatrix} \varphi \\ \psi \end{Bmatrix}_{p=i\omega}} \quad (3.3\text{-}3)$$

and

$$\begin{Bmatrix} \Phi_1 \\ \Psi_1 \end{Bmatrix} = \frac{1}{2\pi i} \int_{C_U + C_L} \begin{Bmatrix} \varphi \\ \psi \end{Bmatrix} e^{pt} dp = \frac{\mathrm{Re}}{\pi} \int_{0}^{\infty} \begin{Bmatrix} \varphi \\ \psi \end{Bmatrix} e^{-i\omega t}\, d\omega, \quad (3.3\text{-}4)$$

in which

$$\varphi \Big|_{p=-i\omega} = \varphi^{inc}(r, \theta, -i\omega) + \varphi^{sc}(r, \theta, -i\omega), \quad (3.3\text{-}5)$$

$$\psi \Big|_{p=-i\omega} = \psi^{sc}(r, \theta, -i\omega), \quad (3.3\text{-}6)$$

where $\varphi^{inc}(r, \theta, p)$, $\varphi^{sc}(r, \theta, p)$, and $\psi^{sc}(r, \theta, p)$ are given by equations (3.2-2) and (3,2-10). The infinite sums in (3.3-5) and (3.3-6) will be approximated in the next section for $\omega \to \infty$. The subscript $p = -i\omega$ is henceforth deleted.

3.4. Watson's Transformation

Before writing the particular form of the Watson transformation to be used in the problem, it is convenient to introduce the notation

$$\mathcal{F}(\nu, \Omega) = \frac{d}{d\Omega}(\ln H_\nu^{(1)}(\Omega) \quad , \quad \mathcal{N}(\nu) = \frac{\pi i}{2} e^{i\pi\nu/2} \tag{3.4-1}$$

where $H_\nu^{(1)}(\Omega)$ is the Hankel function of the first kind. With this notation and the relation

$$K_\nu(\Omega e^{-i\pi/2}) = \mathcal{N}(\nu) H_\nu^{(1)}(\Omega) \ , \tag{3.4-2}$$

one immediately finds that*

$$\frac{r^2(mve^{-i\pi/2})^{1/2}}{\mu \mathcal{N}(\nu)} \cdot \frac{\tilde{A}}{H_\nu^{(1)}(mv)} = \left(\frac{3+4\nu^2}{2} - v^2\right) - 4mv\, \mathcal{F}(\nu, mv), \tag{3.4-3}$$

$$\frac{r^2(ve^{-i\pi/2})^{1/2}}{\mu \mathcal{N}(\nu)} \cdot \frac{\tilde{B}}{H_\nu^{(1)}(v)} = -\left(\nu^2 - \frac{1}{4}\right)\left(2v\, \mathcal{F}(\nu, v) - 3\right), \tag{3.4-4}$$

---

* $p = i\omega$ had been substituted into equations (2.2-10) before writing equations (2.4-4)-(2.4-7). Here the substitution is $p = -i\omega$.

$$\frac{r^2(mve^{-i\pi/2})^{1/2}}{\mathcal{N}(\nu)}\cdot\frac{\tilde{\mathcal{D}}}{H_\nu^{(1)}(mv)} = 2mv\,\mathcal{F}(\nu,mv) - 3\,, \tag{3.4-5}$$

$$\frac{r^2(ve^{-i\pi/2})^{1/2}}{\mathcal{N}(\nu)}\cdot\frac{\tilde{\mathcal{E}}}{H_\nu^{(1)}(v)} = 2v\,\mathcal{F}(\nu,v) + \left(\frac{3-4\nu^2}{2}+v^2\right), \tag{3.4-6}$$

$$\tilde{\mathcal{G}} = \tilde{\mathcal{G}}^*\,e^{-i\pi/2(\nu-1/2)}, \tag{3.4-7}$$

$$\tilde{\mathcal{S}} = \tilde{\mathcal{S}}^*\,e^{-i\pi/2(\nu-1/2)}, \tag{3.4-8}$$

$$\frac{\Delta(r_0,-i\omega,\nu-1/2)}{H_\nu^{(1)}(\Omega)\;H_\nu^{(1)}(m\Omega)} = \frac{4\sqrt{m}\,\mu\,\mathcal{N}^2(\nu)\,\Omega(\nu^2-9/4)}{r_0^4\,e^{-i\pi/2}}\,f_3(\nu), \tag{3.4-9}$$

where

$$\frac{1}{\mu}\tilde{\mathcal{G}}^* = \left[\frac{J_\nu(mv)}{(mv)^{1/2}}\left(\frac{3+4\nu^2}{2}-v^2\right) - 4mv\,\frac{J_\nu'(mv)}{(mv)^{1/2}}\right]\frac{1}{r^2}\,, \tag{3.4-10}$$

$$\tilde{\mathcal{S}}^* = \left[2mv\,\frac{J_\nu'(mv)}{(mv)^{1/2}} - 3\,\frac{J_\nu(mv)}{(mv)^{1/2}}\right]\frac{1}{r^2} \tag{3.4-11}$$

$$f_3(\nu) = -\frac{\nu^2-1/4}{m\Omega^2}\left(1-\frac{\Omega^2}{2(\nu^2-9/4)}\right)^2 + \left\{\mathcal{F}(\nu,m\Omega) - \frac{1}{2m\Omega}\left(1+\frac{\Omega^2}{\nu^2-9/4}\right)\right\}\times \tag{3.4-12}$$

$$\times\left\{\mathcal{F}(\nu,\Omega)+\frac{1}{2\Omega}\left(1-\frac{2\Omega^2}{\nu^2-9/4}\right)\right\}.$$

On applying formula (2.4-1) to the expressions for φ and ψ, one obtains

$$\phi = \sqrt{\frac{\pi}{2}}\,\phi_0(-i\omega)\int_{C_W} \nu\, \frac{\phi_{\nu-1/2}(r, r_0, \nu-1/2)}{\Delta(r_0, -i\omega, \nu-1/2)} \cdot \frac{P_{\nu-1/2}(\cos\theta)}{\cos\nu\pi}\, \exp\left[-i\frac{\pi}{2}(\nu+1/2)\right] d\nu, \quad (3.4\text{-}13)$$

$$\psi = \sqrt{\frac{\pi}{2}}\,\phi_0(-i\omega)\int_{C_W} \nu\, \frac{\psi_{\nu-1/2}(r, r_0, \nu-1/2)}{\Delta(r_0, -i\omega, \nu-1/2)} \cdot \frac{dP_{\nu-1/2}(\cos\theta)}{d\theta} \cdot \frac{\exp\left[-i\frac{\pi}{2}(\nu+1/2)\right]}{\cos\nu\pi}\, d\nu, \quad (3.4\text{-}14)$$

where

$$\phi_{\nu-1/2}(r, r_0, \nu) = \frac{J_\nu(m\nu)}{(m\nu)^{1/2}}\,\Delta(r_0, -i\omega, \nu-1/2) + \left[\tilde{\mathcal{B}}_0\,\tilde{\mathcal{G}}_0^* - \tilde{\mathcal{G}}_0^*\,\tilde{\mathcal{E}}_0\right] \frac{\mathcal{N}(\nu)\, H_\nu^{(1)}(m\nu)}{(m\nu e^{-i\pi/2})^{1/2}}, \quad (3.4\text{-}15)$$

$$\psi_{\nu-1/2}(r, r_0, \nu) = \left[\tilde{\mathcal{D}}_0\,\tilde{\mathcal{G}}_0^* - \tilde{\mathcal{A}}_0\,\tilde{\mathcal{G}}_0^*\right] \frac{\mathcal{N}(\nu)\, H_\nu^{(1)}(\nu)}{(\nu e^{-i\pi/2})^{1/2}}, \quad (3.4\text{-}16)$$

and C_W is the contour shown in Figure 4. Using the relations

$$H_{-\nu}^{(1)}(z) = e^{+i\nu\pi}\, H_\nu^{(1)}(z),$$

$$J_{-\nu}(z) = e^{-i\nu\pi}\, J_\nu(z) + i \sin\nu\pi\, H_\nu^{(1)}(z), \quad (3.4\text{-}17)$$

$$P_{-\lambda-\frac{1}{2}}(\cos\theta) = P_{\lambda-\frac{1}{2}}(\cos\theta),$$

it is seen that the integrands are odd functions of ν. By the arguments given in section 2.4, it follows that

$$\phi = \sqrt{2\pi}\,\phi_0(-i\omega)\, e^{-i\pi/4} \sum_{s=0}^{\infty} (-1)^s \int_{-\infty}^{\infty} \nu \frac{\phi_{\nu-1/2}}{\Delta} P_{\nu-1/2}(\cos\theta) \exp\left[i\nu(2\pi s + \tfrac{\pi}{2})\right] d\nu, \quad (3.4\text{-}18)$$

$$\psi = \sqrt{2\pi}\,\phi_0(-i\omega)\, e^{-i\pi/4} \sum_{s=0}^{\infty} (-1)^s \int_{-\infty}^{\infty} \nu \frac{\psi_{\nu-1/2}}{\Delta} \cdot \frac{dP_{\nu-1/2}(\cos\theta)}{d\theta} \exp\left[i\nu(2\pi s + \tfrac{\pi}{2})\right] d\nu. \quad (3.4\text{-}19)$$

The application of Poisson's summation formula to equations (3.3-5) and (3.3-6) yields

$$\phi = \sqrt{2\pi}\,\phi_0(-i\omega) \sum_{s=-\infty}^{\infty} (-1)^s \int_{0}^{\infty} \nu \frac{\phi_{\nu-1/2}}{\Delta} P_{\nu-1/2}(\cos\theta)\, e^{i\frac{\pi}{2}(\nu-1/2)} \exp(2\pi i s\nu)\, d\nu,$$

$$\psi = \sqrt{2\pi}\,\phi_0(-i\omega) \sum_{s=-\infty}^{\infty} (-1)^s \int_{0}^{\infty} \nu \frac{\psi_{\nu-1/2}}{\Delta} \cdot \frac{dP_{\nu-1/2}(\cos\theta)}{d\theta}\, e^{i\pi/2(\nu-1/2)} \exp(2\pi i s\nu)\, d\nu.$$

By substituting $-\nu$ for ν in the integrals from $s = -1$ to ∞ and using equations (3.4-17), the above expressions become precisely equations (3.4-18) and (3.4-19). Thus, Poisson's summation formula and Watson's transformation are also equivalent for this problem.

To deform the path of integration in (3.4-13) and (3.4-14) away from the real axis, it is necessary to know the roots of $\Delta(r_o, -i\omega, \nu-\frac{1}{2})$ for large values of Ω. These roots may be easily determined from those of $\Delta(r_o, i\omega, \nu-\frac{1}{2})$ because the relation

$$\overline{H_{\nu}^{(1)}(\Omega)} = H_{\overline{\nu}}^{(2)}(\Omega), \quad \Omega \text{ real},$$

implies that

$$f_3(\nu) = \overline{f_2(\overline{\nu})}$$

and

$$\Delta(r_o, -i\omega, \nu-\tfrac{1}{2}) = \overline{\Delta(r_o, i\omega, \overline{\nu}-\tfrac{1}{2})} \quad , \tag{3.4-20}$$

where the vinculum indicates the complex conjugate. Hence the roots of $\Delta(r_o, -i\omega, \nu-\frac{1}{2})$ are precisely the complex conjugate of the roots of $\Delta(r_o, i\omega, \nu-\frac{1}{2})$.

3.5. The Residue Series

The next step in the solution is to determine the conditions under which the integrals in (3.4-13) and (3.4-14) may be reduced to a series of residues evaluated at the zeros of $\Delta(r_o, -i\omega, \nu-\frac{1}{2})$. This is done by considering a sequence of paths L_n, shown in Figure 13, which passes between these zeros and is such that

$$\lim_{n\to\infty} \int_{L_n} f(r, \theta; \nu)\, d\nu = 0, \tag{3.5-1}$$

where $f(r, \theta; \nu)$ is a generic expression for the integrands of (3.4-13) and (3.4-14). Since the integrands are odd functions of ν, the integrals along the imaginary axis vanish.

On Γ_1, and Γ_2, the dominant terms of $J_\nu(z)$ and $H_\nu^{(1)}(z)$ are

$$J_\nu(z) \sim \frac{1}{\sqrt{2\pi\nu}} \left(\frac{e\,z}{2\nu}\right)^\nu \quad ,$$

$$H_\nu^{(1)}(z) = \frac{J_{-\nu}(z) - J_\nu(z)\, e^{-i\pi\nu}}{i \sin \pi\nu} \sim \frac{1}{i \sin \pi\nu} \left[\frac{\left(\frac{z}{2}\right)^{-\nu}}{\Gamma(1-\nu)} - \frac{\left(\frac{z}{2}\right)^{+\nu} e^{-\pi\nu i}}{\Gamma(1+\nu)} \right],$$

where the second term in the brackets is significant only in the neighborhood of the imaginary axis. Therefore

$$\frac{\varphi_{\nu-\frac{1}{2}}}{\Delta} \sim \frac{1}{\nu} \left(\frac{em\nu}{2\nu}\right)^\nu + \frac{1}{r_o^2\, \nu^{3/2}} \left(\frac{em\Omega}{2\nu}\right)^\nu \left(\frac{r_o}{r}\right)^{\frac{1}{2}} \left[\left(\frac{r_o}{r}\right)^\nu \text{ or} \left(\frac{r}{r_o}\right)^\nu \right],$$

$$\frac{\psi_{\nu-\frac{1}{2}}}{\Delta} \sim \frac{1}{\nu} \sqrt{\frac{2m\Omega}{\pi\nu}} \left(\frac{em\Omega}{2\nu}\right)^\nu \left(\frac{r_o}{r}\right)^{\frac{1}{2}} \left[\left(\frac{r_o}{r}\right)^\nu \text{ or } \left(\frac{r}{r_o}\right)^\nu \right],$$

where the second term in each braket applies close to the imaginary axis. Above the real axis the expansion

$$\frac{1}{\cos \nu\pi} = 2 \sum_{s=o}^{\infty} (-1)^s \exp\left[i\pi\nu(2s+1)\right] \qquad (3.5\text{-}2)$$

is valid. Below the real axis, the corresponding expansion is

$$\frac{1}{\cos \nu\pi} = 2 \sum_{s=o}^{\infty} (-1)^s \exp\left[-i\pi\nu(2s+1)\right] .$$

From Appendix D, for $0 < \theta < \pi$,

$$P_{\nu-\frac{1}{2}}(\cos\theta) \sim \left(\frac{2}{\nu\pi \sin}\right)^{\frac{1}{2}} \cos \nu\theta , \qquad |\nu| \to \infty .$$

When these results are applied to the integrands of equations (3.4-13) and (3.4-14), one finds that

$$f(r, \theta; \nu) \exp\left[-i\pi\nu(2s+1)\right] \sim \exp i\nu\left[(\theta - \frac{3\pi}{2}) - 2\pi s\right] \text{ on } \Gamma_2 ,$$

$$f(r, \theta; \nu) \exp\left[i\pi\nu(2s+1)\right] \sim \exp i\nu\left[2\pi s + (\frac{\pi}{2} - \theta)\right] \text{ on } \Gamma_1 .$$

Since the paths of integration avoid the singularities of the integrands it follows that

$$\lim_{n \to \infty} \int_{\Gamma_2} f(r, \theta; \nu) \exp\left[-i\pi\nu(2s+1)\right] d\nu = 0 , \qquad (3.5\text{-}3)$$

for all s when $0 < \theta < \pi$, and that

$$\lim_{n \to} \int_{\Gamma_1} f(r, \theta; \nu) \exp\left[i\pi\nu(2s+1)\right] d\nu = 0 \qquad (3.5\text{-}4)$$

for all θ, $0 < \theta < \pi$ when $s \geq 1$. However, for $s = 0$ Jordan's lemma gives

$$\theta < \frac{\pi}{2} \qquad (3.5\text{-}5)$$

as the condition under which formula (3.5-4) is valid. Also, since $P_{\nu - \frac{1}{2}}(1) = 1$, it is easily verified that all of the above results remain true if $\theta = 0$. Near $\theta = \pi$, however, the equations (3.4-13) and

(3.4-14) can no longer be employed for $P_{\nu-\frac{1}{2}}(\cos\theta)$ has a logarithmic singularity at this point.

It is appropriate to indicate here that, for the case of a scalar plane wave, Nussenzveig (2) also found the term with s=0 to be the critical one in determining the solution in the illuminated zone. He showed that only this term needs to be considered for obtaining the solution outside of the shadow zone.

In view of the foregoing discussion, it follows that the functions $\varphi|_{p=-i\omega}$ and $\psi|_{p=-i\omega}$ can be written as

$$\phi = e^{i\pi/4}(2\pi)^{3/2}\phi_0(-i\omega)\sum_{s=0}^{\infty}(-1)^s\sum_{\nu_j}\nu\frac{\phi_{\nu-1/2}}{\partial\Delta/\partial\nu}P_{\nu-1/2}(\cos\theta)\exp\left[i\nu\left(2\pi s+\frac{\pi}{2}\right)\right], \qquad (3.5\text{-}6)$$

$$\psi = (2\pi)^{3/2}e^{i\pi/4}\phi_0(-i\omega)\sum_{s=0}^{\infty}(-1)^s\sum_{\nu_j}\nu\frac{\psi_{\nu-1/2}}{\partial\Delta/\partial\nu}\cdot\frac{dP_{\nu-1/2}(\cos\theta)}{d\theta}\exp\left[i\nu\left(2\pi s+\frac{\pi}{2}\right)\right], \qquad (3.5\text{-}7)$$

for $0 \le \theta < \frac{\pi}{2}$, where the ν_j are the zeros of $\Delta(r_o, -i\omega, \nu-\frac{1}{2})$ in the first quadrant.

3.6. Evaluation of the Transient Response

3.6.1. Introduction. The analytical evaluation of the solution will now be performed; the technique to be followed has already been employed in section 2.7. In sections 3.2 and 3.3 it was indicated that the series in (3.2-10) and (3.2-11) are meromorphic functions of p with poles at the origin and to the left of the imaginary axis; the path C in

Fig. 3 was shown to be equivalent to the Bromwich contour. In section (3.4) and section (3.5) several properties of the functions $\varphi(r, \theta, p=-i\omega)$ and $\psi(r, \theta, p=-i\omega)$ were deduced. The final forms obtained in section 3.5 give the behavior of the functions for $\omega \to \infty$. Hence, using for φ and ψ the expressions given in (3.5-6) and (3.5-7), one finds that

$$\begin{Bmatrix} \Phi \\ \Psi \end{Bmatrix} = \frac{1}{2\pi i}\int_C e^{-i\omega t} \begin{Bmatrix} \varphi \\ \psi \end{Bmatrix} d(-i\omega) = \frac{1}{2\pi i}\int_{Br_1} e^{pt} \begin{Bmatrix} \varphi \\ \psi \end{Bmatrix}_{-i\omega=p} dp, \quad (3.6\text{-}1)$$

which is valid for short times.

A similar analysis shows that the transformed displacements possess the same properties found for φ and ψ. Hence, one may write, for $0 \le \theta < \frac{\pi}{2}$,

$$u_r = \sum_{s=o}^{\infty} (-1)^s \sum_{\nu_j} \nu P_{\nu-\frac{1}{2}}(\cos\theta) \exp\left[i\nu(2\pi s+\frac{\pi}{2})\right] u_r^{**} \quad (3.6\text{-}2)$$

$$u_\theta = \sum_{s=o}^{\infty} (-1)^s \sum_{\nu_j} \nu \frac{dP_{\nu-\frac{1}{2}}(\cos\theta)}{d\theta} \exp\left[i\nu(2\pi s+\frac{\pi}{2})\right] u_\theta^{**} \quad (3.6\text{-}3)$$

where

$$u_r^{**} = \frac{\varphi_o(-i\omega)\, e^{i\pi/4}(2\pi)^{3/2}}{r} \left\{ \varphi_{\nu-\frac{1}{2}}(mv\vartheta(\nu, mv) - \frac{1}{2}) - (\nu^2 - \frac{1}{4})\, \psi_{\nu-\frac{1}{2}} \right\} \left(\frac{\partial\Delta}{\partial\nu}\right)^{-1},$$

$$u_\theta^{**} = \frac{\varphi_o(-i\omega)\, e^{i\pi/4}(2\pi)^{3/2}}{r} \left\{ \varphi_{\nu-\frac{1}{2}} - \psi_{\nu-\frac{1}{2}}(v\vartheta'(\nu, v) + \frac{1}{2}) \right\} \left(\frac{\partial\Delta}{\partial\nu}\right)^{-1},$$

and the ν_j are the roots of $\Delta(r_o, -i\omega, \nu-\frac{1}{2})$ in the first quadrant. Thus,

to find the displacements at the wave fronts it remains only to apply one of the inversion formulas (3.6-1) to (3.6-2) and (3.6-3). Again this will be done for the displacements at $r=r_o$. A step-function input will be assumed. The normalization constant

$$U_1 = \frac{\tau_o r_o}{\lambda + 2\mu} \tag{3.6-4}$$

is introduced in the final expressions.

3.6.2. Contributions from the Roots ν_{2j} Corresponding to Dilatational Waves. The contributions from the roots ν_{2j} are found in a similar manner as those from the roots ν_{2j} of the point load case. In the vicinity of the roots, the dominant term of $\Delta(r_o, -i\omega, \nu-\frac{1}{2})$ is given by

$$\Delta(r_o, -i\omega, \nu-\tfrac{1}{2}) \sim \frac{\mathcal{N}^2(\nu)\,\mu e^{-i\pi/2}}{\sqrt{m\,\Omega\, r_o^4}} (2\nu^2-\Omega^2)^2 H_\nu^{(1)}(\Omega)\, H_\nu^{(1)}(m\Omega) \,. \tag{3.6-5}$$

Consequently, in this region the zeros of $\Delta(r_o, -i\omega, \nu-\frac{1}{2})$ are the same as the zeros of $H_\nu^{(1)}(m\Omega)$. These zeros are given by

$$\nu_{2j} \sim m\Omega + 2^{-1/3} e^{i\pi/3} (e^{-i\pi} z_j) (m\Omega)^{1/3} , \quad j = 1, 2, \ldots , \tag{3.6-6}$$

where the z_j are the zeros of Ai(z). From equations (A.39), (A.40), (E.11), and (E.12), it follows that

$$J_\nu(m\Omega)\Big|_{\nu=\nu_{2j}} = \left(\frac{2}{\nu_{2j}}\right)^{1/3} \frac{e^{i\pi/6}}{2}\, Bi(z_j) \quad ,$$

where Bi(z) is defined by equation (E. 11). Using these results and equations (3. 6-2), (3. 6-3), one finds that

$$u_r = -\frac{(2\pi)^{3/2}\phi_0(-i\omega)\,2^{1/3}m^2}{(2m^2-1)\,r_0\sqrt{2\pi\sin\theta}}\left(-\frac{i\omega r_0}{C_d}\right)^{2/3} \times$$

$$\times \sum_{s=0}^{\infty}(-1)^s \sum_{\nu_{2j}} \left\{\exp i\nu\left[2\pi s+\left(\tfrac{\pi}{2}-\theta\right)\right]+\exp i\nu\left[2\pi s+\left(\tfrac{\pi}{2}+\theta\right)\right]\right\} Bi(z_j), \qquad (3.6\text{-}7)$$

$$u_\theta = \frac{(2\pi)^{3/2}\phi_0(-i\omega)\,2^{1/3}(1-m^2)^{1/2}}{(2m^2-1)\,r_0\sqrt{2\pi\sin\theta}}\left(-\frac{i\omega r_0}{C_d}\right)^{2/3} \times \qquad (3.6\text{-}8)$$

$$\times \sum_{s=0}^{\infty}(-1)^s \sum_{\nu_{2j}} \left\{\exp i\nu\left[2\pi s+\left(\tfrac{\pi}{2}-\theta\right)\right]-\exp i\nu\left[2\pi s+\left(\tfrac{\pi}{2}+\theta\right)\right]\right\} Bi(z_j).$$

By comparison with the series (2. 7-9) and (2. 7-10), it is concluded that the above series are useful in the deep shadow region, $\theta \ll \frac{\pi}{2}$.

The infinite sums appearing here have the same physical interpretation as those in (2. 7-9) and (2. 7-10). Here, however, no diffraction starts until the incident wave front reaches the ring $(r, \theta) = (r_o, \frac{\pi}{2})$; that is, the diffracted waves have their origin at $r=r_o$, $\theta = \frac{\pi}{2}$, when t=0.

Substituting p for -iω in (3. 6-6), (3. 6-7), and (3. 6-8), one

obtains

$$i\nu_{2j} = -p\,\frac{r_o}{C_d} - 2^{-1/3}(e^{-i\pi}z_j)\left(\frac{p\,r_o}{C_d}\right)^{1/3} \quad , \tag{3.6-9}$$

and by applying (3.6.1),

$$\frac{U_r}{U_1} = -\frac{2\pi m^2 2^{1/3}}{(2m^2-1)\sqrt{\sin\theta}}\sum_{s=0}^{\infty}(-1)^s\sum_{z_{2j}}\left[E_j\left(t, 2\pi s+\tfrac{\pi}{2}-\theta\right)+E_j\left(t, 2\pi s+\tfrac{\pi}{2}+\theta\right)\right], \tag{3.6-10}$$

$$\frac{U_\theta}{U_1} = \frac{2\pi(1-m^2)^{1/2}2^{1/3}}{(2m^2-1)\sqrt{\sin\theta}}\sum_{s=0}^{\infty}(-1)^s\sum_{z_{2j}}\left[E_j\left(t, 2\pi s+\tfrac{\pi}{2}-\theta\right)-E_j\left(t, 2\pi s+\tfrac{\pi}{2}+\theta\right)\right], \tag{3.6-11}$$

where

$$E_j(t,\theta) = \frac{\mathrm{Bi}(z_j)}{2\pi i}\int_{B_{r_1}} \frac{r_o}{C_d}\left(\frac{p\,r_o}{C_d}\right)^{-1/3} y(\theta)\,dp \quad , \tag{3.6-12}$$

and $y(\theta)$ is given by equation (2.7-17). The above integrals also have the form of equation (2.7-18) and, therefore, the final expressions here are

$$\frac{U_r}{U_1} = -\frac{8.05m^2\sqrt{\pi}}{(2m^2-1)\sqrt{\sin\theta}}\cdot\frac{Bi(z_1)}{\left(\frac{\pi}{2}-\theta\right)^{11/4}}T_5^{9/4}\,x$$

$$x\ \exp\left[-0.9742\left(\tfrac{\pi}{2}-\theta\right)^{3/2}T_5^{-1/2}\right]H(T_5), \tag{3.6-13}$$

$$\frac{U_\theta}{U_1} = - \frac{(1-m^2)^{\frac{1}{2}}}{m^2} \frac{U_r}{U_1} \quad , \tag{3.6-14}$$

in which

$$T_s = \frac{t C_d}{r_o} - \left(\frac{\pi}{2} - \theta\right) \quad , \tag{3.6-15}$$

and the inequalities (corresponding to (2.7-24))

$$0 < \theta \quad , \quad 1 < \frac{\pi}{2} - \theta \quad , \quad \frac{t C_d}{r_o} < \min\left(\frac{1}{m}\left(\frac{\pi}{2} - \theta\right), \frac{\pi}{2} + \theta\right) \tag{3.6-16}$$

must be satisfied. When $m = 0.5$, these expressions reduce to

$$\frac{U_r}{U_1} = - \frac{3.26}{\sqrt{\sin\theta}} \frac{T_5^{9/4}}{\left(\frac{\pi}{2} - \theta\right)^{11/4}} \exp\left[-0.9742 \left(\frac{\pi}{2} - \theta\right)^{5/2} T_5^{-\frac{1}{2}}\right] H(T_5) \quad , \tag{3.6-17}$$

$$\frac{U_\theta}{U_1} = -2\sqrt{3} \frac{U_r}{U_1} \quad . \tag{3.6-18}$$

these results are shown in Figure 14 for $\theta = \frac{\pi}{6}$.

3.6.3. Contributions from the Rayleigh Root. In the context of this chapter, the Rayleigh root is given by

$$\text{Re } \nu_R \sim \nu_o = \zeta_o^{\frac{1}{2}} \Omega \, ,$$

$$\text{Im } \nu_R = \sigma_o \sim + \text{const } \Omega \, e^{-\text{const } \Omega} \quad ,$$

where ν_o and σ_o have been defined in section 2.7.

From Table A1 it follows that in the first quadrant, close to the Rayleigh root,

$$J_\nu(m\,\Omega) = \frac{1}{2}\, S_\nu^{(1)}(m\,\Omega) \;;$$

hence equation (A.7) can be used directly to give

$$J_\nu(m\,\Omega) \sim \frac{1}{2}\sqrt{\frac{\pi}{2}}\,(\nu^2 - \Omega^2)^{-1/4}\, e^{\nu(\tanh\gamma - \gamma)}\,, \quad \nu = m\Omega\cosh\gamma\,,$$

or

$$J_\nu(m\,\Omega) \sim \frac{1}{2}\;\frac{\pi}{2}\;\Omega^{-\frac{1}{2}}\left(\frac{\nu^2}{\Omega^2} - 1\right)^{1/4} \exp\nu\left[\left(\frac{\nu^2}{\Omega^2} - m^2\right)\frac{\Omega}{\nu} - \cosh^{-1}\frac{\nu}{m\Omega}\right]$$

Using these results and equations (3.6-2), (3.6-3), one finds that when m=0.5

$$\frac{u_{rR}}{U_1} = \frac{0.250\,(2\pi)^{3/2}}{\sqrt{\sin\theta}}\cdot\frac{r_o}{C_d}\, e^{i\,7\pi/4}\, \nu_R^{-1/2} \times$$
$$\times \sum_{s=0}^{\infty}(-1)^s e^{-0.507\nu_R}\left\{\exp i\nu_R\left(2\pi s + \tfrac{\pi}{2} - \theta\right) + \exp i\nu_R\left(2\pi s + \tfrac{\pi}{2} + \theta\right)\right\}, \qquad (3.6\text{-}19)$$

$$\frac{u_{\theta R}}{U_1} = -\frac{0.128\,(2\pi)^{3/2}}{\sqrt{\sin\theta}}\cdot\frac{r_o}{C_d}\, e^{i\,7\pi/4}\, \nu_R^{-1/2} \times$$
$$\times \sum_{s=0}^{\infty}(-1)^s e^{-0.507\nu_R}\left\{\exp i\nu_R\left(2\pi s + \tfrac{\pi}{2} - \theta\right) - \exp i\nu_R\left(2\pi s + \tfrac{\pi}{2} + \theta\right)\right\}. \qquad (3.6\text{-}20)$$

From the discussion given after equation (2. 7-31), one concludes that the perdominant disturbance for long time is given by the Rayleigh root, in accordance with Miklowitz (3, 4) who showed this to be the case for the cylindrical cavity diffraction problems.

The application of (3. 6-1) gives

$$\begin{Bmatrix} U_{rR} \\ U_{\theta R} \end{Bmatrix} = \frac{1}{2\pi i} \int_C \begin{Bmatrix} u_{rR} \\ u_{\theta R} \end{Bmatrix}_{-i\omega = p} e^{pt}\, dp \quad , \tag{3.6-21}$$

and, since the semi-circle C_o in Fig. 3 gives no contribution to the integrals, these integrals reduce to

$$\begin{Bmatrix} U_{rR} \\ U_{\theta R} \end{Bmatrix} = \frac{Re}{\pi} \int_0^\infty \begin{Bmatrix} u_{rR} \\ u_{\theta R} \end{Bmatrix}_{p=-i\omega} e^{-i\omega t}\, d\omega \quad , \tag{3.6-22}$$

where property (3. 3-3) has been used. More explicitly,

$$\frac{U_{rR}}{U_1} = \frac{Re}{\pi} \cdot \frac{e^{i7\pi/4}\, 0.250\, (2\pi)^{3/2}}{\sqrt{\sin\theta}} \sum_{s=0}^{\infty} (-1)^s \int_0^\infty \nu_R^{-1/2}\, e^{-0.507\nu_R}\, g(\nu_R, s)\, e^{-i\omega \frac{r_o}{C_d}}\, d\omega, \tag{3.6-23}$$

$$\frac{U_{\theta R}}{U_1} = \frac{Re}{\pi} \cdot \frac{(-0.128)(2\pi)^{3/2}}{\sqrt{\sin\theta}}\, e^{i7\pi/4} \sum_{s=0}^{\infty} (-1)^s \int_0^\infty \nu_R^{-1/2}\, e^{-0.507\nu_R \frac{r_o}{C_d}}\, h(\nu_R, s)\, e^{-i\omega t}\, d\omega, \tag{3.6-24}$$

where

$$i\nu_R = i\nu_o - \sigma_o \quad , \tag{3.6-25}$$

$$g(\nu_R, s) = \exp i\nu_R\left(2\pi s + \frac{\pi}{2} - \theta\right) + \exp i\nu_R\left(2\pi s + \frac{\pi}{2} + \theta\right), \qquad (3.6\text{-}26)$$

$$h(\nu_R, s) = \exp i\nu_R\left(2\pi s + \frac{\pi}{2} - \theta\right) - \exp i\nu_R\left(2\pi s + \frac{\pi}{2} + \theta\right). \qquad (3.6\text{-}27)$$

For the approximations being determined here, it is sufficient to assume, as was done in reference (4), a certain constant value of σ_o, denoted by a small number and accounting for a correction term so generated. The qualitative features of the Rayleigh waves are then contained in

$$\frac{U_{rR}}{U_1} = \frac{Re^{i7\pi/4}}{\pi}\frac{0.250(2\pi)^{3/2}}{\sqrt{\sin\theta}}\sum_{s=0}^{\infty}(-1)^s\left\{d\left(T_6, 2\pi s + \frac{\pi}{2} - \theta\right) + d\left(T_7, 2\pi s + \frac{\pi}{2} + \theta\right)\right\}, \qquad (3.6\text{-}28)$$

$$\frac{U_{\theta R}}{U_1} = -\frac{Re^{i7\pi/4}}{\pi}\frac{0.128(2\pi)^{3/2}}{\sqrt{\sin\theta}}\sum_{s=0}^{\infty}(-1)^s\left\{d\left(T_6, 2\pi s + \frac{\pi}{2} - \theta\right) + d\left(T_7, 2\pi s + \frac{\pi}{2} + \theta\right)\right\}, \qquad (3.6\text{-}29)$$

obtained from (3,6-23) and (3.6-24), where

$$d(T, \theta) = e^{-\sigma_A \theta}\int_o^{\infty} \nu_o^{-\frac{1}{2}}\, e^{-0.507\nu} \exp(-i\nu_o T)\, d\Omega, \qquad (3.6\text{-}30)$$

$$T_6 = \frac{tC_R}{r_o} - 2\pi s - \left(\frac{\pi}{2} - \theta\right), \qquad (3.6\text{-}31)$$

$$T_7 = \frac{t\, C_R}{r_o} - 2\pi s - \left(\frac{\pi}{2} + \theta\right) \quad . \tag{3.6-32}$$

These integrals may be evaluated by using the formula (20)

$$\int_0^\infty \frac{e^{-ax}}{\sqrt{x}} e^{-ixT} dx = \frac{\Gamma(1/2)}{(a^2+T^2)^{1/4}} \exp\left\{-\frac{i}{2}\arctan\frac{T}{a}\right\}, \quad a>0. \tag{3.6-33}$$

Thus,

$$\frac{U_{rR}}{U_1} = \frac{0.75}{\sqrt{\sin\theta}} \sum_{s=0}^{\infty} \left[D\left(T_6, 2\pi s + \frac{\pi}{2} - \theta\right) + D\left(T_7, 2\pi s + \frac{\pi}{2} + \theta\right)\right], \tag{3.6-34}$$

$$\frac{U_{\theta R}}{U_1} = -\frac{1.41}{\sqrt{\sin\theta}} \sum_{s=0}^{\infty} \left[D\left(T_6, 2\pi s + \frac{\pi}{2} - \theta\right) - D\left(T_7, 2\pi s + \frac{\pi}{2} + \theta\right)\right], \tag{3.6-35}$$

where

$$D(T,\theta) = \frac{e^{-\sigma_A \theta}}{(0.507)^2 + T^2}\left[\cos\left(\frac{1}{2}\arctan\frac{T}{0.507}\right) - \sin\left(\frac{1}{2}\arctan\frac{T}{0.507}\right)\right] \tag{3.6-36}$$

3.6.4. Discussion of the Results. As can be seen from equations (3.6-17), (3.6-18), and Figure 14, the diffracted wave fronts are smooth and have the same form as equation (2.7-43) which was derived from the general theory of diffraction. Recall that this agreement was also found in the case of a point load.

The contributions from the Rayleigh root, in the plane wave case, present a different behavior than was found for the point load case, as Miklowitz found for the cylindrical case. The significant difference is the non-singular nature of the Rayleigh waves at their arrival time. This means that the heads and tails of these waves have to be included in the solution (ref. (4) gives a scheme for considering these which could be applied here). This leads to the approximate form of the resultant disturbances given in Fig. 15.

BIBLIOGRAPHY

1. Nagase, M., "Diffraction of Elastic Waves by a Spherical Surface", J. Physical Society of Japan, Vol 11, pp. 279-301 (1956).

2. Nussenzveig, H. M., "High-Frequency Scattering by an Impenetrable Sphere", Annals of Physics, Vol. 34, no. 1 (1965).

3. Miklowitz, J., "Pulse Propagation in a Viscoelastic Solid with Geometric Dispersion", Stress Waves in Anelastic Solids, Springer-Verlag, Berlin, pp. 255-276 (1964).

4. Miklowitz, J., "Scattering of a Plane Elastic Compressional Pulse by a Cylindrical Cavity", Proc. Eleventh International Congress of Applied Mechanics, Springer-Verlag, 1966.

5. Peck, J. C., "Plane-Strain Diffraction of Transient Elastic Waves by a Circular Cavity", Ph. D. Thesis, Calif. Inst. of Technology, 1965.

6. Friedlander, F. G., Sound Pulses, Cambridge University Press (1958).

7. Mow, C. C., "On the Effects of Stress-Wave Diffraction on Ground Measurements: Part I", The Rand Corporation Res. Rep. Memorandum RM-4341-PR, January 1965.

8. Levy, R. B. and J. B. Keller, "Diffraction by a Smooth Object", Comm. Pure Appl. Math., Vol. 12, pp. 159-209 (1959).

9. Franz, W., "Uber die Greenschen Funktionen des Zylinders und der Kugel, Z. Naturforschung, Vol. 9a, pp. 705-716 (1954).

10. Nagase, M., "On the Zeros of Certain Transcendental Functions Related to Hankel Functions, Parts I and II," J. Physical Society of Japan, Vol. 9, pp. 826-853 (1954).

11. Bremmer, H., Terrestrial Radio Waves, Elsevier Pub. Co., New York, 1946.

12. Watson, G. N., "The Diffraction of Electric Waves by the Earth", Proc. Roy. Soc., Ser. A, Vol. 95, 1918.

13. Morse, P. M. and H. Feshbach, Methods of Theoretical Physics, McGraw-Hill, New York, 1953.

14. Titchmarsh, E. C., Introduction to the Theory of Fourier Integrals, second edition, Oxford University Press, p. 60, 1937.

15. Gilbert, F. and L. Knopoff, "Scattering of Impulsive Elastic Waves by a Rigid Cylinder", J. Acoust. Soc. Amer., pp. 1169-1175 (1959).

16. Ragab, F. M., "The Inverse Laplace Transform of an Exponential Function", Comm. Pure Appl. Math., Vol. 11, 1958.

17. de Hoop, A. T., Seismic Scattering Project, Second Annual Report, Institute of Geophysics, University of California, Los Angeles (1957).

18. Miklowitz, J., "Scattering of Transient Elastic Waves by a Circular Cylindrical Cavity", Air Force Special Weapons Center Report SWC TDR 63-43, November 1963.

19. Ewing, W. M., W. S. Jardetzky, and F. Press, Elastic Waves in Layered Media, McGraw-Hill, New York, 1957.

20. Oberhettinger, F., Tabellen zur Fourier Transformation, Die Grundlehren der Mathematischen Wissenschafter, Springer-Verlag, Berlin, 1957.

21. Chao, C. C., H. H. Bleich, and J. Sackman, "Surface Waves in an Elastic Half-Space", ASME Trans., 83E (J. Appl. Mech.), pp. 300-301 (1961); AMR, vol. 15, Rev. 558 (1962).

22. Gilbert, F., "Scattering of Impulsive Elastic Waves by a Smooth Convex Cylinder", J. Acoust. Soc. Amer., pp. 841-857 (1960).

23. Rosenfeld, R. L. and J. Miklowitz, "Wave Fronts in Elastic Rods and Plates", Proc. Fourth U. S. Nat. Cong. Appl. Mech.

24. Watson, G. N., Theory of Bessel Functions, second edition, Cambridge Univ. Press, 1962.

25. Keller, J. B., S. I. Rubinow, and M. Goldstein, "Zeros of Hankel Functions and Poles of Scattering Amplitudes", J. Mathematical Physics, vol. 4, pp. 829-832 (1963).

26. Nagase, M., "Asymptotic Expansions of Bessel Functions in the Transitional Regions", J. Physical Soc. of Japan, Vol. 9, pp. 296-297 (1954).

27. Watson, G. N., "Bessel Functions of Large Order", Proc. Camb. Phil. Soc., Vol. 19, pp. 96-110 (1918).

28. Abramowitz, M. and I. A. Stegun, editors, Handbook of Mathematical Functions, Natl. Bur. Stds. Appl. Math. Series 55, pp. 367, 446 (1964).

29. Sakai, Takuzo, "On the Propagation of Tremors over Plane Surface of an Elastic Solid Produced by an Internal Source", Geophysical Magazine, Vol 8, pp. 1-74. (1934).

30. Victorov, I. A., "Rayleigh-Type Waves on a Cylindrical Surface", Soviet Physics-Acoustics, Vol. 4, pp. 131-136 (1958).

31. Erdelyi, A., W. Magnus, F. Oberthettinger, and F. G. Tricomi, Higher Transcendental Functions, Vol. 2, Bateman Manuscript Project, McGraw-Hill, New York, 1953.

32. Watson, G. N., "Asymptotic Expansions of Hypergeometric Functions", Trans. Cambr. Phil. Soc., Vol. 22, no. 14, pp. 277-308.

33. Robin, L., Fonctions Spheriques de Legendre et Fonctions Spheroidales, Tome II, Gauthier-Villars, Paris, 1958.

34. Szegö, G., "Uber Einige Asymptotische Entwicklungen der Legendreschen Funktionen", Proc. London Math. Soc., (2) 36, p. 427 (1934).

35. Olver, F. W. J., "The Asymptotic Expansion of Bessel Functions of Large Order", Roy. Soc. of London, Philos. Trans., Vol. 27, pp. 328-368, 1954-55.

36. Olver, F. W. J., "Some New Asymptotic Expansions for Bessel functions of Large Order", Proc. Camb. Phil. Soc., Vol. 48, pp. 414-427 (1952).

37. Yeh, Gordon C. K., "The Diffraction of a Plane Compressional Wave by a Spherical Cavity in an Elastic Medium", ZAMP, Vol. 15, pp. 237-252 (1964).

38. Levey, H. C., and J. J. Mahoney, "The Interaction of a Plane Shock and a Cylindrical Body", Australian Defense Scientific Service, Aeronautical Research Laboratories, Aerodynamics Report 121, November 1961, ARL/A-121.

39. Ying, C. F., and R. Truell, "Scattering of a Plane Longitudinal Wave by a Spherical Obstacle in an Isotropically Elastic Solid", J. Appl. Phys., Vol. 27, pp. 1086-1097 (1956).

40. Sezawa, K., "On the Propagation of Rayleigh Waves on Plane and Spherical Surfaces," Bull. Earthquake Research Institute (Tokyo), Vol. 2, pp. 21-28 (1927).

41. Sezawa, K., "Propagation of Love Waves on a Spherical Surface and Allied Problems", Bull. Earthquake Research Inst. (Tokyo), Vol. 7, pp. 437-456 (1928).

42. McLachlan, N. W., Complex Variable Theory and Transform Calculus, second edition, Cambridge University Press, London, 1963.

43. Fock, V. A., Electromagnetic Diffraction and Propagation Problems, Pergamon Press, New York, 1965.

44. Lloyd, J. R., and J. Miklowitz, "On the Use of Double Integral Transforms in the Study of Dispersive Elastic Wave Propagation", Proc. Fourth U. S. Natl. Cong. Appl. Mechs., ASME, pp. 255-267, New York, 1962.

45. Erdelyi, A., W. Magnus, F. Oberthettinger, and F. G. Tricomi, Higher Transcendental Functions, Vol. 1, Bateman Manuscript Project, McGraw-Hill, New York, 1953.

46. Copson, E. T., An Introduction to the Theory of Functions of a Complex Variable, Oxford at the Clarendon Press, 1960.

47. Miklowitz, J., "Elastic Wave Propagation" Applied Mechanics Surveys, Spartan Books, Washington, D. C., pp. 809-839 (1966).

48. Van Der Pol, B., and H. Bremmer, Operational Calculus Based on the Two-Sided Laplace Integral, Cambridge at the University Press, 1964.

APPENDIX A. ASYMPTOTIC APPROXIMATIONS FOR BESSEL FUNCTIONS OF LARGE COMPLEX ORDER

Introduction

The primary purpose of this appendix is to present the asymptotic approximations for the Hankel functions of the second kind, $H_\nu^{(2)}(\Omega)$, valid as $|\nu| \to \infty$ and $\Omega \to \infty$. The results shown here are taken from Watson's Theory of Bessel Functions, reference (24), and from references (2), (10), (25), (26), (27), and (28). A common notation is used. Only a brief exposition of the results is intended here; for further details one should refer to the aforementioned references.

Expansions for Large ν and Ω with $|\nu|$ Larger than Ω

This section contains the asymptotic expansions for the region usually denoted as non-transitional (5) or non-oscillatory (10). These expansions are employed for $|\nu| >> \Omega$; more specifically, for

$$\lim_{|\nu| \to \infty} \left| \nu^{3/3} \left(\frac{\Omega}{\nu} - 1 \right) \right| = \infty . \tag{A. 1a}$$

For ν in the transitional region a separate analysis should be given. The transitional region is governed by

$$\lim_{|\nu| \to \infty} \left| \nu^{2/3} \left(\frac{\Omega}{\nu} - 1 \right) \right| < \infty \tag{A. 1b}$$

This case will be treated in a later section.

In Watson's work is is assumed that

$$\nu = \Omega \cosh \gamma = \Omega \cosh (\lambda + i\beta) , \tag{A. 2}$$

where $0 < \beta < \pi$ and λ is any real number. Consideration is then given to the integrals

$$H_{\nu}^{(1)}(\Omega) = \frac{1}{\pi i} \int_{-\infty}^{\infty+\pi i} e^{-\Omega f(w)}\, dw, \qquad (A.3)$$

$$H_{\nu}^{(2)}(\Omega) = -\frac{1}{\pi i} \int_{-\infty}^{\infty-\pi i} e^{-\Omega f(w)}\, dw = -\frac{1}{\pi i} \int_{-\infty+\pi i}^{\infty} e^{-\Omega f(w)}\, dw, \qquad (A.4)$$

where $f(w) \equiv w \cosh \gamma' - \sinh w$.

A stationary point of the integrands is at $w = \gamma'$. Hence, to evaluate the above integrals one should choose the contours that correspond to the steepest descent through the stationary point $w = \gamma'$; that is, the curve whose equation is $\mathrm{Im}\, f(w) = \mathrm{Im}\, f(\gamma')$. There are two such branches through $w = \gamma'$; their slopes at the point are

$$\pm \frac{\pi}{4} + \frac{1}{2} \tan^{-1} (\tanh \lambda \cot \beta),$$

where the $\tan^{-1}$ denotes an acute angle; $\mathrm{Re}\, f(w)$ increases as w moves away from γ' on the first branch, while it decreases as w moves away from γ' on the second branch.

The integrals along these branches [say (i) and (ii)] are denoted, respectively, by

$$S_{\nu}^{(1)}(\Omega) = \frac{1}{\pi i} \int_{(i)} e^{-\Omega f(w)}\, dw, \qquad (A.5)$$

$$S_{\nu}^{(2)}(\Omega) = \frac{1}{\pi i} \int_{(ii)} e^{\Omega f(w)}\, dw\,, \qquad (A.6)$$

With the aid of Watson's lemma these integrals yield the asymptotic expansions

$$S_{\nu}^{(1)}(\Omega) \sim A(\nu,\Omega)\, e^{\alpha} \sum_{m=0}^{\infty} \frac{\Gamma(m+\frac{1}{2})}{\Gamma(\frac{1}{2})} A_m \left(\frac{\nu}{2}\tanh\gamma\right)^{-m}\,, \qquad (A.7)$$

$$S_{\nu}^{(2)}(\Omega) \sim iA(\nu,\Omega)\, e^{-\alpha} \sum_{m=0}^{\infty} \frac{\Gamma(m+\frac{1}{2})}{\Gamma(\frac{1}{2})} A_m \left(-\frac{\nu}{2}\tanh\gamma\right)^{-m}\,, \qquad (A.8)$$

where

$$\left.\begin{aligned} A(\nu,\Omega) &= \left(-\frac{\nu\pi i}{2}\tanh\gamma\right)^{-\frac{1}{2}} e^{-i\pi/4} = \left(\frac{2}{\pi}\right)^{\frac{1}{2}} (\nu^2 - \Omega^2)^{-\frac{1}{4}}, \\ \alpha &= \nu(\tanh\gamma - \gamma) = (\nu^2 - \Omega^2)^{\frac{1}{2}} - \nu \ln\left[\frac{\nu}{\Omega} + \frac{(\nu^2-\Omega^2)^{\frac{1}{2}}}{\Omega}\right], \end{aligned}\right\} \qquad (A.9)$$

with

$$\arg\left(-\frac{\nu\pi i}{2}\tanh\gamma\right) = \arg\left(-i\sinh\gamma\right)\,, \qquad (A.10)$$

where the value of $\arg(-i\sinh\gamma)$ lies between $-\frac{\pi}{2}$ and $\frac{\pi}{2}$; the values of A_1, A_2, ..., are

$$A_0 = 1 , \qquad A_1 = \frac{1}{8} - \frac{5}{24} \coth^2 \gamma' ,$$

$$A_2 = \frac{3}{128} - \frac{77}{576} \coth^2 \gamma' + \frac{385}{3456} \coth^4 \gamma' , \ldots . \qquad (A.11)$$

These asymptotic expansions are invalid for the values of ν corresponding to small γ' because (A.1a) is violated; this case is the transitional case which will be presented in the next section.

Obviously, since $S_\nu^{(1)}(\Omega)$ and $S_\nu^{(2)}(\Omega)$ are solutions of Bessel's differential equation, they represent linear combinations of $H_\nu^{(1)}(\Omega)$ and $H_\nu^{(2)}(\Omega)$; the coefficients in the asymptotic expansions of the latter are determined by identifying the terminal points of the particular contours (i), (ii) in (A.5) and (A.6) with the terminal points of the paths in (A.3) and (A.4).

The location of the end points of (i) and (ii) depends on the values of ν . For some regions in the ν - plane, and the corresponding γ' -plane, shown in Figure A1, one obtains the end points which correspond to those of $H_\nu^{(1)}(\Omega)$ and $H_\nu^{(2)}(\Omega)$. Table A1 gives the end-points for the various regions in Fig. A1 and also the relationships between $S_\nu^{(1)}(\Omega)$, $S_\nu^{(2)}(\Omega)$ and $H_\nu^{(1)}(\Omega)$, $H_\nu^{(2)}(\Omega)$. Table A2 is obtained from Table A1 by a suitable rearrangement. In the tables, M and N denote respectively, the smallest integer for which

$$1 - \lambda \tan \lambda + \left[(M + 1)\pi - \beta\right] \cot \beta > 0 ,$$

when $\cot \beta > 0$, and

$$1 - \lambda \tan \lambda - (N\pi + \beta) \cot \beta > 0 ,$$

when $\cot\beta < 0$. The preceding two relations arise from generalizations of the equation

$$1 - \beta\cot\beta - \lambda\tanh\lambda = 0 .$$

The curves AB and AC in Fig. A1 correspond to this equation. The generalizations stem from extensions of the γ-plane depicted in Fig. A1.

The values of $H_\nu^{(2)'}(\Omega)$ corresponding to various values of are obtained when $S_\nu^{(1)}(\Omega)$, $S_\nu^{(2)}(\Omega)$, and $H_\nu^{(2)}(\Omega)$ in Tables A1 and A2 are replaced by $S_\nu^{(1)'}(\Omega)$, $S_\nu^{(2)'}(\Omega)$, and $H_\nu^{(2)'}(\Omega)$. The asymptotic expansions for $S_\nu^{(1)'}(\Omega)$ and $S_\nu^{(2)'}(\Omega)$, obtained by differentiating the above expressions for $S_\nu^{(1)}(\Omega)$ and $S_\nu^{(2)}(\Omega)$, are as follows:

$$S_\nu^{(1)'}(\Omega) \sim \sinh\gamma\, A(\nu,\Omega)\, e^{\alpha}\left[1 + C_1(\nu\tanh\gamma)^{-1} + C_2(\nu\tanh\gamma)^{-2} + \ldots\right], \quad (A.12)$$

$$S_\nu^{(2)'}(\Omega) \sim -i\sinh\gamma\, A(\nu,\Omega)\, e^{-\alpha}\left[1 - C_1(\nu\tanh\gamma)^{-1} + C_2(\nu\tanh\gamma)^{-2} + \ldots\right], \quad (A.13)$$

where

$$C_1 = -\frac{3}{8} + \frac{7}{24}\coth^2\gamma ,$$

$$C_2 = -\frac{15}{128} + \frac{33}{64}\coth^2\gamma - \frac{455}{1152}\coth^4\gamma .$$

The information in the tables is presented graphically in

Figure A2 for the various regions of the ν-plane. Additional information is also depicted. Construction of the figure is given in Appendix B because it is more pertinent to the discussion of the function $F(\nu,\Omega)$. The following comments apply (2): in the figure the notation of (A.9) has been used, where the branch of $(\nu^2-\Omega^2)^{1/2}$ was indicated in (A.10), more specifically, one must have

$$(\nu^2-\Omega^2)^{1/2} \longrightarrow \nu = |\nu| \exp(i\phi), \quad (-\pi < \phi \leq \pi), \quad \text{for } |\nu| \to \infty \qquad (A.14)$$

Thus,

$$A(\nu,\Omega) \longrightarrow \left(\frac{2}{\pi\nu}\right)^{1/2}, \qquad e^{\alpha} \longrightarrow \left(\frac{e\Omega}{2\nu}\right)^{\nu} \qquad \text{for } |\nu| \to \infty \ . \qquad (A.15)$$

The asymptotic behavior of $H_\nu^{(1)}(\Omega)$ and $H_\nu^{(2)}(\Omega)$ changes (Stokes' phenomenon) across certain "Stokes" lines, shown as thick lines in Fig. A2. For $H_\nu^{(1)}(\Omega)$, one has the curve $h_1(\mathrm{Re}\,\alpha = 0, \ \mathrm{Im}\,\nu > 0)$ and $h_{-1}(\mathrm{Re}(\alpha - i\pi\nu) = 0, \ \mathrm{Im}\,\nu < 0)$. These curves are symmetrical with respect to the origin and the zeros of $H_\nu^{(1)}(\Omega)$ are asymptotically located on them. The curve h_1 cuts the real axis at $\nu = \Omega$ at an angle of $\pi/3$. The tangent to this curve tends to the vertical direction for $|\nu| \to \infty$. Asymptotically, the curve approaches $\nu = \sigma|\nu|, \eta \longrightarrow -\frac{\pi}{2}$ where σ and η are defined as

$$\sigma = \exp\left[i\left(\frac{\pi}{2} + \epsilon\right)\right] \ , \qquad (A.16)$$

$$\eta = \epsilon \ln \left| \frac{2\nu}{e\Omega} \right| \quad , \qquad \text{(A. 17)}$$

and $\epsilon \to 0$ in such a way that η approaches a constant value.

For $H_\nu^{(2)}(\Omega)$, one has the Stokes lines $h_2(\mathrm{Re}\,\alpha = 0,\ \mathrm{Im}\,\nu < 0)$ and $h_{-2}(\mathrm{Re}\,(\alpha + i\pi\nu) = 0,\ \mathrm{Im}\,\nu > 0)$, which are complex conjugate to h_1 and h_{-1}, respectively, and where the zeros of $H_\nu^{(2)}(\Omega)$ are asymptotically located. In addition, one has the portions of the real axis denoted in Fig. A2 by j' (from $-\infty$ to $-\Omega$) and j (from $-\Omega$ to Ω), where the zeros of $J_\nu(\Omega)$ are located.

These curves divide the ν-plane into the five regions A to E shown in Fig. A2. The asymptotic behavior of $H_\nu^{(1)}(\Omega)$, $H_\nu^{(2)}(\Omega)$, $J_\nu(\Omega)$, and $J_{-\nu}(\Omega)$ in these regions is shown in the figure. Note that

$$J_\nu(\Omega) \longrightarrow (2\pi\nu)^{-1/2} \left| \frac{e\Omega}{2\nu} \right|^\nu \quad , \quad (|\nu| \to \infty) \qquad \text{(A. 18)}$$

in all regions. For each function there is a domain where it tends to zero for $|\nu| \to \infty$, whereas it tends to infinity outside this domain. For $J_\nu(\Omega)$, this domain is the region A. For $H_\nu^{(1)}(\Omega)$, it is the domain E between h_2 and the curve $\nu = -\sigma|\nu|$, $\eta \to -\frac{3\pi}{2}$ in the lower half-plane. For $H_\nu^{(2)}(\Omega)$, it is the domain B between h_1 and the curve $\nu = \sigma|\nu|$, $\eta \to \frac{3\pi}{2}$ in the upper half-plane. Finally, $J_{-\nu}(\Omega) \to 0$ in the regions C and D.

These results have to be modified in the neighborhood of each of the Stokes lines, where the two representations for the same function become of comparable order. One must then add the two represen-

tations to obtain the asymptotic expansions valid in these neighborhoods. Note that the function is the sum of the two representations in the two regions adjacent to a given Stokes line. However, one of them becomes negligible in comparison to the other away from the Stokes line. These neighborhoods are indicated by the shaded region in Fig. A2. Thus, to the first order, one has

$$H_\nu^{(1)}(\Omega) \sim 2A\, e^{i\pi/4} \sinh(\alpha - \tfrac{i\pi}{4}) \quad \text{in AB,} \tag{A.19}$$

$$H_\nu^{(1)}(\Omega) \sim -2A \exp(-i\pi\nu - \tfrac{i\pi}{4}) \sinh(\alpha - i\pi\nu + \tfrac{i\pi}{4}) \quad \text{in DE,} \tag{A.20}$$

$$H_\nu^{(2)}(\Omega) \sim -2A \exp(i\pi\nu + \tfrac{i\pi}{4}) \sinh(\alpha - i\pi\nu - \tfrac{i\pi}{4}) \quad \text{in BC,} \tag{A.21}$$

$$H_\nu^{(2)}(\Omega) \sim 2A e^{-i\pi/4} \sinh(\alpha + \tfrac{i\pi}{4}) \quad \text{in EA .} \tag{A.22}$$

In region BE, in the neighborhood of the real axis, one may employ the Debye asymptotic expansions

$$H_\nu^{(1,2)}(\Omega) = \sqrt{\tfrac{2}{\pi}} (\Omega^2 - \nu^2)^{-1/4} \exp\left\{ \pm i \left[(\Omega^2 - \nu^2)^{1/2} - \nu \cos\tfrac{\nu}{\Omega} - \tfrac{\pi}{4} \right] \right\} \times$$
$$\times \left[1 \mp \frac{i}{8(\Omega^2 - \nu^2)^{1/2}} \left(1 + \frac{5}{3} \frac{\nu^2}{\Omega^2 - \nu^2} + \cdots \right) + \cdots \right] \tag{A.23}$$

where the upper signs refer to $H_\nu^{(1)}(\Omega)$ and the lower ones to $H_\nu^{(2)}(\Omega)$, and $(\Omega^2 - \nu^2)^{-1/4} > 0$, $0 < \cos^{-1}\frac{\nu}{\Omega} < \frac{\pi}{2}$ for $-\Omega < \nu < \Omega$.

Asymptotic Approximations in the Transition Region

The transition region corresponds to the neighborhood of $\nu = \pm z$ where the asymptotic expansions given in the previous section are not valid. In this case, with

$$\nu = z \cosh \gamma \,, \tag{A. 24}$$

$$\gamma = O(z^{-1/3}) \prec\prec 1 \,, \tag{A. 25}$$

and therefore $|\nu - z|$ becomes comparable to $|\nu^{1/3}|$, that is

$$\lim_{\nu \to \infty} \left| \nu^{2/3} \left(\frac{z}{\nu} - 1 \right) \right| < \infty \,. \tag{A. 26}$$

As in reference (5), this case will be termed "transitional".

The formulas of the first approximation were investigated by Watson in (27). The results are

$$H_\nu^{(1)}(z) = -3^{-1/2} e^{i\pi/3} \eta \left[H_{-1/3}^{(1)}(\xi) - \frac{3}{5} \eta^2 \xi H_{2/3}^{(1)}(\xi) + O(\eta^4) \right] \,, \tag{A. 27}$$

$$H_\nu^{(2)}(z) = 3^{-1/2} e^{-i\pi/3} \eta \left[H_{-1/3}^{(2)}(\xi) - \frac{3}{5} \eta^2 \xi H_{2/3}^{(2)}(\xi) + O(\eta^4) \right] \tag{A. 28}$$

where

$$\xi = \frac{i\nu}{3} \tanh^3 \gamma \quad , \qquad \eta = \tanh \gamma \quad , \tag{A. 29}$$

and z, ν are unrestricted complex numbers. These results were improved (10) by noticing the form of (A. 27) and (A. 28) and assuming for $H_\nu^{(2)}(z)$ the following expansion with unknown coefficients:

$$H_\nu^{(2)}(z)=3^{-1/2}e^{-i\pi/3}\left[\eta H_{-1/3}^{(2)}(\xi)+\sum_{n=1}^{\infty} q_n(\xi)\eta^{2n+1}\right] \qquad \text{(A. 30)}$$

By substituting into Bessel's differential equation,

$$\frac{d^2H_\nu^{(2)}(z)}{dz^2}+\frac{1}{z}\cdot\frac{dH_\nu^{(2)}(z)}{dz}=-\left(1-\frac{\nu^2}{z^2}\right)H_\nu^{(2)}(z)=\sinh^2\gamma\, H_\nu^{(2)}(z) \qquad \text{(A. 31)}$$

and equating coefficients of the same powers of η , one obtains a system of differential equations for the q_n's, for example,

$$\begin{aligned} q_1''(\xi)+\frac{7}{3\xi}q_1'(\xi)+\left(1+\frac{1}{3\xi^2}\right)q_1(\xi)&=-2H_{-1/3}^{(2)}(\xi)-\frac{2}{3\xi}H_{2/3}^{(2)}(\xi), \\ q_2''(\xi)+\frac{11}{3\xi}q_2'(\xi)+\left(1+\frac{5}{3\xi^2}\right)q_2(\xi)&=-H_{-1/3}^{(2)}(\xi)+q_1''(\xi)+\frac{3}{\xi}q_1'(\xi) \\ &\quad+\left(-1+\frac{1}{\xi^2}\right)q_1(\xi). \end{aligned} \qquad \text{(A. 32)}$$

By an iterative process one obtains expressions for the q_n's , for example, $q_1(\xi)$ is given by

$$q_1(\xi)=\frac{1}{10}H_{-1/3}^{(2)}(\xi)-\frac{3}{5}H_{2/3}^{(2)}(\xi)\,. \qquad \text{(A. 33)}$$

Thus one finds that

$$H_\nu^{(2)}(z) \sim 3^{-1/2} e^{-i\pi/3} \eta \left[(a_1(\xi') + a_2(\xi') + \cdots) H_{-1/3}^{(2)}(\xi') + (b_1(\xi') + b_2(\xi') + \cdots) \xi'^{-1} H_{2/3}^{(2)}(\xi') \right] \quad \text{(A. 34)}$$

in which

$$\left.\begin{aligned} a_1(\xi') &= 1 + \frac{1}{10}\eta^2 \quad , \quad b_1 = -\frac{3}{5}\xi'^2\eta^2 , \\ a_2(\xi') &= \left(\frac{13}{280} - \frac{9}{50}\xi'^2\right)\eta^4 + \left(\frac{803}{25200} - \frac{921}{3500}\xi'^2\right)\eta^6 + \\ &\quad + \left(-\frac{1.3959}{\xi'^2} + 1.3329 - 0.61168\xi'^2 + 0.0054\xi'^4\right)\eta^8 , \\ b_2(\xi') &= \left(\frac{1}{210} - \frac{3}{7}\xi'^2\right)\eta^4 + \left(\frac{37}{18900} - \frac{197}{600}\xi'^2 + \frac{9\xi'^4}{950}\right)\eta^6 + \\ &\quad + \left(-2.0929 + 0.51938\xi'^2 - 0.038541\xi'^4\right)\eta^8 . \end{aligned}\right\} \quad \text{(A. 35)}$$

By a similar process one finds that

$$H_\nu^{(1)}(z) \sim -3^{-1/2} e^{-i\pi/3} \eta \left[(a_1(\xi') + a_2(\xi') + \cdots) H_{-1/3}^{(1)}(\xi') + (b_1(\xi') + b_2(\xi') + \cdots) \xi'^{-1} H_{2/3}^{(1)}(\xi') \right] \quad \text{(A. 36)}$$

Differentiation with respect to z yields

$$H_\nu^{(2)\prime}(z) \sim -i 3^{-1/2} e^{-i\pi/3} \eta^2 (\cosh\gamma)^{-1} \left[c_1(\xi') \xi'^{-1} H_{-1/3}^{(2)}(\xi') + c_2(\xi') H_{2/3}^{(2)}(\xi') \right] , \quad \text{(A. 37)}$$

where

$$\left.\begin{aligned} c_1(\zeta) &= \left(\frac{1}{15} - \frac{3}{5}\zeta^{1/2}\right)\eta^2 + \left(\frac{1}{15} - \frac{36}{35}\zeta^{1/2}\right)\eta^4 + \cdots, \\ c_2(\zeta) &= -1 - \frac{9}{10}\eta^2 + \left(-\frac{253}{280} + \frac{9}{50}\zeta^{1/2}\right)\eta^4 + \cdots, \end{aligned}\right\} \qquad \text{(A. 38)}$$

with a similar expression for $H_\nu^{(1)'}(\Omega)$.

Reference (28), pages 367 and 446, gives another form of the expansions

$$H_\nu^{(1,2)}(\Omega) = 2\exp\left(\mp i\frac{\pi}{3}\right)\left(\frac{2}{\nu}\right)^{1/3} Ai\left[\exp\left(\pm i\frac{2\pi}{3}\right)\left(\frac{2}{\nu}\right)^{1/3}(\nu - \Omega)\right] + O(\Omega^{-1}), \qquad \text{(A. 39)}$$

$$J_\nu(\Omega) = \left(\frac{2}{\nu}\right)^{1/3} Ai\left[\left(\frac{2}{\nu}\right)^{1/3}(\nu - \Omega)\right] + O(\Omega^{-1}), \qquad \text{(A. 40)}$$

where Ai denotes the Airy function defined in Appendix E.

TABLE A1

Regions	End-points	$S_\nu^{(1)}(z)$
1, 3, 4	$-\infty,\ \infty + \pi i$	$H_\nu^{(1)}(z)$
2, 6a	$\infty - \pi i,\ \infty + \pi i$	$2J_\nu(z)$
5, 7b	$-\infty,\ -\infty + 2\pi i$	$2e^{-\nu\pi i}J_{-\nu}(z)$
6b	$-\infty - 2N\pi i,\ \infty + \pi i$	$e^{N\nu\pi i}H_\nu^{(1)}(ze^{-N\pi i})$
7a	$-\infty,\ \infty + (2M+1)\pi i$	$e^{-M\nu\pi i}H_\nu^{(1)}(ze^{-M\pi i})$
Regions	**End-points**	$S_\nu^{(2)}(z)$
1, 2, 5	$-\infty + \pi i,\ \infty$	$H_\nu^{(2)}(z)$
3, 7a	$-\infty + \pi i,\ -\infty - \pi i$	$2J_\nu(z)$
4, 6b	$\infty + 2\pi i,\ \infty$	$2e^{\nu\pi i}J_{-\nu}(z)$
6a	$-\infty + (2M+1)\pi i,\ \infty$	$e^{M\nu\pi i}H_\nu^{(2)}(ze^{M\pi i})$
7b	$-\infty + \pi i,\ \infty - 2N\pi i$	$e^{-N\nu\pi i}H_\nu^{(2)}(ze^{N\pi i})$

TABLE A2

Regions	$H_\nu^{(1)}(a)$	$H_\nu^{(2)}(a)$
1	$S_\nu^{(1)}(a)$	$S_\nu^{(2)}(a)$
2	$S_\nu^{(1)}(a) - S_\nu^{(2)}(a)$	$S_\nu^{(2)}(a)$
3	$S_\nu^{(1)}(a)$	$S_\nu^{(2)}(a) - S_\nu^{(1)}(a)$
4	$S_\nu^{(1)}(a)$	$S_\nu^{(2)}(a) - e^{2\nu\pi i} S_\nu^{(1)}(a)$
5	$S_\nu^{(1)}(a) - e^{-2\nu\pi i} S_\nu^{(2)}(a)$	$S_\nu^{(2)}(a)$
6a	$\frac{\sin(M+1)\nu\pi}{\sin \nu\pi} e^{M\nu\pi i} S_\nu^{(1)}(a) - S_\nu^{(2)}(a)$	$S_\nu^{(2)}(a) - \frac{\sin M\nu\pi}{\sin \nu\pi} e^{(M+1)\nu\pi i} S_\nu^{(1)}(a)$
6b	$S_\nu^{(1)}(a) - \frac{\sin N\nu\pi}{\sin \nu\pi} e^{(N-1)\nu\pi i} S_\nu^{(2)}(a)$	$\frac{\sin(N+1)\nu\pi}{\sin \nu\pi} e^{N\nu\pi i} S_\nu^{(2)}(a) - e^{2\nu\pi i} S_\nu^{(1)}(a)$
7a	$S_\nu^{(1)}(a) - \frac{\sin M\nu\pi}{\sin \nu\pi} e^{-(M+1)\nu\pi i} S_\nu^{(2)}(a)$	$\frac{\sin(M+1)\nu\pi}{\sin \nu\pi} e^{-M\nu\pi i} S_\nu^{(2)}(a) - S_\nu^{(1)}(a)$
7b	$\frac{\sin(N+1)\nu\pi}{\sin \nu\pi} e^{-N\nu\pi i} S_\nu^{(1)}(a) - e^{-2\nu\pi i} S_\nu^{(2)}(a)$	$S_\nu^{(2)}(a) - \frac{\sin N\nu\pi}{\sin \nu\pi} e^{-(N-1)\nu\pi i} S_\nu^{(1)}(a)$

APPENDIX B. ASYMPTOTIC EXPANSION OF $F(\nu,\Omega)$ AS A FUNCTION OF FOR LARGE

Introduction

In this appendix a summary of the asymptotic properties of the function $F(\nu,\Omega)$ is given. These properties were derived in detail in reference (10) and were rederived by the author. Here it is shown that some of the results can be obtained and extended by techniques simpler than those of (10). Only the results needed in the text are given.

Basic Formulas

$$F(\nu,\Omega) = \frac{d}{d\Omega}(\ln H_\nu^{(2)}(\Omega)) = -\frac{J_2 + \pi i/4\Omega}{J_1}, \qquad \text{(B. 1)}$$

where

$$\left.\begin{aligned} J_1 &\equiv \int_0^\infty K_0(t)\cosh 2\nu\xi' d\xi' = \frac{\pi^2}{8} H_\nu^{(1)}(\Omega)\, H_\nu^{(2)}(\Omega) \ , \\ J_2 &\equiv -\frac{1}{2}\cdot\frac{\partial J_1}{\partial \Omega} = \int_0^\infty K_1(t)\sinh\xi' \cosh 2\nu\xi' d\xi' \ , \\ t &= 2\Omega\sinh\xi' \ , \end{aligned}\right\} \qquad \text{(B. 2)}$$

valid for any complex ν and $\mathrm{Re}\,\Omega > 0$.

Preliminary Analysis

In reference (10) a preliminary analysis of $F(\nu,\Omega)$ was performed by considering equation (B. 1) and separating the values of $\nu = \tau + i\sigma$ (τ, σ real) into real, imaginary, and complex values.

Since $F(\nu,\Omega)$ is even in ν, only Re $\nu > 0$ was considered.

The results of the analysis are given schematically in Figures B1, B2, and B3. The poles of $F(\nu,\Omega)$ are the fourth quadrant series of points indicated by "o" in Fig. B3. From the analysis in (10) it is concluded that $F(\nu,\Omega)$ has an infinite number of poles of the first order within a relatively narrow region extending from $\nu = \Omega$ to $-i\infty$; this region will henceforth be termed the oscillatory region or the transitional region (5).

On the basis of the preliminary analysis in (10), it was postulated that, for $|\nu| > \Omega$ in the whole ν-plane except the transitional regions,

$$F(\nu,\Omega) = -\left(\frac{\nu^2}{\Omega^2} - 1\right)^{1/2}\left\{1 + O(\Omega^{-1})\right\} \qquad \text{(B. 3)}$$

to the first approximation. The required Riemann surface has a cut in the right half-plane as shown in Figure B4. The cut starts at $\nu = \Omega$ and goes off to $-i\infty$, always within the oscillatory region. The argument of $\left(\frac{\nu^2}{\Omega^2} - 1\right)^{1/2}$ vanishes when ν tends to $+\infty + i\epsilon$, $\epsilon \ll 1$. The validity of this formula will be shown in the next section.

Note that the Riemann surface here is different from that of equations (A. 2) and (A. 14) and therefore one must scrutinize the arguments of multi-valued functions when applying the formulas. The coexistence of two different surfaces on the discussion merely means that the two surfaces are complementary, as will be seen later.

Closer Evaluation of $F(\nu,\Omega)$

In accordance with Appendix A, away from the cuts of Figure B4,

$H^{(2)}_{\nu}(\Omega)$ is a linear combination of $S^{(1)}_{\nu}(\Omega)$ and $S^{(2)}_{\nu}(\Omega)$. Using relations (A. 2), (A. 7), (A. 8), (A. 12), and (A. 13), one obtains

$$H^{(2)}_{\nu}(\Omega) = A(\nu,\Omega)\,(c_1 e^{\alpha} + i c_2 e^{-\alpha}),$$

$$H^{(2)\prime}_{\nu}(\Omega) = A(\nu,\Omega)\,(c_1 e^{\alpha} - i c_2 e^{-\alpha})\,(\tfrac{\nu^2}{\Omega^2} - 1)^{1/2}\left\{1 + O(\Omega^{-1})\right\},$$

where c_1 and c_2 are some functions of ν.

Hence, using Table A2 and considering the sign of α and of the imaginary part of ν, it follows that

$$F(\nu,\Omega) = -\,(\nu^2\Omega^{-2} - 1)^{1/2}\left\{1 + O(\Omega^{-1})\right\} \qquad \text{(a)}$$

in regions A and B of Fig. A2, and

$$F(\nu,\Omega) = +\,(\nu^2\Omega^{-2} - 1)^{1/2}\left\{1 + O(\Omega^{-1})\right\} \qquad \text{(b)}$$

in regions C, D, and E of Fig. A2.

Equation (b) is the analytic continuation of equation (a) into the other sheet of the Riemann surface of $(\nu^2\Omega^{-2} - 1)^{1/2}$. However, since $F(\nu,\Omega)$ is a meromorphic function of ν, this surface is not really a property of $F(\nu,\Omega)$; it was introduced in approximating $H^{(2)\prime}_{\nu}(\Omega)$. In fact, the approximations given here for $F(\nu,\Omega)$ are not valid in the vicinity of the cuts shown in Fig. B4. On the basis of equation (B. 3), it follows that equation (a) above is valid in the whole ν-plane except the transitional regions.

Location of the poles of $F(\nu,\Omega)$. The estimates of $F(\nu,\Omega)$ are simply given by the ratio of the expressions in Appendix A for

$H^{(2)}_{\nu}(\Omega)$ and $H^{(2)'}_{\nu}(\Omega)$ for ν in the various regions of the ν-plane.

$F(\nu,\Omega)$ will now be closely analyzed to determine its poles. The poles of $F(\nu,\Omega)$ correspond to the zeros of $H^{(2)}_{\nu}(\Omega)$ and, therefore, the results in (25) serve as a check on the results given here.

*Observe that $S^{(1)}_{\nu}(\Omega)$ and $S^{(2)}_{\nu}(\Omega)$ never vanish. This is so because the expressions

$$S^{(1)}_{\nu}(\Omega) = \frac{1}{\pi i}\, e^{-\Omega \mathrm{Im}\, f(\gamma')} \int_{(i)} e^{-\Omega \mathrm{Re}\ f(w)}\, dw\,, \qquad w = u + iv\,,$$

$$= \frac{1}{\pi i}\, e^{-\Omega \mathrm{Im}\, f(\gamma')} \left\{ \int_{(i)} e^{-\Omega \mathrm{Re}\, f(w)} du + i \int_{(i)} e^{-\Omega \mathrm{Re}\, f(w)} dv \right\},$$

$$S^{(2)}_{\nu}(\Omega) = -\frac{1}{\pi i}\, e^{\Omega \mathrm{Im}\, f(\gamma')} \left\{ \int_{(ii)} e^{-\Omega \mathrm{Re}\, f(w)} du + i \int_{(ii)} e^{-\Omega \mathrm{Re}\ f(w)} dv \right\},$$

are derived by using the property of the integration contour. These contours, as shown in the figures on pages 264-266, reference (24), are such that neither du nor dv changes its sign in the intervals contributing to the integrals; in the case of γ being finite this is also deducible from the expansion formulas (A. 7) and (A. 8).

Using Table A2 and considering the order of magnitude of $e^{\nu \pi i}$, it is clear that $H^{(2)}_{\nu}(\Omega)$ never vanishes in the regions 6a and 7b, Fig. A1, but vanishes only in a part of regions 3, 7a and 4, 6b, where $S^{(2)}_{\nu}(\Omega)$ and $S^{(1)}_{\nu}(\Omega)$ are of the same order.

In view of equation (A. 21), the zeros of $H^{(2)}_{\nu}(\Omega)$ are given by

---

* This discussion is applicable to the construction of Fig. A2.

such values of ν that correspond to γ satisfying

$$\Omega(\gamma\cosh\gamma - \sinh\gamma) = i(m\pi - \frac{\pi}{4})\left\{1 + O(\Omega^{-1})\right\} , \quad [\nu = \Omega\cosh\gamma]$$

for large values of γ, where m denotes any positive integer; in other words, the zeros of $H_\nu^{(2)}(\Omega)$ lie close to the curve

$$\mathrm{Re}(\gamma\cosh\gamma - \sinh\gamma) = 0$$

(or, equivalently, $\mathrm{Re}\,\alpha = \mathrm{Re}\,\nu(\tanh\gamma - \gamma) = 0$ as shown in Fig. A2), or

$$\lambda\coth\lambda - \beta\tan\beta - 1 = 0 .$$

The curve starts from the point $\nu = \Omega$ forming an angle $-\frac{\pi}{3}$ with the real axis, passes through the middle part of region 3 and goes off to $-i\infty$, as shown by the dotted line in Fig. A1 and by the branch line h_2 in Fig. A2. For large m it is easily seen that the zeros of $H_\nu^{(2)}(\Omega)$ are given by

$$\nu_m \cong -\frac{(m-\frac{1}{4})\pi i}{\log m} .$$

For values of ν close to Ω which are of greatest importance for the applications in the text, the zeros of $H_\nu^{(2)}(\Omega)$ are discussed another way in the following.

Poles of $F(\nu, \Omega)$ close to Ω. Relation (A. 34) suggests to the first approximation, that the zeros of $H_\nu^{(2)}(\Omega)$ near Ω are given by those corresponding to the values of ξ satisfying

$$H_{-1/3}^{(2)}(\xi) = \frac{\pi}{\mathcal{M}(-1/3)} \cdot \sqrt{\frac{3}{z}}\ \mathrm{Ai}(z) = 0 \ , \qquad \text{(B. 4)}$$

which is the highest order term, where

$$\xi = \frac{i\nu}{3} \tanh^3 \gamma$$

$$\xi = \rho e^{\pi i}, \quad z = e^{i\pi} \left(\frac{3}{2}\rho\right)^{2/3}, \quad \rho = \frac{2}{3}\left(e^{-i\pi} z\right)^{3/2}, \qquad \text{(B. 5)}$$

and $\mathrm{Ai}(z)$ is the Airy function discussed in Appendix E. Table E1 gives the first ten values of z for which (B. 4) is satisfied. From the values of z one finds that the first few values of ρ are*

$$\rho = \left\{ \begin{array}{lll} 2.3834466, & 5.5101956, & 8.6473577, \\ 11.7868429, & 14.9272068, & .... \end{array} \right\} . \qquad \text{(B. 6)}$$

The first approximate values of γ are those which correspond to these values of ρ, that is

$$\gamma \sim \left(\frac{3\rho}{\Omega}\right)^{1/3} e^{5/6 \pi i} \ , \qquad \text{(B. 7)}$$

---

* Nagase found these values of ρ by using the tables on pages 714-729, reference (24).

choosing among the three possible arguments of γ the one which is compatible with the previous discussion. Therefore, since $\nu = \Omega \cosh \gamma$, the required zeros of $H_\nu^{(2)}(\Omega)$ are given, to the first approximation, by

$$\nu = \Omega \left[1 + \frac{1}{2} \left(\frac{3\varsigma}{\Omega} \right)^{2/3} e^{5/3 \pi i} \right], \tag{B.8}$$

where the values of ς are given by (B.6). This result is in agreement with references (5) and (25).

APPENDIX C. RAYLEIGH ROOT OF THE FREQUENCY EQUATION

Introduction

The primary purpose of this appendix is to derive approximate expressions for the Rayleigh root of the frequency equation. This appendix follows closely the plan and outline of reference (10) where the root has been approximated. It differs from the aforementioned reference in that it has the correction to some errors made in (10).

Rayleigh Root

In the vicinity of the Rayleigh root,

$$F(\nu,\Omega)=-\left(\frac{\nu^2}{\Omega^2}-1\right)^{1/2}\left\{1+O(\Omega^{-1})\right\}, \quad F(\nu,m\Omega)=-\left(\frac{\nu^2}{m^2\Omega^2}-1\right)^{1/2}\left\{1+O(\Omega^{-1})\right\};$$

therefore equation (2.4-9) may be written as*

$$\left.\begin{aligned} f_2(\nu)&=-\frac{\nu^2-1/4}{m\Omega^2}\left\{1-\frac{\Omega^2}{2(\nu^2-9/4)}\right\}^2+\left[-\left(\frac{\nu^2}{\Omega^2}-1\right)^{1/2}+\frac{1}{2\Omega}\left(1-\frac{2\Omega^2}{\nu^2-9/4}\right)\right]\times \\ &\qquad\times\left[-\left(\frac{\nu^2}{m^2\Omega^2}-1\right)^{1/2}\frac{1}{2m\Omega}\left(1+\frac{\Omega^2}{\nu^2-9/4}\right)\right]\left\{1+O(\Omega^{-1})\right\} && \text{(a)}\\ &=\left[\left(\frac{\nu^2}{\Omega^2}-1\right)^{1/2}\left(\frac{\nu^2}{m^2\Omega^2}-1\right)^{1/2}-\frac{\nu^2}{m\Omega^2}\left(1-\frac{\Omega^2}{2\nu^2}\right)^2\right]\left\{1+O(\Omega^{-1})\right\} && \text{(b)}\\ &=-\frac{\Omega^2}{4m\nu^2}\left[\left(2\frac{\nu^2}{\Omega^2}-1\right)^2-4\frac{\nu^2}{\Omega^2}\left(\frac{\nu^2}{\Omega^2}-m^2\right)^{1/2}\left(\frac{\nu^2}{\Omega^2}-1\right)^{1/2}\right] && \text{(c)}\\ &=-\frac{r_0^4}{4m\nu^2\Omega^2}\left[\left(2\frac{\nu^2}{r_0^2}-\frac{\Omega^2}{r_0^2}\right)^2-\frac{4\nu^2}{r_0^2}\left(\frac{\nu^2}{r_0^2}-\frac{\Omega^2}{r_0^2}\right)^{1/2}\left(\frac{\nu^2}{r_0^2}-\frac{m^2\Omega^2}{r_0^2}\right)^{1/2}\right] && \text{(d)} \end{aligned}\right\} \quad \text{(C.1)}$$

---

* See Figure 6 for the required branch cuts.

When the expressions [ ] in (C. 1c) and (C. 1d) are set equal to zero, they become, respectively, equation (32), reference (29), and equation (2-38), reference (19).

By setting the above expressions for $f_2(\nu)$ equal to zero, the following equations are obtained

$$(2\nu^2-\Omega^2)^2=4\nu^2(1-\Omega^2\nu^{-2})^{1/2}(1-m^2\Omega^2\nu^{-2})^{1/2}, \qquad \text{(C. 2)}$$

$$S(S-1)^{1/2}(S-m^2)^{1/2}-(S-1/2)^2=0, \qquad \text{(C. 3)}$$

where

$$S=\frac{\nu^2}{\Omega^2}. \qquad \text{(C. 4)}$$

Formula (C. 2) corresponds to formula (3. 11), reference (5), and formula (C. 3) is precisely formula (3. 27), page 850, reference (10). It was also deduced in a related way in references (30) and (3). As in the cylindrical case, (C. 2) or (C. 3) establishes the fact that $f_2(\nu)$ contains a real root which corresponds to the Rayleigh surface wave. Using the definition of phase velocity, $c=\frac{\omega r_o}{\nu}$, formula (C. 3) can be written as

$$\left(2-\frac{c^2}{C_s^2}\right)^2=4\left(1-\frac{c^2}{C_s^2}\right)^{1/2}\left(1-\frac{c^2}{C_d^2}\right)^{1/2}. \qquad \text{(C. 5)}$$

Squaring equation (C. 5) gives

$$\frac{c^2}{C_S^2}\left[\frac{c^6}{C_S^6} - 8\frac{c^4}{C_S^4} + \frac{c^2}{C_S^2}\left(24 - 16\frac{C_S^2}{C_d^2}\right) - 16\left(1 - \frac{C_S^2}{C_d^2}\right)\right] = 0, \qquad \text{(C. 6)}$$

which is equation (2-29), reference (19).

The preceding equations are discussed at length in the references indicated. In particular, from the analysis given in reference (29), page 9, it follows that there is only one root which approaches the real ν-axis as $|\nu| \to \infty$ and whose limiting phase velocity is the Rayleigh velocity. The real part of this root is given asymptotically by

$$\nu_R \sim \nu_0 = \varsigma_0^{1/2}\Omega, \qquad \text{(C. 7)}$$

where ς_0 is the unique real root of the cubic equation

$$16(1-m^2)\varsigma^3 - 8(3-2m^2)\varsigma^2 + 8\varsigma - 1 = 0 \; ; \qquad \text{(C. 8)}$$

ς_0 is greater than one.

To estimate the imaginary part of the root, it is necessary to retain the first term of the expansion for $F(\nu,\Omega)$ that contains i. In accordance with equations (3. 47), (3. 48), (3. 50), and (3. 51), reference (10), part I, the expression needed is

$$F(\nu_R,\Omega) = -\left(\frac{\nu_R^2}{\Omega^2} - 1\right)^{1/2}\left[1 + iE(\nu_R,\Omega)\right],$$

where $\nu_R = \nu_0 + i\sigma_0$, and

$$E(\nu,\Omega)=\exp\left[-2\Omega\left(\frac{\nu}{\Omega}\cosh^{-1}\frac{\nu}{\Omega}-\left(\frac{\nu^2}{\Omega^2}-1\right)^{1/2}\right)\right] \qquad \text{(C. 9)}$$

By assuming the inequality $|\sigma_0| << \nu_0$, the substitution of this expression into (2.4-9) yields

$$f_2(\nu_R)=-\frac{\nu_R^2}{m\Omega^2}\left\{1-\frac{\Omega^2}{2\nu_R^2}\right\}^2+\left(\frac{\nu_R^2}{\Omega^2}-1\right)^{1/2}\left[1+iE(\nu_R,\Omega)\right]\left(\frac{\nu_R^2}{m^2\Omega^2}-1\right)^{1/2}\left[1+iE(\nu_R,m\Omega)\right]$$

$$=-\frac{\Omega^2}{m\nu_0^2}\left(\frac{\nu_0^2}{\Omega^2}-\frac{1}{2}\right)^2\left[1+\left(\frac{4}{\frac{\nu_0^2}{\Omega^2}-\frac{1}{2}}-\frac{2\Omega^2}{\nu_0^2}\right)\frac{i\sigma_0\nu_0}{\Omega^2}\right]$$

$$+\frac{1}{m}\left(\frac{\nu_0^2}{\Omega^2}-1\right)^{1/2}\left(\frac{\nu_0^2}{\Omega^2}-m^2\right)^{1/2}\left[1+\left\{\left(\frac{\nu_0^2}{\Omega^2}-m^2\right)^{-1}+\left(\frac{\nu_0^2}{\Omega^2}-1\right)^{-1}\right\}\frac{i\sigma_0\nu_0}{\Omega^2}+\right.$$

$$\left.+iE(\nu_0,\Omega)+iE(\nu_0,m\Omega)\right].$$

By setting this expression equal to zero, and in view of equation (C. 3), the following equation is obtained:

$$\frac{1}{m}\left(\frac{\nu_0^2}{\Omega^2}-1\right)^{1/2}\left(\frac{\nu_0^2}{\Omega^2}-m^2\right)^{1/2}\left[\left\{\left(\frac{\nu_0^2}{\Omega^2}-m^2\right)^{-1}+\left(\frac{\nu_0^2}{\Omega^2}-1\right)^{1/2}\right\}\frac{i\sigma_0\nu_0}{\Omega^2}+iE(\nu_0,\Omega)+iE(\nu_0,m\Omega)\right]$$

$$-\frac{\Omega^2}{m\nu_0^2}\left(\frac{\nu_0^2}{\Omega^2}-\frac{1}{2}\right)^2\left[\left(\frac{4}{\nu_0^2\Omega^{-2}-1/2}-\frac{2\Omega^2}{\nu_0^2}\right)\frac{i\sigma_0\nu_0}{\Omega^2}\right]=0,$$

or, by solving for σ_0 ,

$$\sigma_0=-\Omega\frac{S_0^{-1/2}}{K(m)}\left[E(\nu_0,\Omega)+E(\nu_0,m\Omega)\right], \qquad \text{(C. 10)}$$

where

$$K(m) = (\sigma_0 - m^2)^{-1} + (\sigma_0 - 1)^{-1} - (\sigma_0 - \tfrac{1}{2})(2\sigma_0 + 1)(\sigma_0 - 1)^{-\frac{1}{2}}(\sigma_0 - m^2)^{-\frac{1}{2}}$$

Note that, just as in the cylindrical case (30, 5), σ_0 has the form

$$\mathrm{Im}\, \nu_R = \sigma_0 \sim -\mathrm{const}\, \Omega\, e^{-\mathrm{const}\, \Omega},$$

where const > 0.

APPENDIX D. ASYMPTOTIC APPROXIMATIONS FOR LEGENDRE POLYNOMIALS OF LARGE COMPLEX ORDER

Introduction

This appendix contains asymptotic approximations for the Legendre functions appearing in the text. These approximations are valid as $|\nu| \to \infty$ in, at least, $|\arg \nu| < \frac{\pi}{2}$ and various regions in θ. Some formulas hold for $|\arg \nu| \leq \pi - \delta$. The results compiled here are taken from references (2), (31), (32), (33), (34), and (28). A common notation is used.

Basic Relations

$$P_{\nu-1/2}(\cos\theta) = F\left(\tfrac{1}{2}-\nu, \tfrac{1}{2}+\nu; 1; \tfrac{1}{2}-\tfrac{1}{2}\cos\theta\right), \quad -1 < \cos\theta < 1 \tag{D. 1}$$

$$P_{\nu-1/2}(\cos\theta) = P_{-\nu-1/2}(\cos\theta), \tag{D. 2}$$

$$P_{\nu-1/2}(-\cos\theta) = P_{\nu-1/2}(\cos\theta)\sin\nu\pi + \tfrac{2}{\pi}Q_{\nu-1/2}(\cos\theta)\cos\nu\pi, \quad 0 < \cos\theta < 1, \tag{D. 3}$$

$$Q_{\nu-1/2}(-\cos\theta) = -Q_{\nu-1/2}(\cos\theta)\sin\nu\pi + \tfrac{\pi}{2}P_{\nu-1/2}(\cos\theta)\cos\nu\pi, \quad 0 < \cos\theta < 1. \tag{D. 4}$$

For integer n,

$$P_n(-\cos\theta) = (-1)^n P_n(\cos\theta), \quad Q_n(-\cos\theta) = (-1)^{n+1} Q_n(\cos\theta) \tag{D. 5}$$

$$P_n(1)=1, P_n(-1)=(-1)^n, P_{2n}(0)=\frac{(-1)^n(2n)!}{2^{2n}(n!)^2}, \quad P_{2n+1}(0)=0, \tag{D. 6}$$

$$\left|P_n(\cos\theta)\right|\leq 1, \quad \left|\frac{dP_n(\cos\theta)}{d\theta}\right|\leq n^2. \tag{D. 7}$$

Asymptotic Expansions

If $0<\theta\leq\pi$, $|\arg\nu|\leq\pi-\delta$, the following asymptotic expansions are valid as $|\nu|\to\infty$ (32), (33):

$$P_{\nu-1/2}(\cos\theta)\sim\left(\frac{2}{\nu\pi\sin\theta}\right)^{1/2}\left[\cos\left(\nu\theta-\frac{\pi}{4}\right)+O\left(\frac{1}{\nu}\right)\right]. \tag{D. 8}$$

If $0\leq\theta\leq\epsilon$, $|\nu|\epsilon\leq 1$, $|\nu|\to\infty$, arg ν arbitrary, (2), (31), (33), then

$$P_{\nu-1/2}(\cos\theta)\sim J_0(u)+\sin^2\frac{\theta}{2}\left[\frac{u}{6}J_3(u)-J_2(u)+\frac{J_1(u)}{2u}\right]+O\left(\sin^4\frac{\theta}{2}\right), \tag{D. 9}$$

where

$$u = 2\nu\sin\frac{\theta}{2} \tag{D. 10}$$

and must remain finite.

A uniform asymptotic expansion of the Legendre function has been given by Szegö (34):

$$P_{\nu-1/2}(\cos\theta) \sim \left(\frac{\theta}{\sin\theta}\right)\left[\nu J_0(\nu\theta) + \frac{1}{8}(\theta\cot\theta - 1)\frac{\nu J_1(\nu\theta)}{\nu\theta} + O(\nu^{-2})\right]. \quad \text{(D. 11)}$$

This reduces to (D. 8) when $|\nu|\theta >> 1$ and remains valid for $\theta \to 0$.

APPENDIX E. THE AIRY FUNCTION

Introduction

This appendix contains some properties of the Airy function which are needed in the text. The results given here may be found in references (2), (28), (35).

Basic Relations

The Airy functions are solutions of the differential equation

$$\frac{d^2 w}{dz^2} = z w \quad . \tag{E. 1}$$

One standard solution is defined by

$$Ai(z) = \frac{3^{1/3}}{\pi} \int_0^\infty \cos(t^3 + 3^{1/3} z t)\, dt \tag{E. 2}$$

which can also be written as

$$Ai(z) = \frac{1}{\pi} \sqrt{\frac{z}{3}}\; K_{1/3}(\zeta) \tag{E. 3}$$

where

$$\zeta = \frac{2}{3} z^{3/2} \tag{E. 4}$$

The functions $Ai(z e^{\pm \frac{2}{3}\pi i})$ also satisfy (E. 1), and one finds it convenient to use the notation

$$R_1(z) = Ai(z), \quad R_2(z) = Ai(z\,e^{\frac{2}{3}\pi i}), \quad R_3(z) = Ai(z\,e^{-\frac{2}{3}\pi i}). \qquad (E.5)$$

Any two of these functions comprise a linearly independent pair of solutions of (E. 1), the Wronskians being

$$W(R_1, R_2) = \frac{e^{-i\pi/6}}{2\pi}, \quad W(R_1, R_3) = \frac{e^{i\pi/6}}{2\pi}, \quad W(R_2, R_3) = \frac{i}{2\pi}. \qquad (E.6)$$

Also

$$R_1(z) + e^{i2\pi/3} R_2(z) + e^{-i2\pi/3} R_3(z) = 0 . \qquad (E.7)$$

Asymptotic Expansions

Ai(z) is an integral function of z and, for large $|z|$, it takes the asymptotic values

$$\left.\begin{aligned} Ai(z) &= \frac{e^{-\zeta}}{2\sqrt{\pi}\, z^{1/4}} \left\{1 + O(|\zeta|^{-1})\right\} \\ Ai'(z) &= -\frac{z^{1/4} e^{-\zeta}}{2\sqrt{\pi}} \left\{1 + O(|\zeta|^{-1})\right\} \end{aligned}\right\} \qquad (E.8)$$

when $|\arg z| < \pi$, and

$$\left.\begin{aligned} Ai(-z) &= \frac{z^{-1/4}}{\sqrt{\pi}}\left\{\sin\left(\zeta+\frac{\pi}{4}\right)\left[1+O(|\zeta|^{-2})\right] - \cos\left(\zeta+\frac{\pi}{4}\right) O(|\zeta|^{-1})\right\} \\ Ai'(-z) &= -\frac{z^{-1/4}}{\sqrt{\pi}}\left\{\cos\left(\zeta+\frac{\pi}{4}\right)\left[1+O(|\zeta|^{-2})\right] + \sin\left(\zeta+\frac{\pi}{4}\right) O(|\zeta|^{-1})\right\} \end{aligned}\right\} \qquad (E.9)$$

when $|\arg z| < \frac{2}{3}\pi$. The expressions in (E. 8) and (E. 9) are equivalent in their common region of validity. From them one may deduce the useful inequalities

$$|\mathrm{Ai}(z)| < C(1+|z|^{1/4})^{-1} \left|\exp(-\tfrac{2}{3} z^{3/2})\right|$$

$$|\mathrm{Ai}'(z)| < C(1+|z|^{1/4}) \left|\exp(-\tfrac{2}{3} z^{3/2})\right| \qquad \text{(E. 10)}$$

valid when $|\arg z| \leq \pi$, where C is some constant.

If the sectors

$$|\arg z| \leq \frac{1}{3}\pi, \quad -\pi \leq \arg z \leq -\frac{1}{3}\pi, \quad \frac{1}{3}\pi \leq \arg z \leq \pi,$$

are denoted by S_1, S_2, S_3, respectively (Fig. E1), then it is seen from (E. 5) and (E. 8) that $R_j(z)$ is exponentially small in $S_j (j=1, 2, 3)$, when $|z|$ is large. Consequently in S_j any independent pair of solutions of (E. 1) must include $R_j(z)$ as a member if it is to be satisfactory from the numerical standpoint.

Another standard solution of (E. 1) is the function

$$\mathrm{Bi}(z) = e^{i\pi/6} R_2(z) + e^{-i\pi/6} R_3(z) \qquad \text{(E. 11)}$$

introduced in the British Association Mathematical Tables (1946). From this definition and equation (E. 7), it follows that

$$\mathrm{Ai}(z e^{\pm 2\pi i/3}) = \frac{1}{2} e^{\pm \pi i/3} \left[\mathrm{Ai}(z) \mp i\, \mathrm{Bi}(z)\right] . \qquad \text{(E. 12)}$$

Zeros of Ai(z) and Ai'(z)

The zeros of the Airy function are all located on the negative real axis. If $-x_n$ denotes the nth zero, one has, for large n (28, p. 450),

$$x_n = \left[\frac{3\pi}{2}\left(n-\frac{1}{4}\right)\right]^{2/3}\left\{1 + O(n^{-2})\right\} \qquad (n >> 1) \qquad \text{(E. 12)}$$

$$Ai'(-x_n) \approx \frac{(-1)^{n-1}}{\sqrt{\pi}}\left[\frac{3\pi}{2}\left(n-\frac{1}{4}\right)\right]^{1/6} \qquad (n >>1) \qquad \text{(E. 13)}$$

The first ten values of $x_n \equiv -a_s$ and the first ten zeros of Ai'(z) are listed in Table E1 (28, p. 478).

TABLE E1. ZEROS AND ASSOCIATED VALUES OF AIRY FUNCTIONS AND THEIR DERIVATIVES

s	a_s	$Ai'(a_s)$	a'_s	$Ai(a'_s)$
1	- 2.33810 741	+0.70121 082	- 1.01879 297	+0.53565 666
2	- 4.08794 944	-0.80311 137	- 3.24819 758	-0.41901 548
3	- 5.52055 983	+0.86520 403	- 4.82009 921	+0.38040 647
4	- 6.78670 809	-0.91085 074	- 6.16330 736	-0.35790 794
5	- 7.94413 359	+0.94733 571	- 7.37217 726	+0.34230 124
6	- 9.02265 085	-0.97792 281	- 8.48848 673	-0.33047 623
7	-10.04017 434	+1.00437 012	- 9.53544 905	+0.32102 229
8	-11.00852 430	-1.02773 869	-10.52766 040	-0.31318 539
9	-11.93601 556	+1.04872 065	-11.47505 663	+0.30651 729
10	-12.82877 675	-1.06779 386	-12.38478 837	-0.30073 083

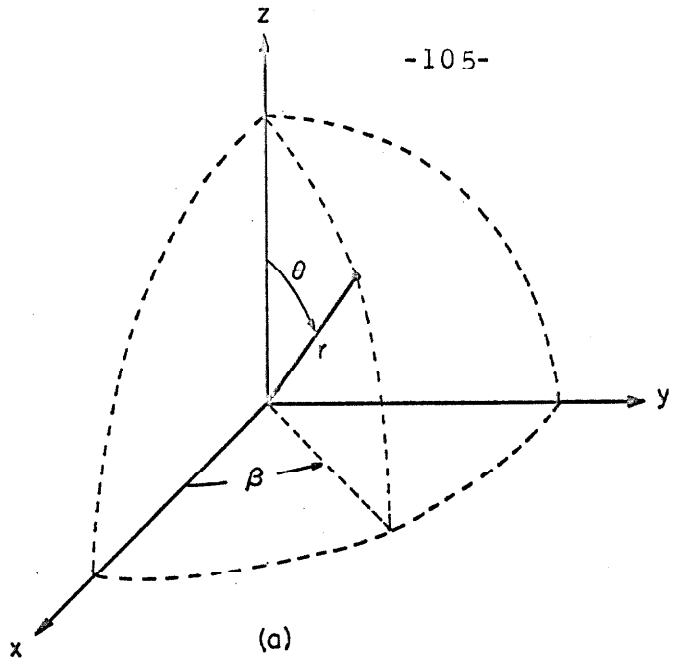

(a)

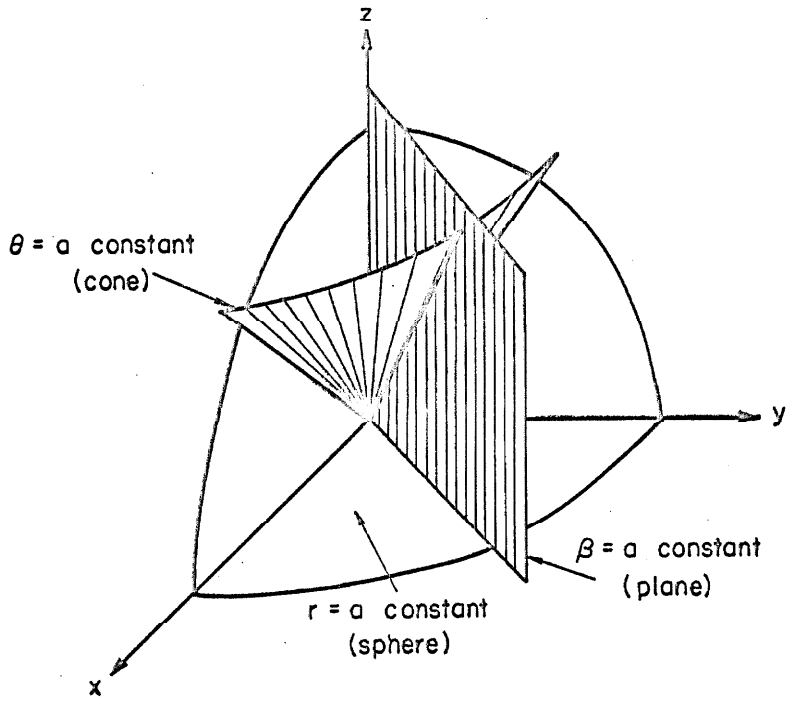

(b)

FIGURE 1

(a) THE THREE SPHERICAL COORDINATES

(b) THE THREE MUTUALLY PERPENDICULAR SURFACES OF THE SPHERICAL COORDINATE SYSTEM

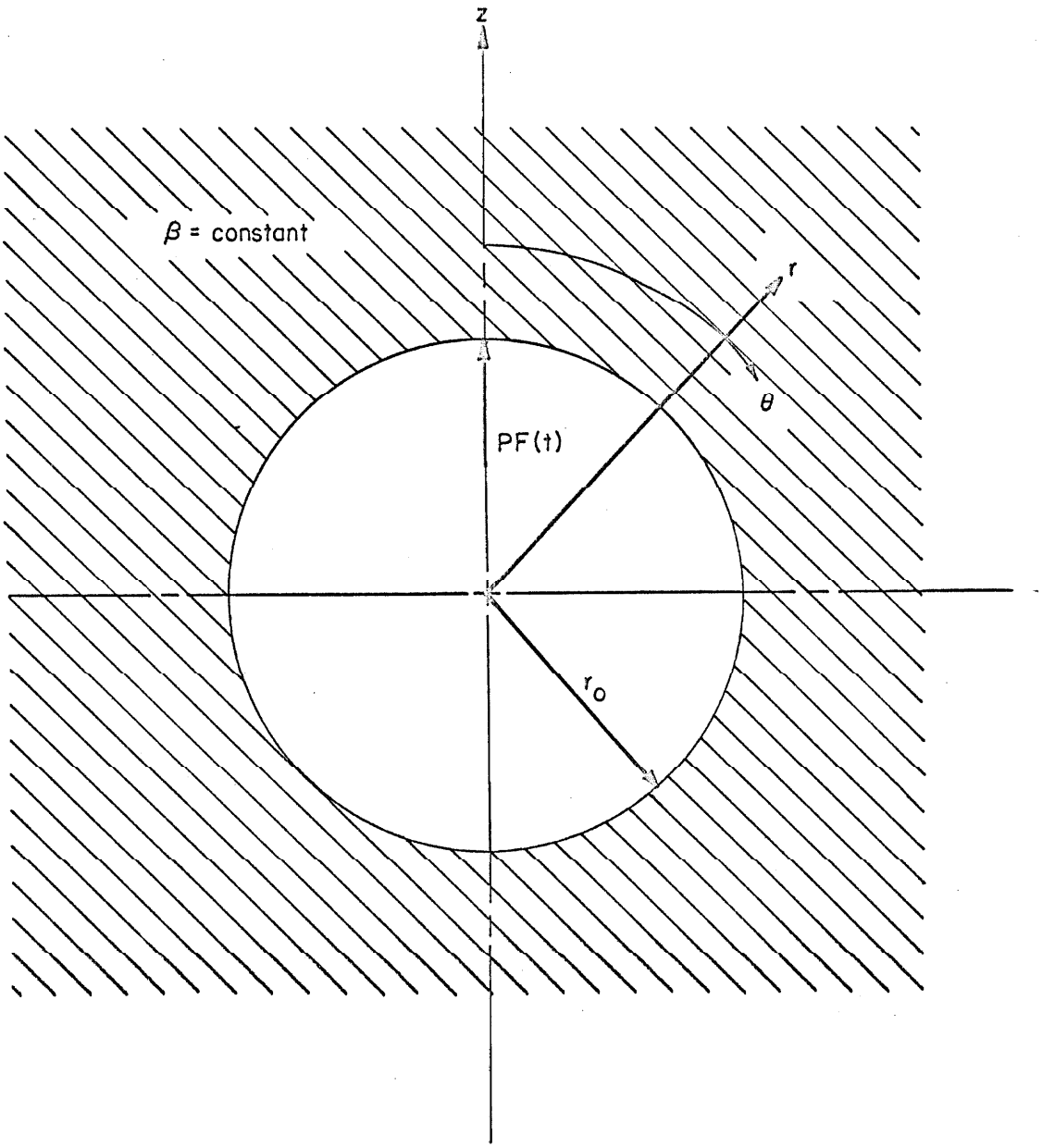

FIGURE 2

PROBLEM OF CAVITY SURFACE NORMAL POINT SOURCE

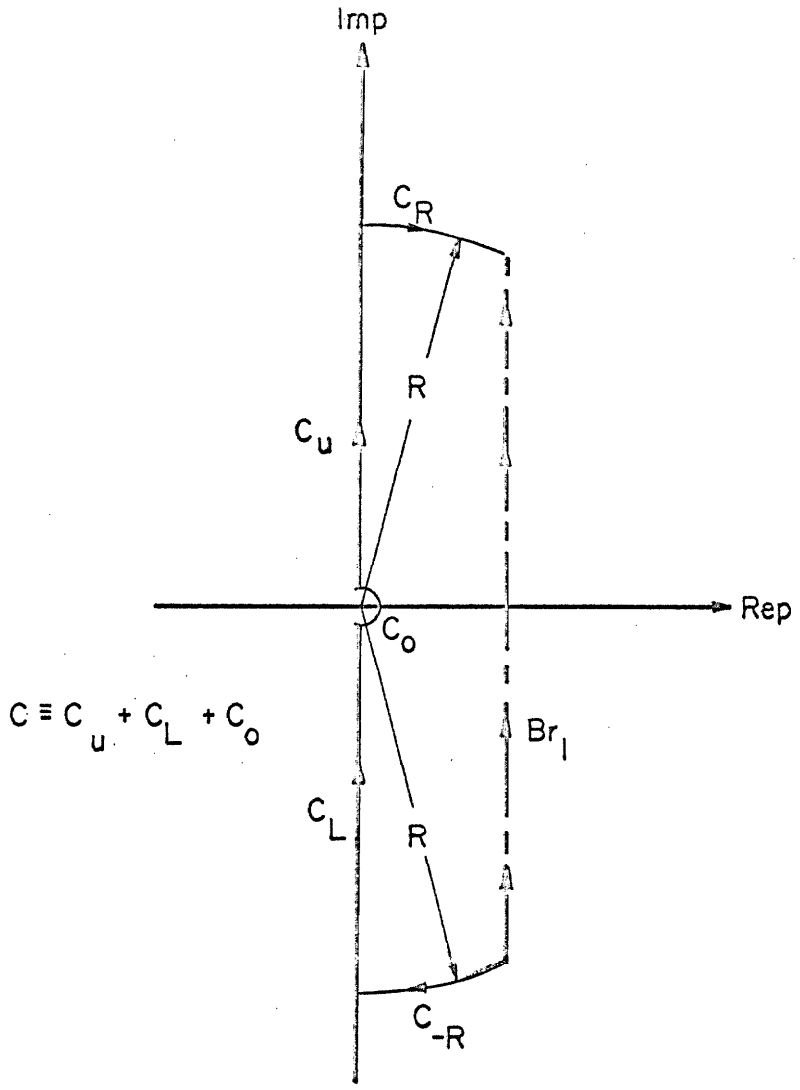

FIG. 3

COMPLETION OF INVERSION CONTOUR FOR LAPLACE TRANSFORM

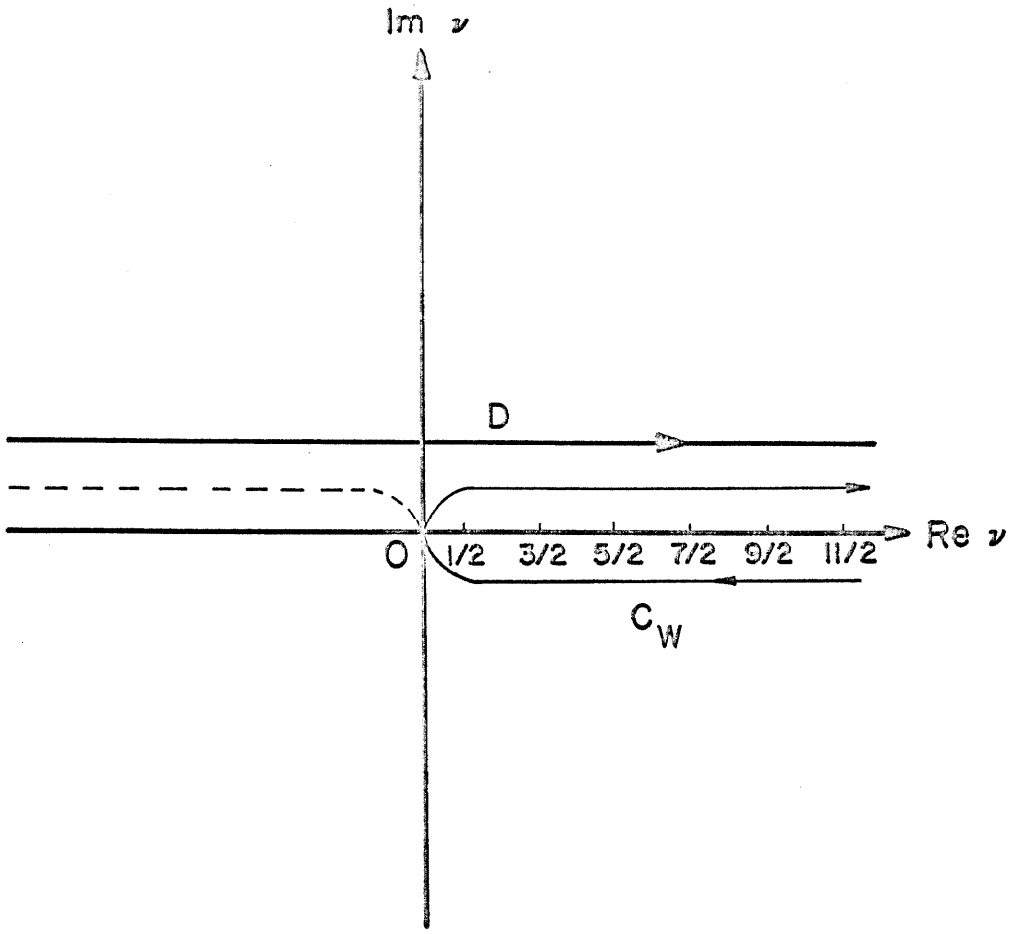

FIGURE 4

INTEGRATION IN THE ν - PLANE

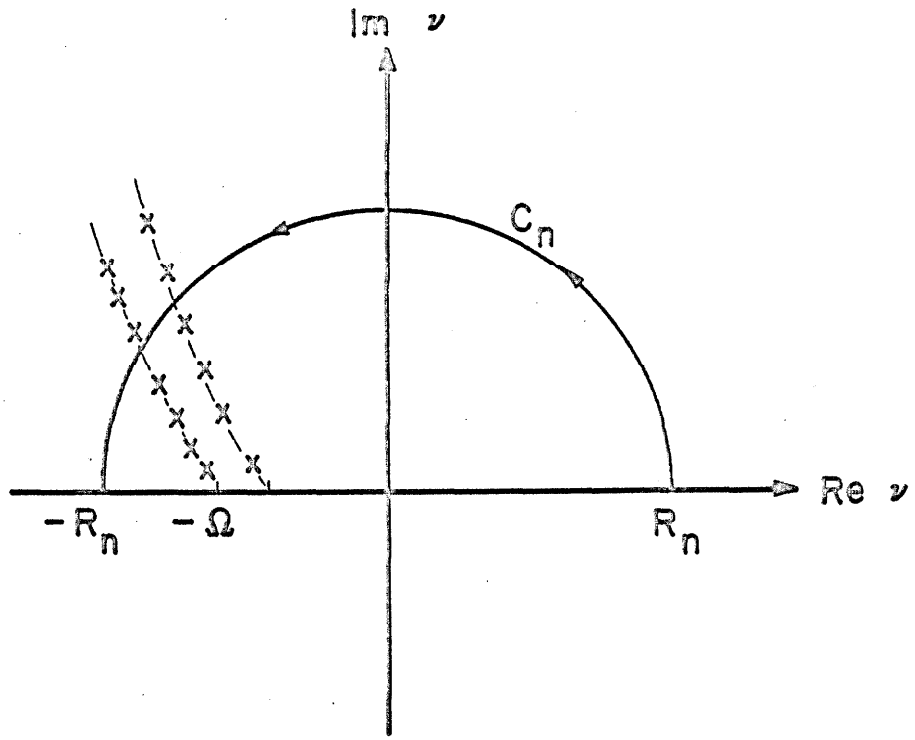

FIGURE 5

INTEGRATION IN THE ν-PLANE

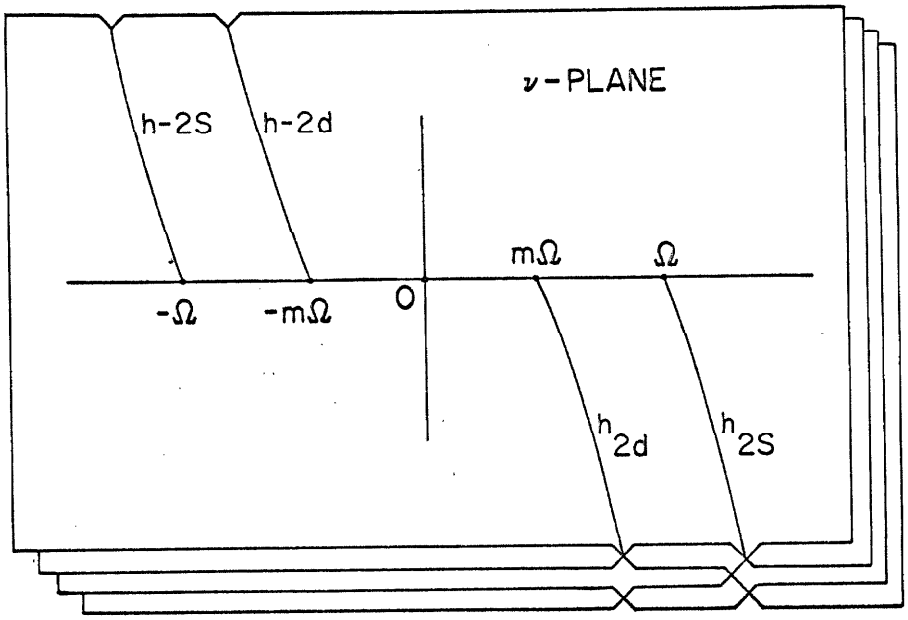

FIGURE 6

BRANCH CUTS IN THE ν-PLANE

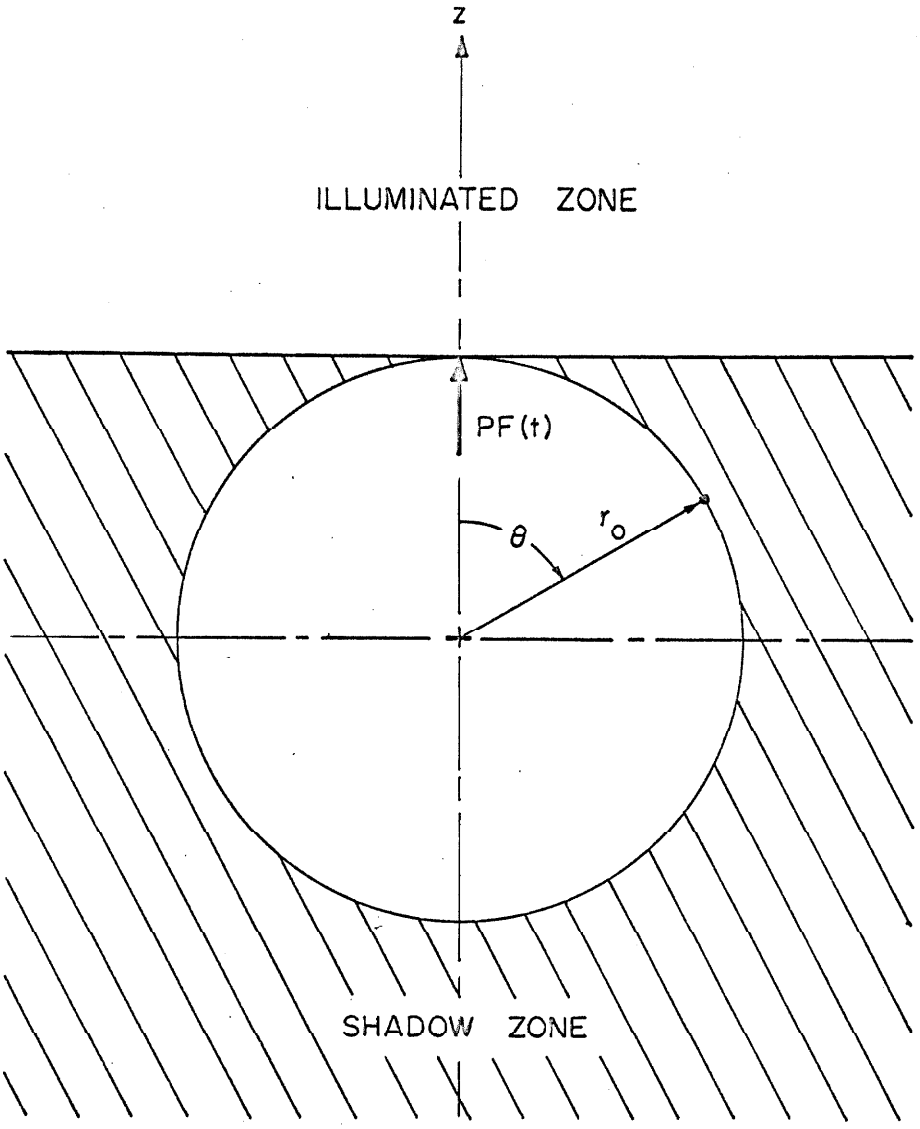

FIGURE 7
GEOMETRICAL ZONES OF THE PROBLEM

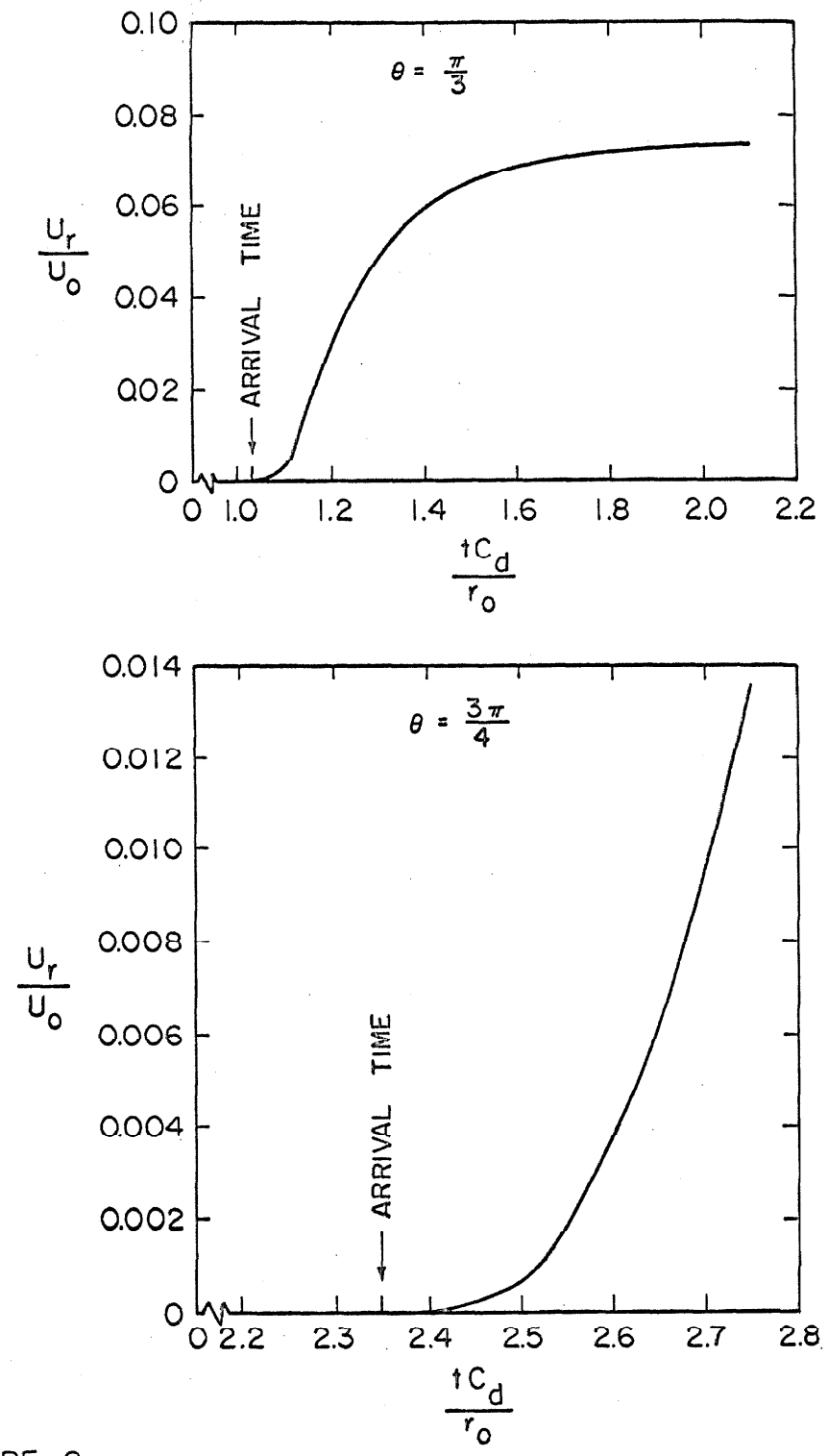

FIGURE 8
RADIAL DISPLACEMENT AT THE CAVITY WALL

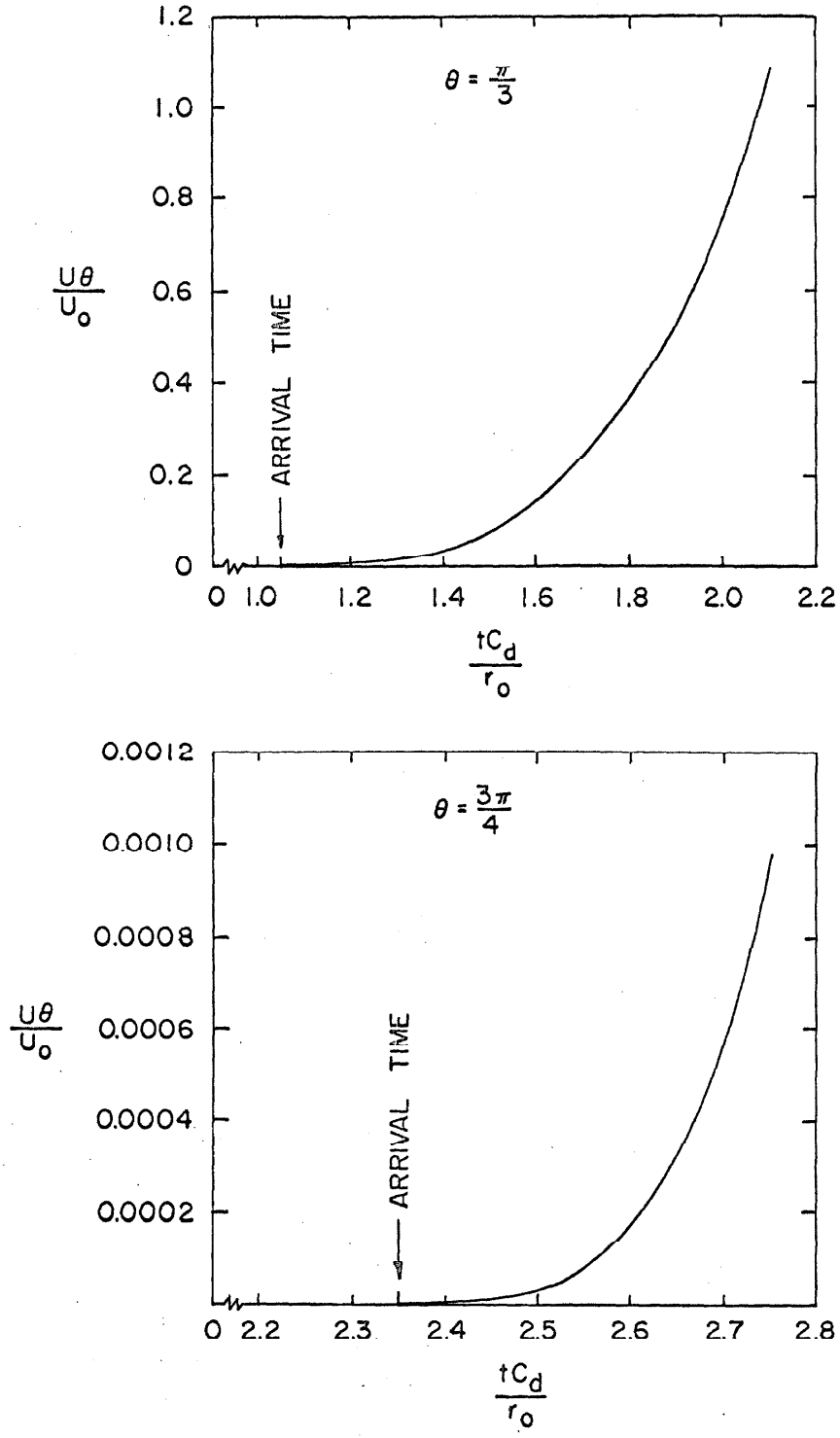

FIGURE 9

TANGENTIAL DISPLACEMENT AT THE CAVITY WALL

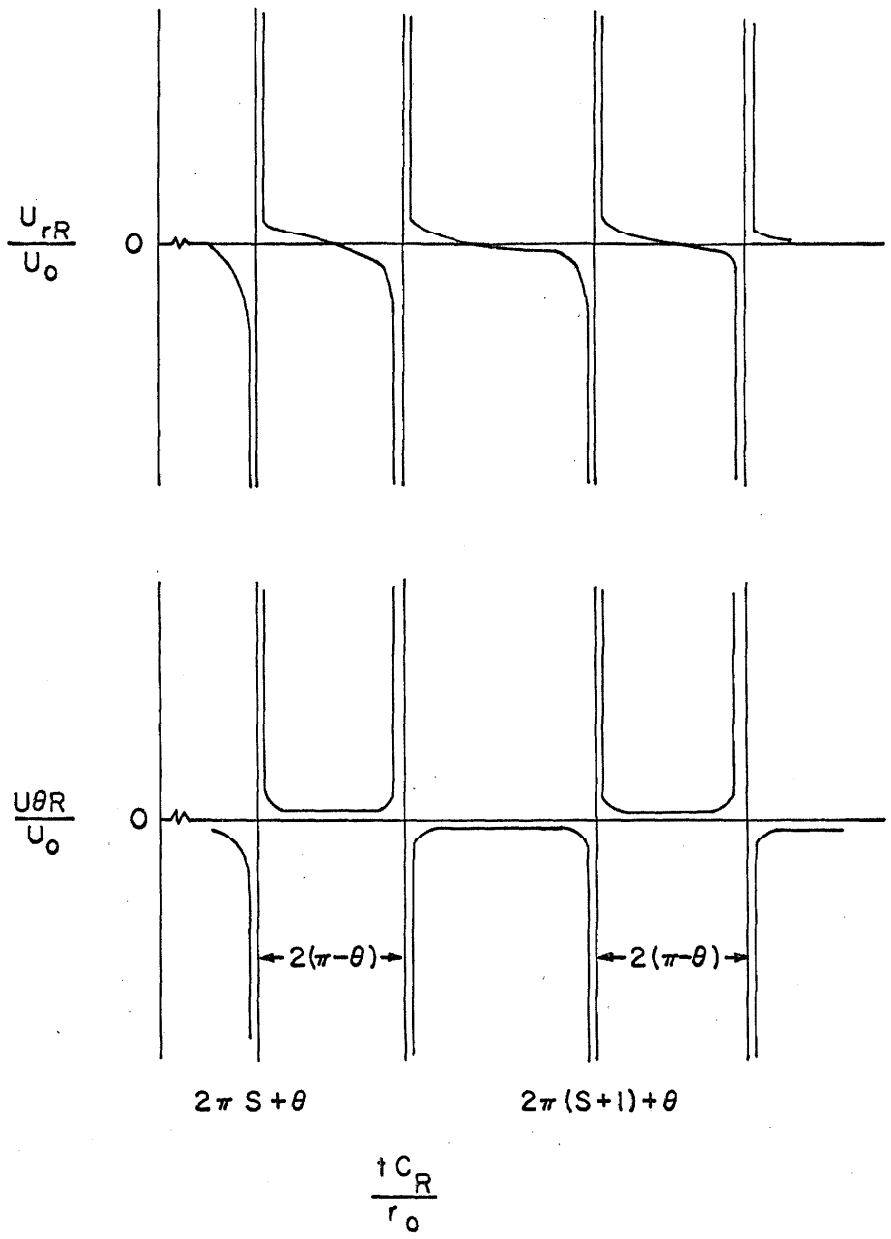

FIGURE 10

TOTAL RESPONSE FOR LONG TIME AT CAVITY WALL DUE TO RAYLEIGH WAVES

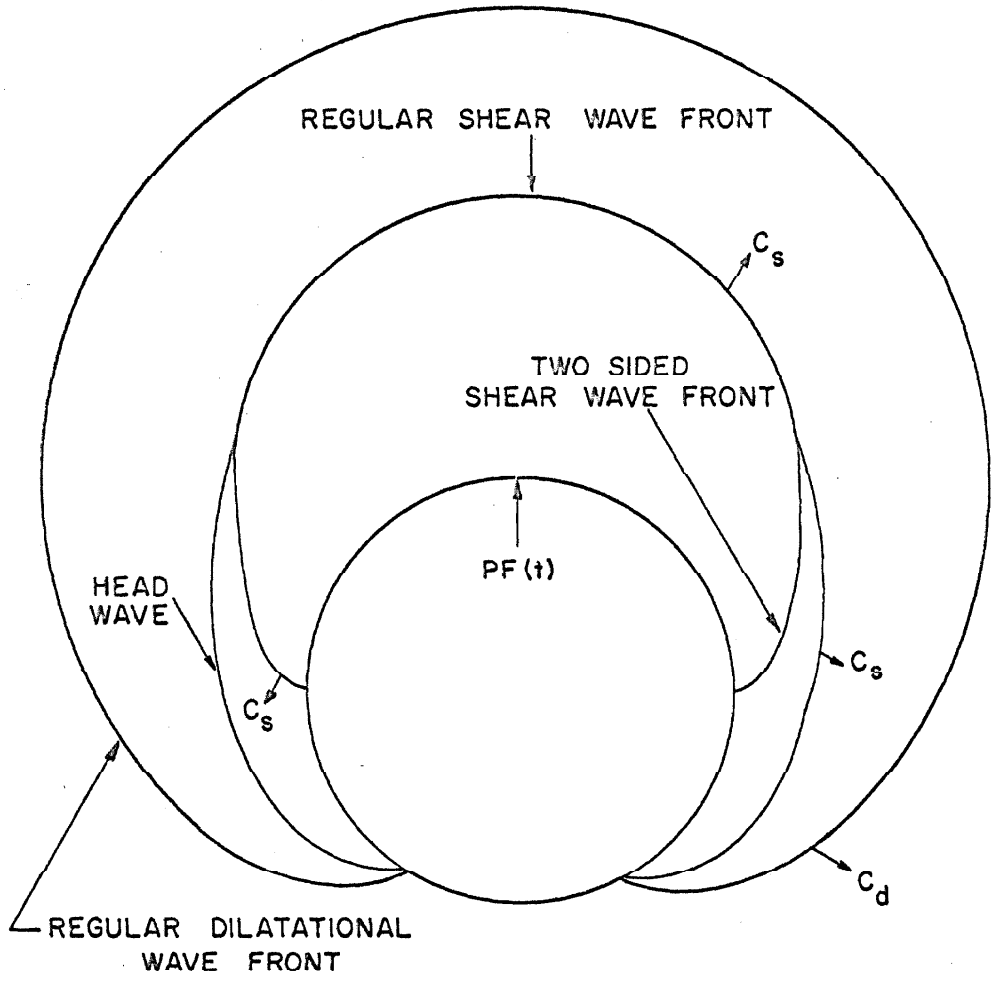

FIGURE II

BASIC WAVE FRONTS FOR SPHERICAL CAVITY PROBLEM

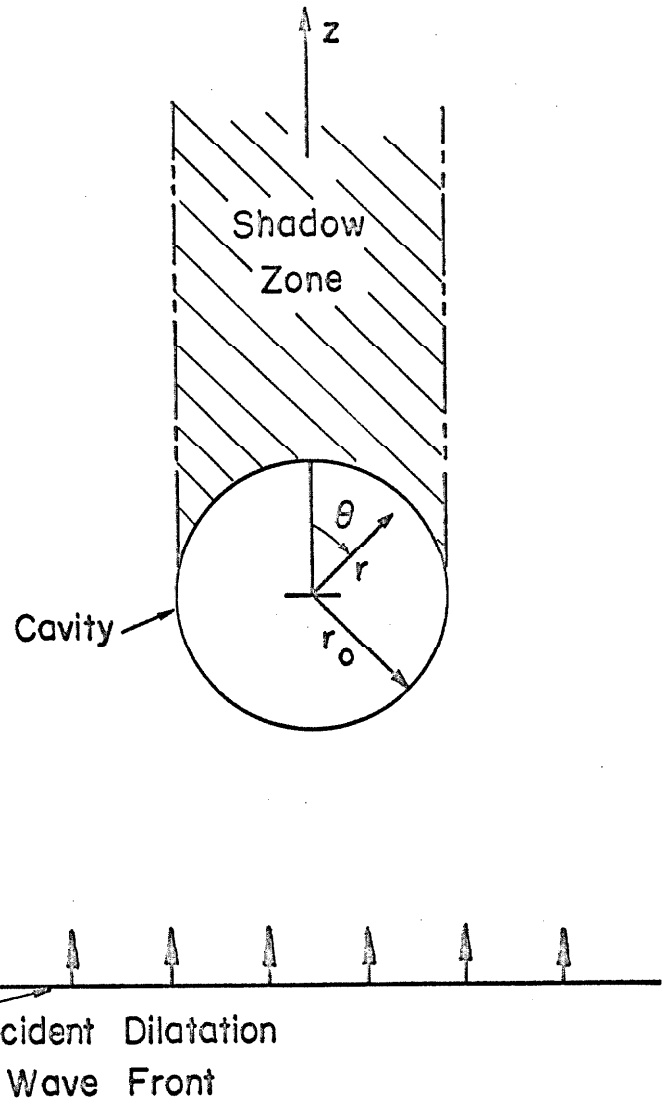

FIGURE 12
PROBLEM OF INCIDENT PLANE WAVE

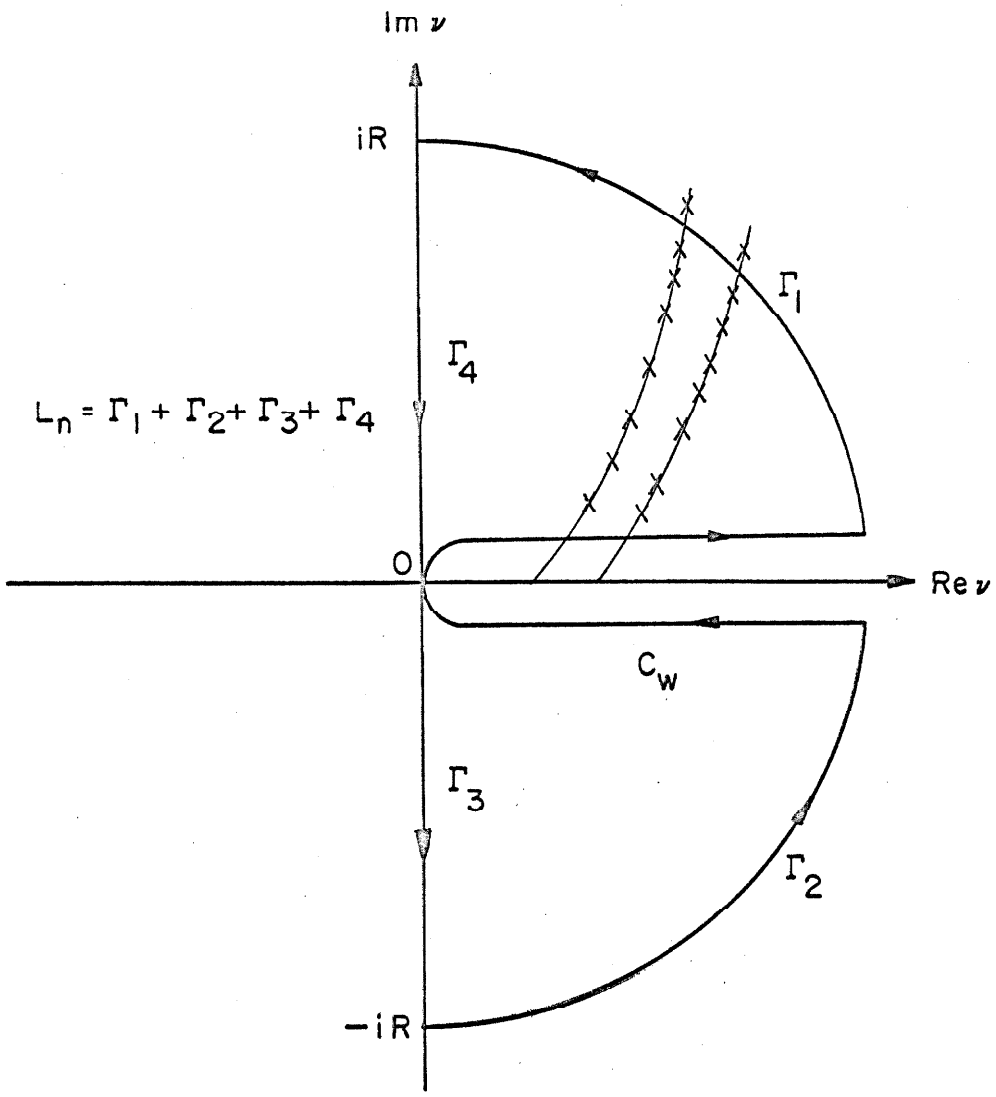

FIGURE 13

INTEGRATION IN THE ν-PLANE

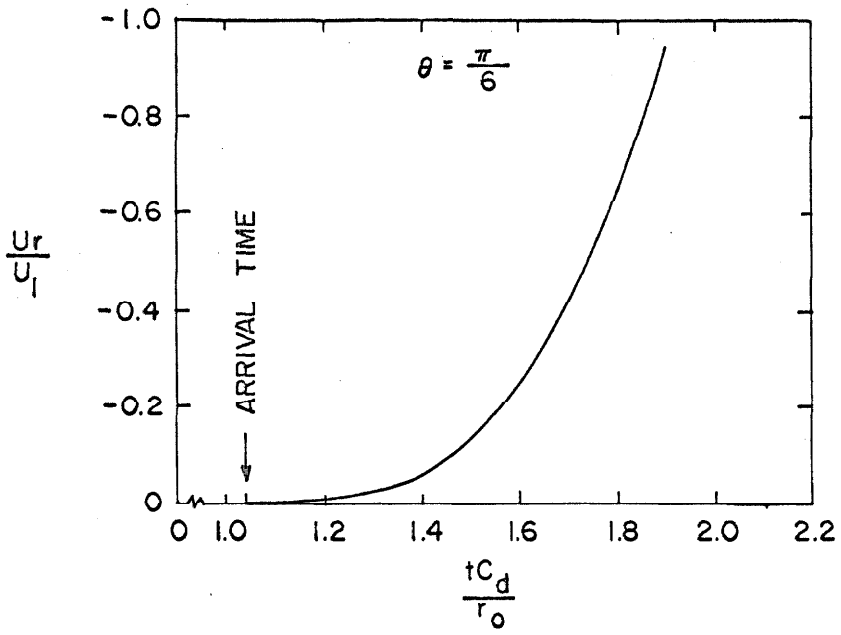

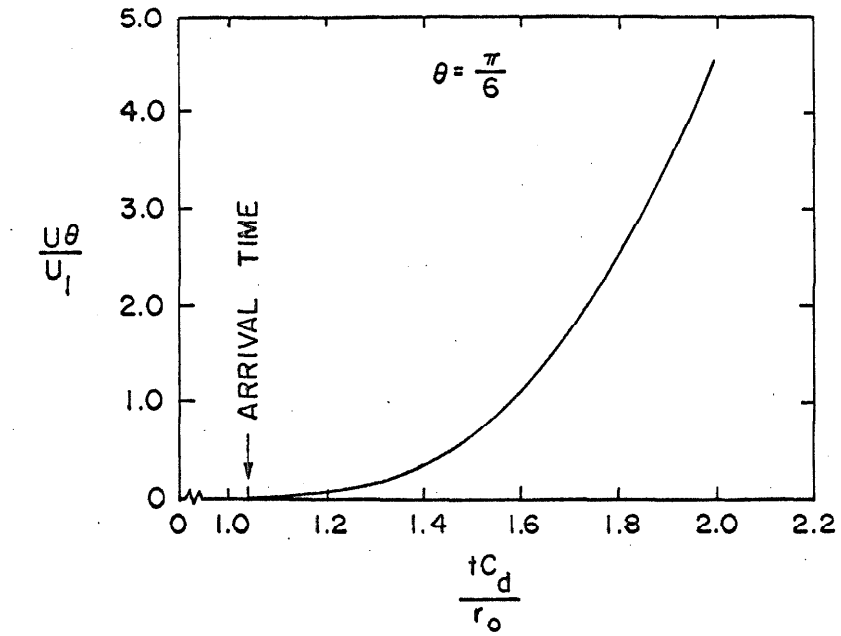

FIGURE 14

DISPLACEMENT COMPONENTS FOR PLANE WAVE CASE

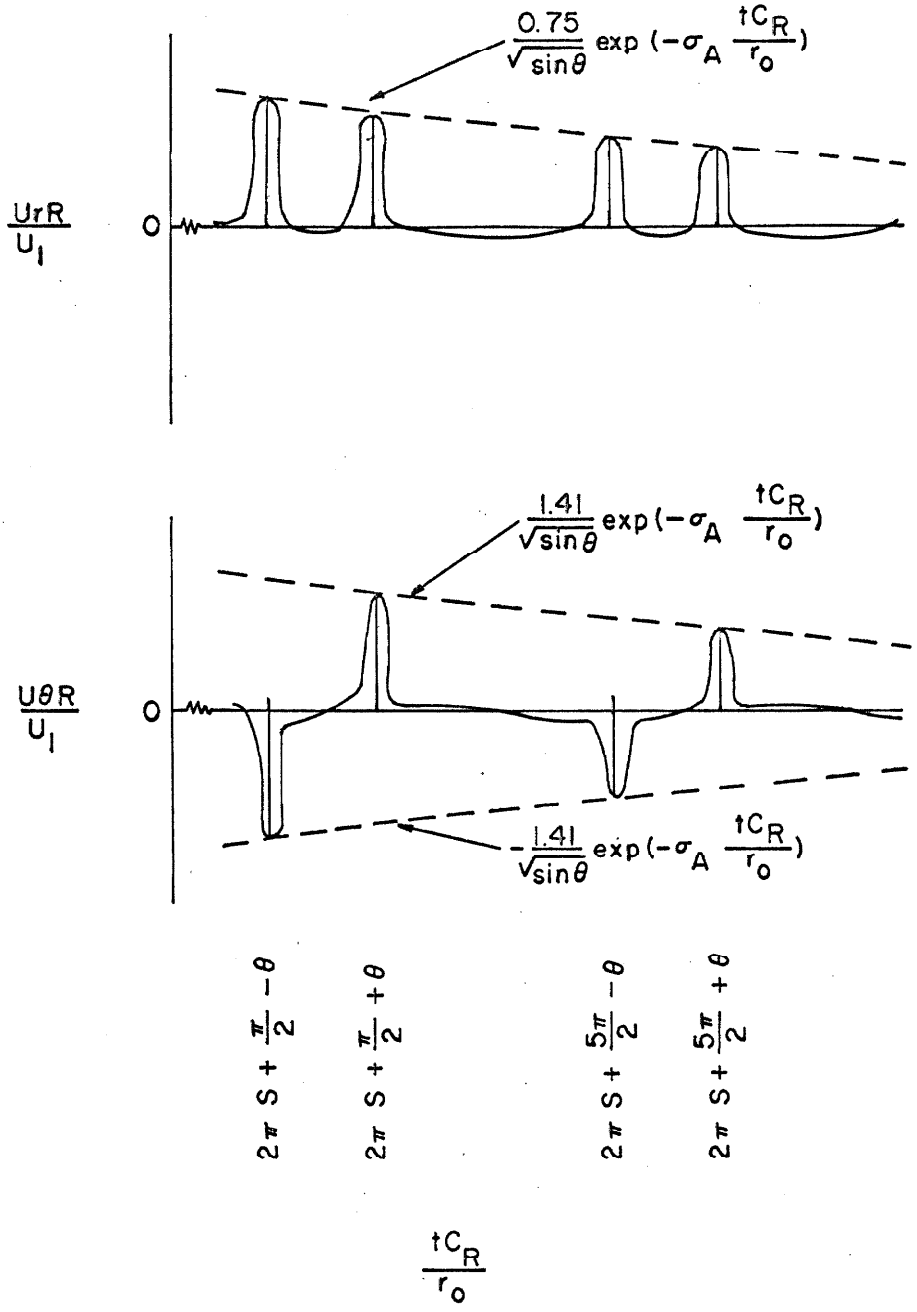

FIGURE 15

RAYLEIGH WAVES AT CAVITY WALL (LONG-TIME SOLUTION) – PLANE WAVE CASE

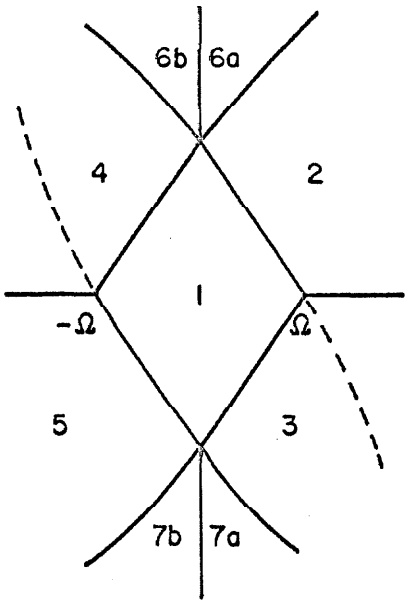

(a)

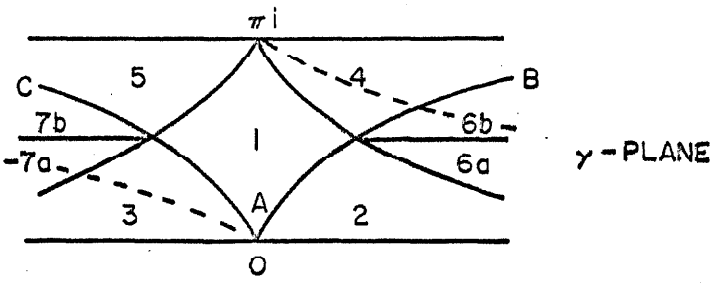

(b)

FIGURE A1

THE ν-γ TRANSFORMATION

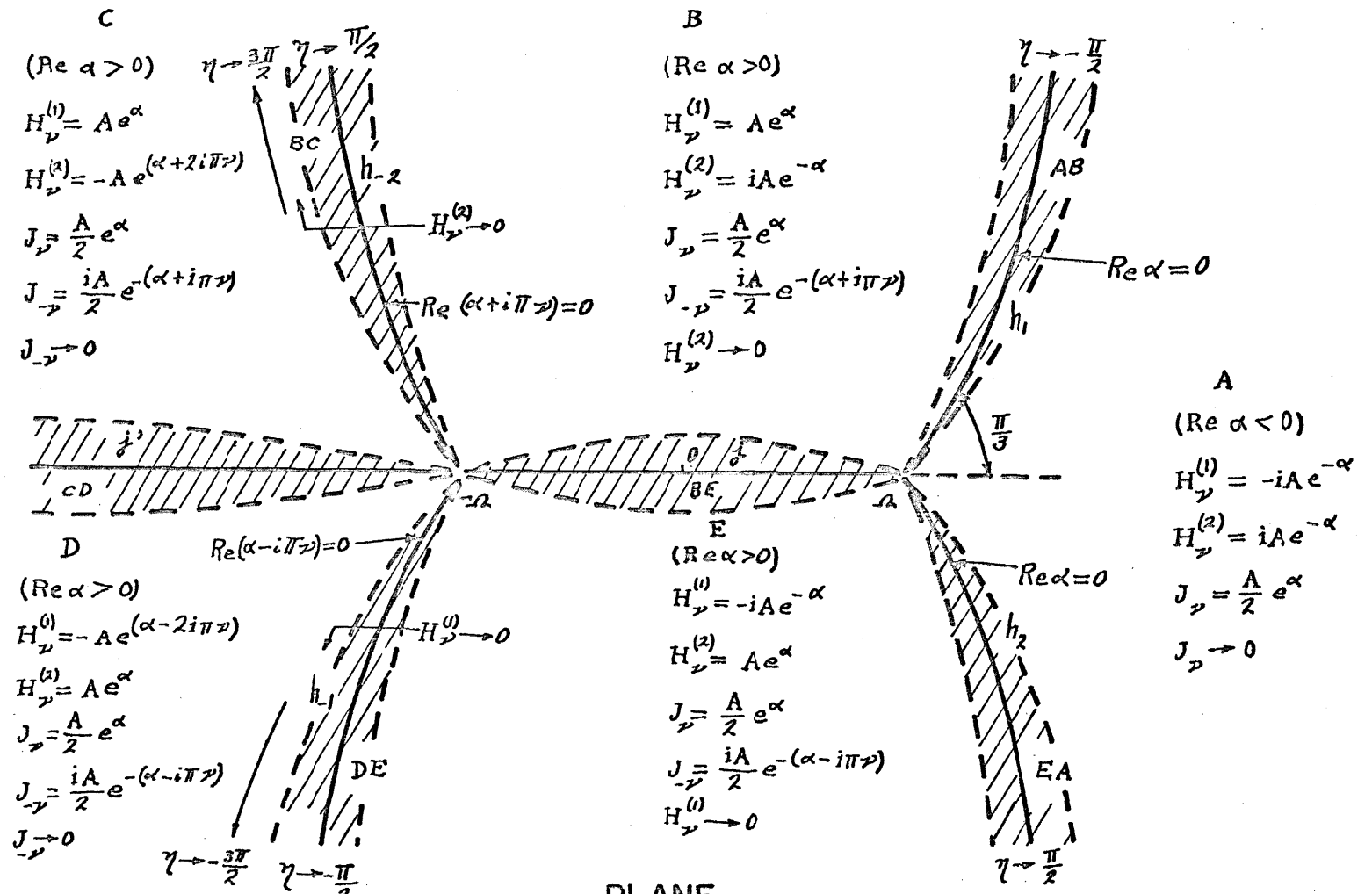

ν - PLANE

FIGURE A2

EXPANSIONS IN THE ν - PLANE

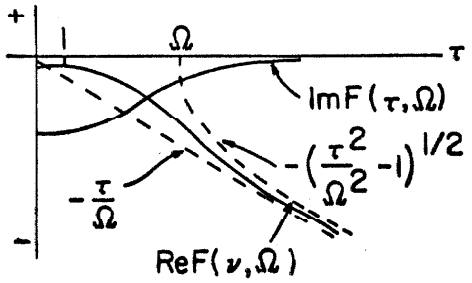

(a)

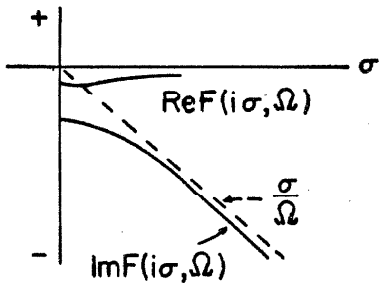

(b)

FIGURE B1

(a) F (ν, Ω) FOR ν REAL

(b) F (ν, Ω) FOR ν IMAGINARY

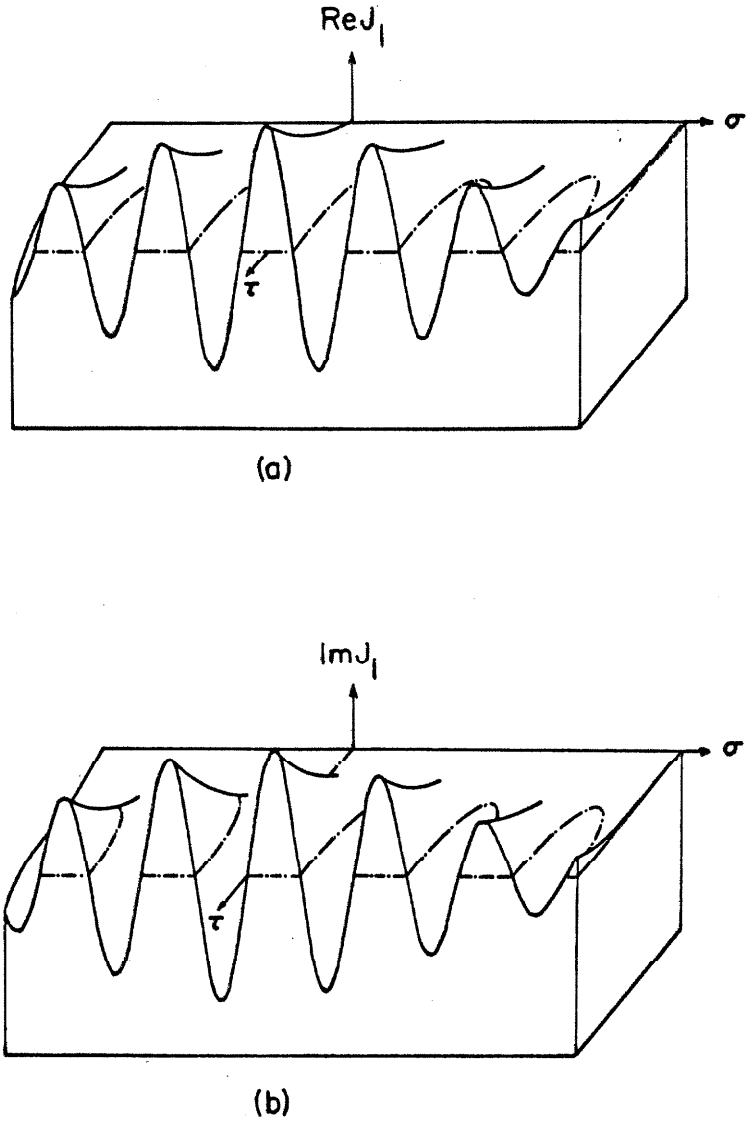

FIGURE B2
RELIEF DIAGRAMS OF ReJ_1 AND ImJ_1

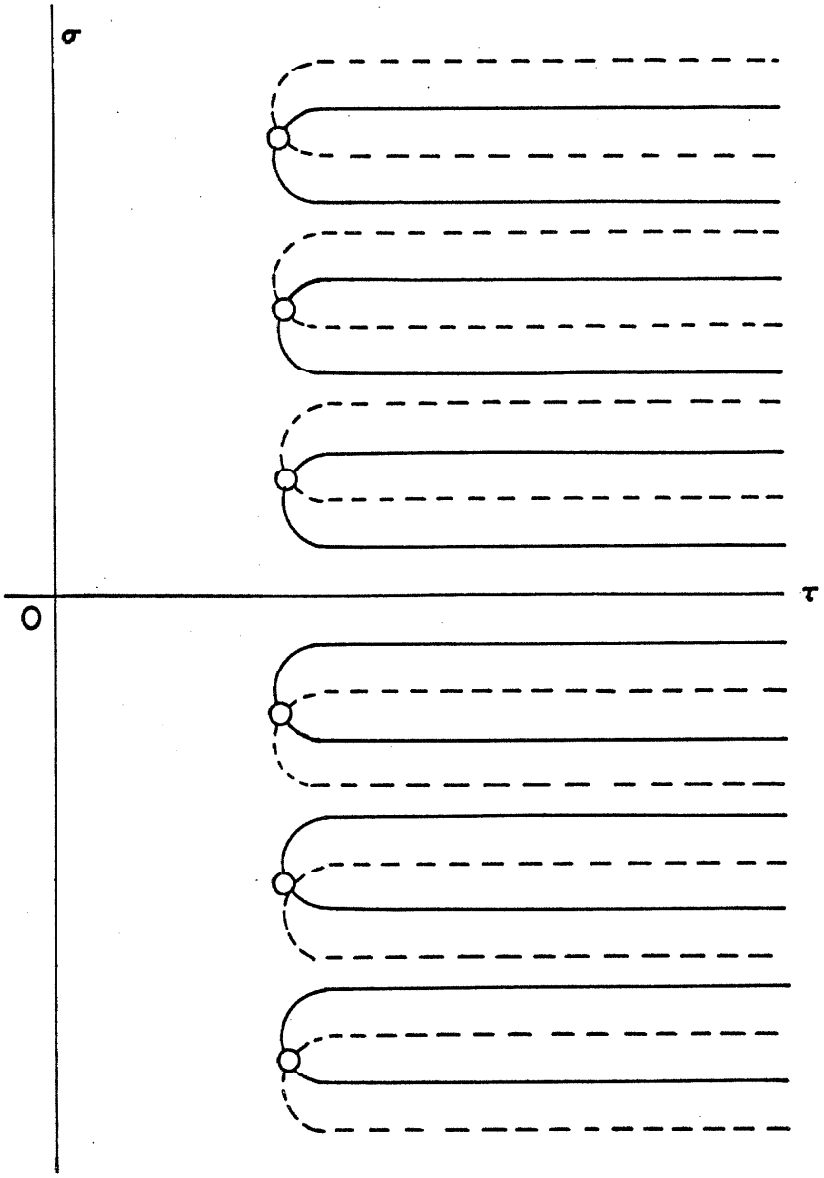

FIGURE B3

SCHEMATIC LOCATION OF THE POLES OF $F(\nu, \Omega)$

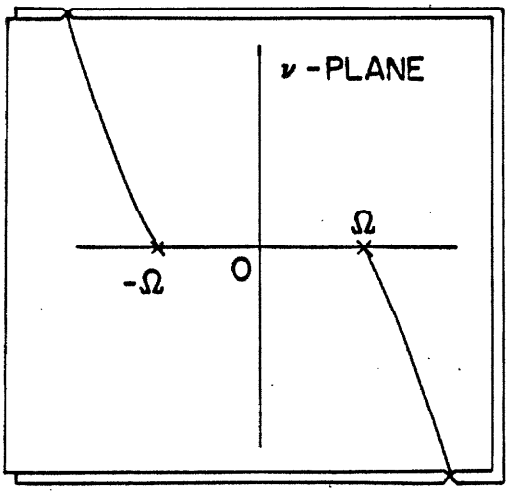

FIGURE B4

BRANCH CUTS IN THE ν -PLANE

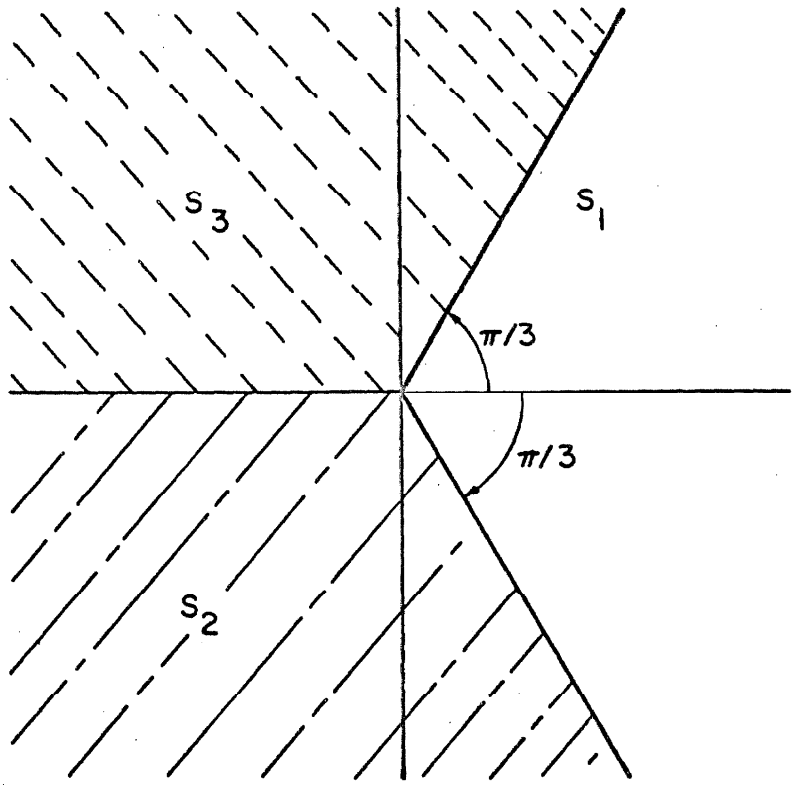

FIGURE E1
CONVERGENCE SECTORS FOR THE AIRY FUNCTION